

**INVESTIGATION OF THE DEFORMATION ALONG AN OBLIQUE
CONVERGENT MARGIN, ALEUTIAN TRENCH**

A Thesis Presented to

the Faculty of the Department of Earth and Atmospheric Sciences

University of Houston

In Partial Fulfillment

of the Requirements for the Degree

Master of Science

By

Cansu Guner

May 2017

**INVESTIGATION OF THE DEFORMATION ALONG AN OBLIQUE
CONVERGENT MARGIN, ALEUTIAN TRENCH**

Cansu Guner

APPROVED:

Dr. Michael A. Murphy, Chairman

Dr. Guaquan Wang

Dr. Veronica Sanchez

Dean, College of Natural Sciences and Mathematics

ACKNOWLEDGEMENTS

I would like to express my sincere gratitude to my committee chair, Dr. Michael A. Murphy and members, Dr. Guaquan Wang and Dr. Veronica Sanchez for their support and academic guidance. I owe special thanks to Turkish Petroleum Corporation for the financial and academic support they provided under all circumstances throughout my graduate studies. Last, but certainly not least; my deepest gratitude goes to my parents and family for their constant encouragement and total support in my attainment of this goal.

**INVESTIGATION OF THE DEFORMATION ALONG AN OBLIQUE
CONVERGENT MARGIN, ALEUTIAN TRENCH**

An Abstract of a Thesis

Presented to

the Faculty of the Department of Earth and Atmospheric Sciences

University of Houston

In Partial Fulfillment

of the Requirements for the Degree

Master of Science

By

Cansu Guner

May 2017

ABSTRACT

Deformation of the Aleutian Arc is widely interpreted to occur due to oblique convergence between the North American and Pacific plates. Due to the obliquity between the relative plate motion and the strike of the margin, the strain within the accretionary prism and forearc is interpreted to be partitioned resulting in the formation of five crustal blocks and a forearc sliver. The aim of this study is to better understand the geometry of these features and their potential kinematic role in accommodating oblique convergence. Forearc partitioning, rotation and translation of the forearc sliver plate are evaluated using: 1) data from 6 GPS stations collected between 2004 and 2015, 2) 1,798 earthquake events (focal mechanisms and depth) that occurred between January 1976 to April 2015, 3) plate convergence directions and velocities, and 4) trends of Holocene magmatic features. My results show that the boundary of blocks including what I interpret as a forearc sliver correlate to the angle of obliquity between the North American and the Pacific plates. Strain-partitioning structures in the Aleutian arc develop where the angle of obliquity is $\geq 20^\circ$. The boundary between blocks undergoing vertical axis rotation and the forearc sliver corresponds to an angle of obliquity equal to 70° ($170E^\circ$). This position in the arc also correlates to a change in the azimuth of Holocene volcanic features where they trend subparallel to the strike of the arc.

Four GPS stations are located within the arc. Velocities of these stations increase toward the west. These GPS stations' velocities cannot represent the blocks' rotations by themselves but they can represent the movement direction of the block limits. To find the pivot axis of the arc, three GPS stations were chosen as fixed locations. My results show

that the Aleutian Arc is undergoing clockwise rotation with respect to Station AB02 in the central portion of the Aleutian at 170°W, which is the pivot point of the localities where these stations exist. This indicates that the angle of obliquity west of 170°W is increasing. Earthquake depths show that the angle of subduction is moderate in the east and shallow in the west. Arc-parallel and arc-normal convergence rates studies correlate with convergence obliquity along the arc.

Table of Contents

1	INTRODUCTION.....	1
1.1	GEOLOGIC SETTING OF THE ALEUTIAN ARC	4
1.2	PLATE TECTONICS OF THE ALEUTIAN ARC	5
1.3	TECTONIC EVOLUTION OF THE ALEUTIAN ARC.....	7
1.4	PREVIOUS STUDIES.....	8
1.4.1	Summit Basins.....	9
1.4.2	Forearc Blocking.....	9
1.4.3	Paleomagnetic Evaluation.....	12
2	DATA & METHOD, AND CALCULATIONS	14
2.1	GLOBAL POSITIONING SYSTEM METHODS AND MEASUREMENTS	14
2.2	GLOBAL POSITIONING SYSTEM CALCULATIONS	15
2.2.1	GPS Station AB01	16
2.2.2	GPS Station AB21	23
2.2.3	GPS Station AC66	30
2.2.4	GPS Station AC60	38
2.2.5	GPS Station PETS	45
2.3	GPS STATIONS HORIZONTAL VELOCITY CALCULATIONS ACCORDING TO REFERENCE STATIONS	52
2.3.1	AB01 FIXED.....	53
2.3.2	AB21 FIXED.....	56
2.3.3	AC66 FIXED.....	59
2.3.4	AC60 FIXED.....	62
2.3.5	PETS FIXED	65
2.3.6	AB02 FIXED.....	69
2.4	GPS STATIONS MOVEMENT DIRECTION CALCULATIONS ACCORDING TO REFERENCE STATIONS TO PREDICT PIVOT LOCATION.....	74
2.4.1	Station AB01 Fixed	74
2.4.2	Station AB21 Fixed	77
2.4.3	Station AB02 Fixed	81
3	EARTHQUAKE DEPTHS AND MAGNITUDES.....	85
4	DISPLACEMENT PARTITIONING.....	90

4.1	ARC-PARALLEL & ARC-NORMAL STRAINS	90
4.2	VOLCANIC ACTIVITY AND MAGMA PATHWAYS	100
5	RESULTS AND CONCLUSIONS	103
	REFERENCES	108

LIST OF FIGURES

Figure 1.1.1.	Block diagram showing sliver plate and convergence parameters	2
Figure 1.1.2.	Bathymetric Map showing major locations.	4
Figure 1.2.1.	Block diagram showing major components of the system	5
Figure 1.3.1.	Schematic illustration of tectonic history of Aleutian Arc.	8
Figure 1.4.1.	Bathymetry map of Aleutian Arc showing major summit basin	10
Figure 2.2.1.	Displacement parameters configurations.....	16
Figure 2.2.2.	Position of Station AB01 at North Direction.....	17
Figure 2.2.3.	Position of Station AB01 at East Direction	17
Figure 2.2.4.	Frequency versus Amount of Daily Displacement Vector for Station AB01	18
Figure 2.2.5.	Frequency versus Direction of Daily Displacement Vector for Station AB01	19
Figure 2.2.6.	Frequency versus Amount of Total Displacement Vector for Station AB01	20
Figure 2.2.7.	Frequency versus Direction of Total Displacement Vector for Station AB01	21
Figure 2.2.8.	Polar Graph of Daily Displacement Vector for Station AB01	21
Figure 2.2.9.	Polar Graph of Total Displacement Vector for Station AB01	22
Figure 2.2.10.	Elevation Graph for Station AB01	23
Figure 2.2.11.	Position of Station AB21 at North Direction.....	24
Figure 2.2.12.	Position of Station AB21 at East Direction	24
Figure 2.2.13.	Frequency versus Amount of Daily Displacement Vector for Station AB21	25
Figure 2.2.14.	Frequency versus Direction of Daily Displacement Vector for Station AB21	26
Figure 2.2.15.	Frequency versus Amount of Total Displacement Vector for Station AB21	26
Figure 2.2.16.	Frequency versus Direction of Total Displacement Vector for Station AB21	28
Figure 2.2.17.	Polar Graph of Daily Displacement Vector for Station AB21	28
Figure 2.2.18.	Polar Graph of Total Displacement Vector for Station AB21	29
Figure 2.2.19.	Elevation Graph for Station AB21	30
Figure 2.2.20.	Position of Station AC66 at North Direction.....	31
Figure 2.2.21.	Position of Station AC66 at East Direction	31

Figure 2.2.22. Frequency versus Amount of Daily Displacement Vector for Station AC66.....	32
Figure 2.2.23. Frequency versus Direction of Daily Displacement Vector for Station AC66.....	33
Figure 2.2.24. Frequency versus Amount of Total Displacement Vector for Station AC66	34
Figure 2.2.25. Frequency versus Direction of Total Displacement Vector for Station AC66	35
Figure 2.2.26. Polar Graph of Daily Displacement Vector for Station AC66	36
Figure 2.2.27. Polar Graph of Total Displacement Vector for Station AC66.....	37
Figure 2.2.28. Elevation Graph for Station AC66	37
Figure 2.2.29. Position of Station AC60 at North Direction.....	39
Figure 2.2.30. Position of Station AC60 at East Direction	39
Figure 2.2.31. Frequency versus Amount of Daily Displacement Vector for Station AC60.....	40
Figure 2.2.32. Frequency versus Direction of Daily Displacement Vector for Station AC60.....	41
Figure 2.2.33. Frequency versus Amount of Total Displacement Vector for Station AC60	42
Figure 2.2.34. Frequency versus Direction of Total Displacement Vector for Station AC60	43
Figure 2.2.35. Polar Graph of Daily Displacement Vector for Station AC60	43
Figure 2.2.36. Polar Graph of Total Displacement Vector for Station AC60.....	44
Figure 2.2.37. Elevation Graph for Station AC60	45
Figure 2.2.38. Position of Station PETS at North Direction.....	46
Figure 2.2.39. Position of Station PETS at East Direction	46
Figure 2.2.40. Frequency versus Amount of Daily Displacement Vector for Station PETS.....	47
Figure 2.2.41. Frequency versus Direction of Daily Displacement Vector for Station PETS.....	48
Figure 2.2.42. Frequency versus Amount of Total Displacement Vector for Station PETS	48
Figure 2.2.43. Frequency versus Direction of Total Displacement Vector for Station PETS	49
Figure 2.2.44. Polar Graph of Daily Displacement Vector for Station PETS.....	50
Figure 2.2.45. Polar Graph of Total Displacement Vector for Station PETS	51
Figure 2.2.46. Elevation Graph for Station PETS.....	51
Figure 2.2.47. Velocity and Directions of GPS Stations	52
Figure 2.3.1. Horizontal Movement of Station AB21 According to Station AB01	54
Figure 2.3.2. Horizontal Movement of Station AC66 According to Station AB01	55
Figure 2.3.3. Horizontal Movement of Station AC60 According to Station AB01	56
Figure 2.3.4. Horizontal Movement of Station AB01 According to Station AB21	57
Figure 2.3.5. Horizontal Movement of Station AC66 According to Station AB21	57
Figure 2.3.6. Horizontal Movement of Station AC60 According to Station AB21	58
Figure 2.3.7. Horizontal Movement of Station AB01 According to Station AC66.....	59

Figure 2.3.8. Horizontal Movement of Station AB21 According to Station AC66.....	60
Figure 2.3.9. Horizontal Movement of Station AC60 According to Station AC66.....	62
Figure 2.3.10. Horizontal Movement of Station AB01 According to Station AC60.....	63
Figure 2.3.11. Horizontal Movement of Station AB21 According to Station AC60.....	64
Figure 2.3.12. Horizontal Movement of Station AC66 According to Station AC60.....	65
Figure 2.3.13. Horizontal Movement of Station AB01 According to Station PETS.....	66
Figure 2.3.14. Horizontal Movement of Station AB21 According to Station PETS.....	67
Figure 2.3.15. Horizontal Movement of Station AC66 According to Station PETS.....	68
Figure 2.3.16. Horizontal Movement of Station AC60 According to Station PETS.....	69
Figure 2.3.17. Horizontal Movement of Station AB01 According to Station AB02.....	70
Figure 2.3.18. Horizontal Movement of Station AB21 According to Station AB02.....	71
Figure 2.3.19. Horizontal Movement of Station AC66 According to Station AB02.....	72
Figure 2.3.20. Horizontal Movement of Station AC60 According to Station AB02.....	73
Figure 2.4.1. Movement Direction of Station AB21 According to Station AB01.....	75
Figure 2.4.2. Movement Direction of Station AC66 According to Station AB01.....	75
Figure 2.4.3. Movement Direction of Station AC60 According to Station AB01.....	76
Figure 2.4.4. Relative Movement Directions When Station AB01 is Fixed.....	77
Figure 2.4.5. Movement Direction of Station AB01 According to Station AB21.....	78
Figure 2.4.6. Movement Direction of Station AC66 According to Station AB21.....	79
Figure 2.4.7. Movement Direction of Station AC60 According to Station AB21.....	80
Figure 2.4.8. Relative Movement Directions When Station AB21 is Fixed.....	80
Figure 2.4.9. Movement Direction of Station AB01 According to Station AB02.....	81
Figure 2.4.10. Movement Direction of Station AB11 According to Station AB02.....	82
Figure 2.4.11. Movement Direction of Station AC66 According to Station AB02.....	83
Figure 2.4.12. Movement Direction of Station AC60 According to Station AB02.....	84
Figure 2.4.13. Relative Movement Directions When Station AB21 is Fixed.....	84
Figure 3.1. Earthquake Hypocenters on Aleutian Arc.....	85
Figure 3.2. Earthquake Depths on Aleutian Arc.....	86
Figure 3.3. Earthquake Depth Data from Surface to 70 km.....	86
Figure 3.4. Earthquake Depth Data from 70 to 300 km.....	87
Figure 3.5. Earthquake Magnitudes on Aleutian Arc.....	88
Figure 4.1.1. Displacement Partitioning Model Along Arcuate Convergent Plate Boundary.....	91
Figure 4.1.2. Earthquake Depths and Velocity Partitioning Locations.....	91

Figure 4.1.3. Relative Convergence Directions between North America and Pacific Plates.....	92
Figure 4.1.4. Relative Plate Convergence Obliquity Angles Between North America and Pacific Plates	92
Figure 4.1.5. Relative Plate Convergence Rate Map	94
Figure 4.1.6. Arc-Parallel Relative Plate Motion Rate Map	94
Figure 4.1.7. Arc-Parallel Relative Plate Motion Rate Along the Trench	95
Figure 4.1.8. Arc-normal Relative Plate Motion Rate Map.....	96
Figure 4.1.9. Arc-Normal Relative Plate Motion Rate Along the Trench	97
Figure 4.1.10. Plate Convergence and Arc-parallel Convergence Directions Along the Trench ..	98
Figure 4.1.11. Plate Convergence and Arc-normal Convergence Directions Along the Trench...	99
Figure 4.1.12. Velocity Components and Relative Plate Convergence Rates Along the Trench ..	99
Figure 4.2.1. Active and Holocene volcanoes belonging to the Aleutian-Alaska Arc and Rotating Blocks	100
Figure 4.2.2. Relative Plate Convergence Direction and Magma Pathway Strikes	101
Figure 5.1.1. Comparison Map of Relative Velocity and Velocity Results of GPS Stations	106
Figure 5.1.2. Plate Convergence Obliquity and GPS Stations.....	107

LIST OF TABLES

Table 2.1: Locations of GPS Stations	14
Table 5.1 Velocity of GPS Stations	104
Table 5.2 Relative Horizontal Velocities.....	105

1 INTRODUCTION

Plate tectonics is a theory which states that the outer shell of the earth is divided into several plates and these plates move relative to each other due to driving forces. Where the plates meet, their relative motion determines the plate boundary type as convergent, divergent, or transform. The Aleutian Arc is an example of an arcuate oceanic-continental convergent margin that extends for 3000 kilometers from the Alaska Peninsula to Kamchatka Peninsula. Convergent plate margins are composed of several components including: subduction zone, volcanic arc, trench, overriding plate, forearc sliver plate, strike-slip faults and cross-orogen structures. All of them affect each other directly or indirectly.

If the subducting plate and overriding plate collide at an angle rather than orthogonally, oblique convergence occurs. Because of oblique convergence, the relative motion and strain regime are partitioned into arc-perpendicular and arc-parallel components along the arc-trench. This process may develop a forearc sliver plate between the arc-trench and strike-slip fault zone. Forearc slivers are known to occur in compressional environments where convergence is oblique (Figure 1.1.1) (McCaffrey, 2009). Additionally, the obliquity may be small to produce a strike-slip faults and arc-parallel translation of parts of the arc. The primary factors affecting the slip rate and strike-slip fault development are the degree of obliquity and convergence rate. The rate of strike-slip faulting increases with increasing obliquity of convergence. Typical migration rate of the forearc sliver plate is 1-2 mm/yr according to earthquake slip vector measurements on the western side of the Aleutian Arc (McCaffrey, 1992).

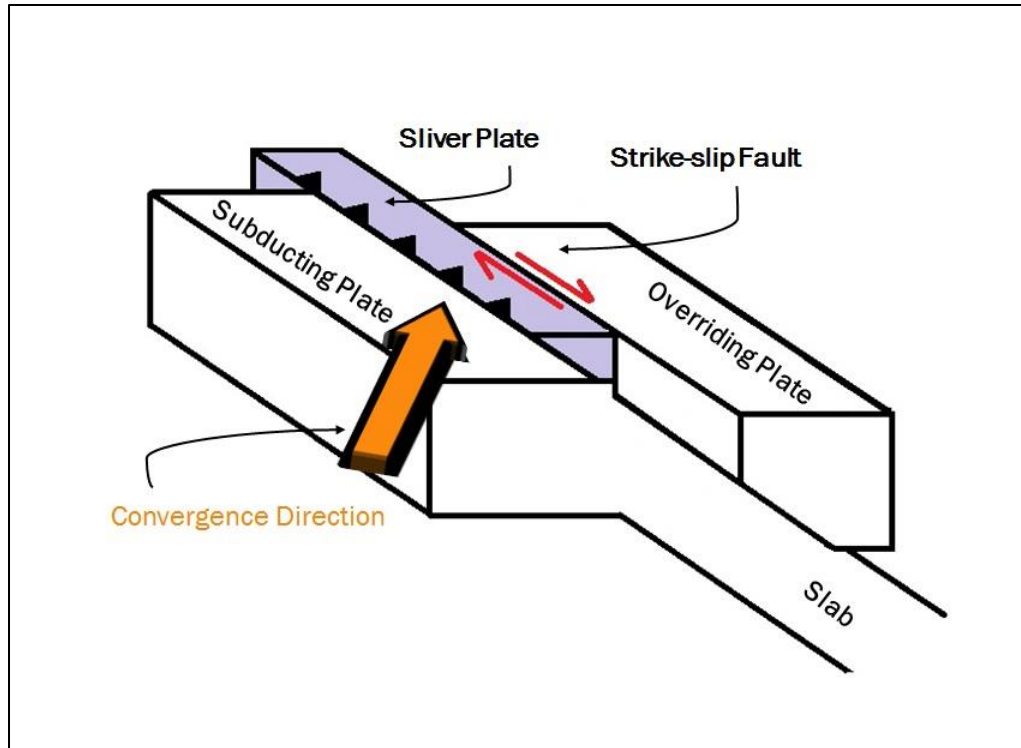


Figure 1.1.1. Block diagram showing sliver plate and convergence parameters (modified from McCaffrey, 2009)

There are two end-member models for the kinematics of arcuate convergent plate boundaries. The first one describes the presence of a single cross-orogen structure in the system that partitions all of the arc-parallel motion along the length of the orogeny; the Sumatra-Java trench is an example of this type. The second one describes several cross-orogen structures that divide the arc-trench region into blocks which rotate about a vertical axis. This is an important issue since the motion of forearc blocks influence the system. The rotation of the blocks and forearc sliver plate change the direction and rate of convergence at the subduction zone affecting their velocities. Since the convergence does not occur between the overriding and subducting plates, the main interaction is between the forearc sliver blocks and subducting plate.

PROJECT SUMMARY

Deformation of the Aleutian Arc is widely thought to be due to oblique convergence between the North American and Pacific plates. The aim of this study is to determine the various convergent plate structures and assess their role in accommodating strain in the Aleutian convergent margin. More specifically, I will investigate the role of forearc partitioning (blocking), rotation and translation of the forearc sliver plate, as well as the shape of the sliver plate and velocity of blocks.

1.1 GEOLOGIC SETTING OF THE ALEUTIAN ARC

The Aleutian Arc results from subduction of the Pacific Plate beneath the Bering Sea region of the North American Plate. It extends 4,000 km from Kamchatka Peninsula to the Gulf of Alaska. The relative convergence rate between the Pacific and North American plates is 48 mm/yr in the east and 78 mm/yr in the west of the arc (Lallemant and Oldow, 2000). The Pacific Plate is thinner and denser, so it subducts underneath the North American Plate. Convergence type changes along the arcuate Aleutian Arc from normal convergence in the east to oblique motion in the central region and nearly pure arc-parallel motion in the west (Lallemant and Oldow, 2000).

The Aleutian Arc is the southern limit of the Aleutian Basin (Figure 1.1.2). The west side of the Aleutian Basin is marked by the Shirshov Ridge which is a west-vergent thrust tectonic unit. Thrusting along the Shirshov Ridge started to develop during the middle Eocene and ceased by the early Oligocene (Chekhovich, 2014).

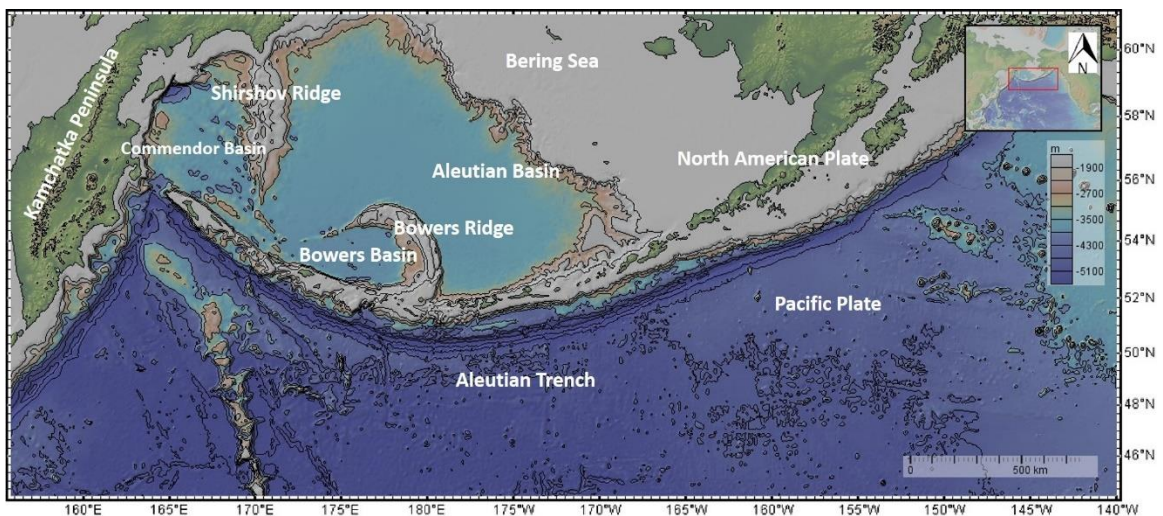


Figure 1.1.2. Bathymetric Map showing major locations. Map is taken from GeoMapApp

The southwest side of the Aleutian Basin is limited by the submarine Bowers Ridge, which is a Paleogene island arc. The age of the island-arc volcanic rocks at the basin is estimated to be 32-26 Ma based on geochemical and $^{40}\text{Ar} / ^{39}\text{Ar}$ age data (Wanke et al., 2012) (Figure 1.1.2).

1.2 PLATE TECTONICS OF THE ALEUTIAN ARC

According to the plate tectonic theory, the outer shell of Earth is composed of several large, thin, rigid plates. The Aleutian Arc, which is a volcanic island arc, that formed at an arcuate convergent margin.

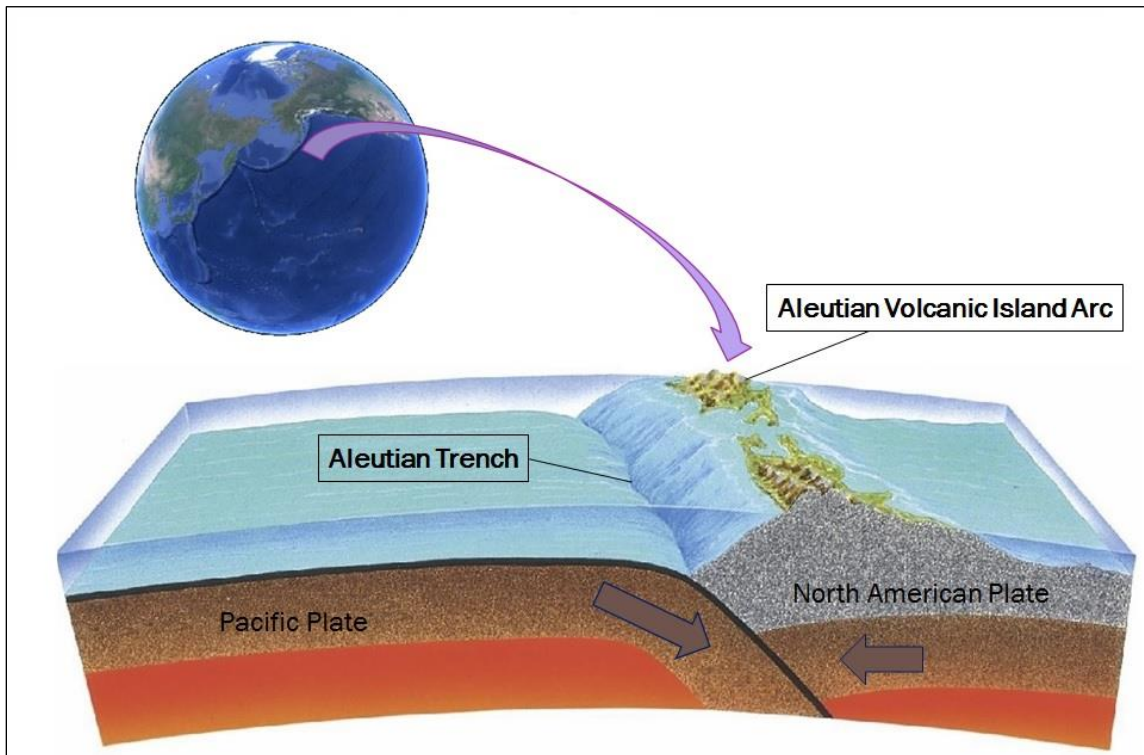


Figure 1.2.1. Block diagram showing major components of the system

(<http://wikifuller.wikispaces.com/Project+PLATE+TECTONICS>)

While subduction occurs between two plates, the subducting slab sinks beneath the overriding plate at an angle which depends on several factors such as plate temperature,

rheologic difference between subducting plate and surrounding mantle, as well as convergence obliquity angle. Where the slab sinks into the mantle, a long and narrow trench is located between the two plates. The Aleutian Trench is located between the subducting Pacific plate and overriding North American plate (Figure 1.2.1).

A megathrust is the interface between two converging plates and is a location of high magnitude earthquakes. The Aleutian Island Arc megathrust is one of them where earthquake activity is concentrated along the boundary of the Pacific and North America plates; as well as in the interior of Alaska where tectonic stresses are translated from the plate boundary into the interior of Alaska. The Pacific Plate subducts along this megathrust beneath the North America Plate, with a relative velocity ranging from 47 to 75 mm/yr. (Wesson et al., 2008). According to Lallemand and Oldow (2000), this rate is about 48 mm/yr in the east and 78 mm/yr in the west.

Oblique convergence between the subducting Pacific and overriding North American (Bering) plates generates the Aleutian Island Arc and results in development of a forearc sliver plate at the westernmost side of the arc with clockwise rotating blocks to the east (Ruppert et al., 2012).

Oblique subduction results in westward transport of the arc and causes arc-parallel translation of the sliver plate between the trench and the island arc as well as vertical axis rotation of crustal blocks. The boundaries of these blocks correlates with the location of fracture zones and the summit basins (Figure 1.4.1). Block margins also spatially coincide with submarine fault-controlled canyons. The southern boundaries of the blocks are restricted by seaward edge of the arc massif and the northern boundaries are defined by the

southern edge of the corresponding summit basins with Kresta Shear Zone (Ruppert et al., 2012 and Lallemand, 1996).

1.3 TECTONIC EVOLUTION OF THE ALEUTIAN ARC

The first appearance of Aleutian Arc magmatism occurred when the North Pacific subduction zone of the Kula plate shifted to the south from the Koryak and Beringian continental margin to its present offshore position of the arc (Figure 1.3.1-A) (Scholl et al., 1987). The oldest rocks dated in the Aleutian Volcanic Islands are 50-55 Ma which indicates that subduction at the Beringian continental margin ended by early Cenozoic time. Most of the volcanic arc was built during the middle Eocene. Magmatic activity waned by 40 Ma ago (Scholl et al., 1987). This decrease in magmatic activity coincides with a change in motion of the Pacific plate and abandonment of the Kula-Pacific spreading center at 43-45 Ma (Figure 1.3.1-B). As a consequence of the new plate configuration, a decrease in subduction rate was estimated as much as 200 km/m.y. for the Kula plate prior to 43 Ma and 58-70 km/m.y. for the Pacific plate (including the remains of the old Kula plate). Another indicator to this decrease of magma generation is the bending in the Emperor-Hawaiian seamount chain which indicates a change in plate motion. This change increased the obliquity of subduction and resulted in a decrease of magma generation at about 43 Ma. (Scholl et al., 1987).

During the Oligocene and Miocene, subduction of the younger and more buoyant Kula Ridge triggered uplift of the region. Subsequent intrusion of epizonal plutons occurred (Scholl et al., 1987).

In the late Cenozoic, subduction of the ridge continued and accompanied by extensional deformation (Figure 1.3.1-C). Moreover, regional subsidence continued until 10 Ma, and is attributed to subduction of the extinct Kula Ridge segments. Summit basins formed in the Late Miocene to early Pliocene. These basins filled with sediments derived from the ridge and late Cenozoic volcanic rocks. The final tectonic stage is from 5 Ma to present and is characterized by an increase in the subduction rate of the Pacific plate up to 87 km/m.y. (Figure 1.3.1-D) (Scholl et al., 1987).

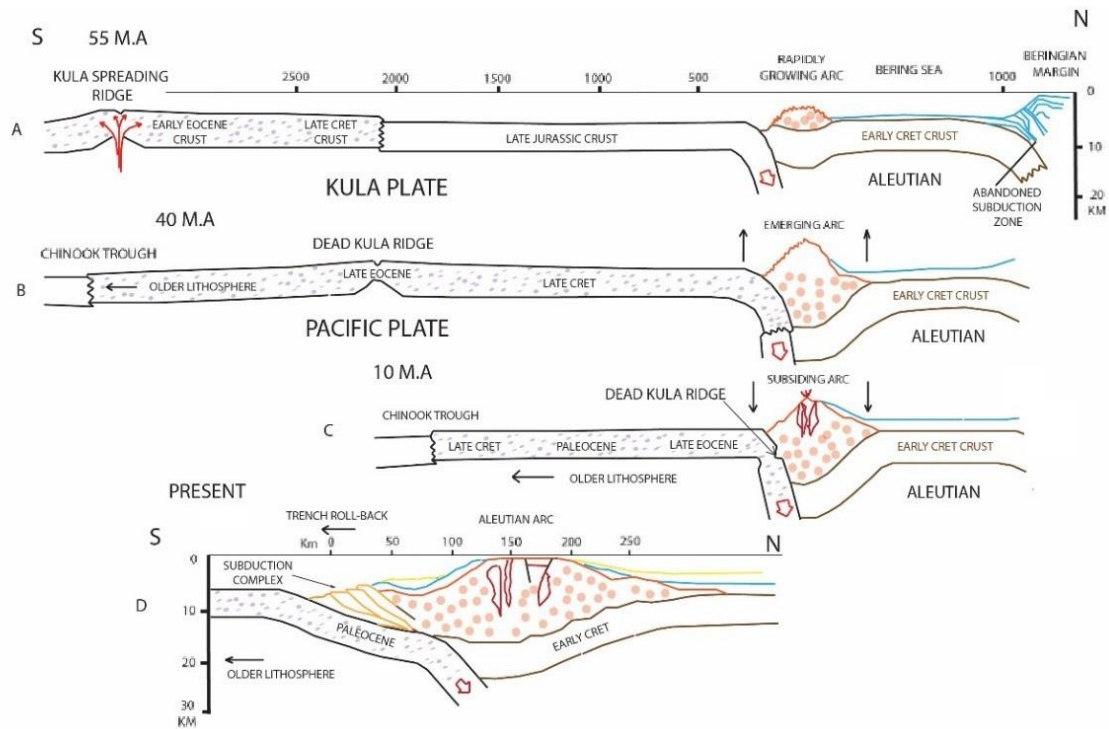


Figure 1.3.1. Schematic illustration of tectonic history of Aleutian Arc (from Scholl et al., 1987). A: Initial formation of the arc and offshore subduction zone, B: Death (subduction) of the Kula-Pacific spreading ridge, C: Subduction of the abandoned Kula-Pacific Ridge, D: Appearance of an accretionary wedge due to faster and more orthogonal direction of underthrusting, and formation of forearc basin of Aleutian Terrace.

1.4 PREVIOUS STUDIES

Convergence rate between the Pacific and North American Plates changes from east to west between 48 mm/year where the obliquity angle is 0° and 78 mm/year where

convergence is almost parallel to the plate boundary (DeMets et al., 1990; Freymueller et al., 2008). This pattern in the rate implies that the magnitude of orthogonal convergence also changes along the strike of the arc from being orthogonal at the eastern part, and oblique in the center. West of 175°E longitude, the direction of the relative plate motion is parallel to the trench.

1.4.1 Summit Basins

Several basins occur along the Aleutian Arc and are interpreted to have formed due to clockwise rotation of the blocks within the arc (Geist et al., 1987). These basins are referred to as the Summit basins and are generally located near or along the axis of late-Cenozoic volcanism. They are interpreted to have formed as arc-parallel graben or half-graben (Geist et al., 1987). Their geomorphic appearance is rhombic shaped and varies in size from ten to hundreds of kilometers in length. The boundaries between the contiguous blocks are composed of fault-controlled canyons that cut the southern slope perpendicular to their regional trend. Along the northern margin of the blocks are triangular shaped summit basins that show evidence of clockwise block rotation (Geist et. al, 1988) (Figure 1.4.1).

1.4.2 Forearc Blocking

Geist et al., (1988) proposed a rotating block model for the central and western part of the Aleutian Arc. In this model, there are five blocks and their margins are interpreted to coincide with geomorphic features such as canyons. The northern boundaries of the blocks are defined as the southern edge of the corresponding summit basins which are shown in the model to form as a result of rotation of the blocks. The boundaries between these five

blocks are defined by submarine fault-controlled canyons. And lastly, the southern boundary of the blocks is the seaward edge of the arc massif.

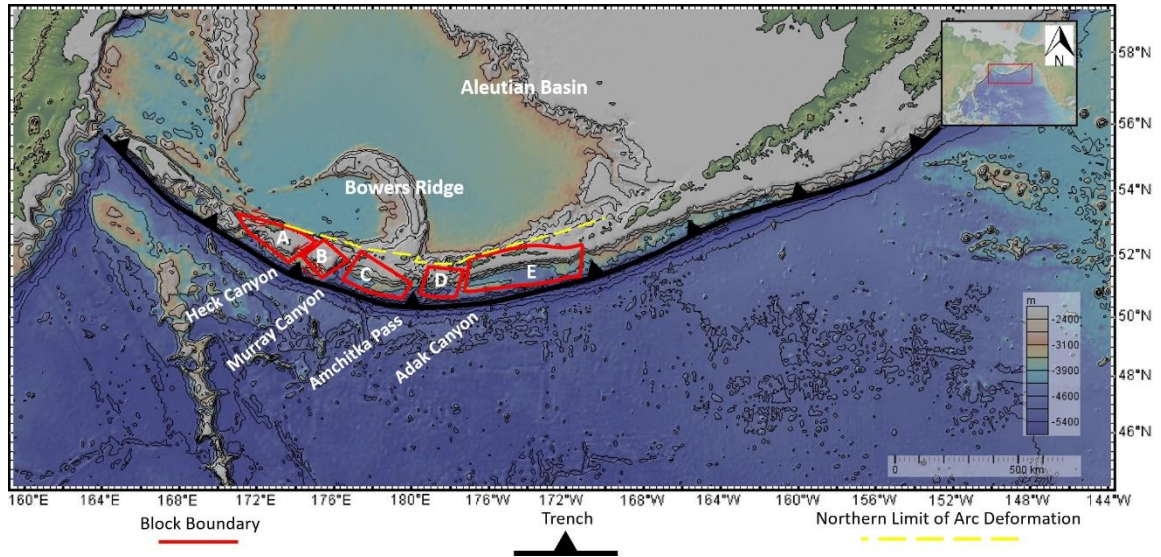


Figure 1.4.1. Bathymetry map of Aleutian Arc showing major summit basin A: Near Block; B: Buldir Block; C: Rat Block; D: Delarof Block; E: Andreanof Block. (Modified from Geist et al., 1988)

The blocks are referred to as the Near Block, Buldir Block, Rat Block, Delarof Block, and Andreanof Block, from west to east (Figure 1.4.1). Block boundaries coincide with normal and strike-slip faults.

The first block, Near Block (A) extends from Kresta Trough to Heck Canyon. It has been deformed by arc-parallel strike-slip faults which show oblique convergence along this part of the Aleutian Arc (Geist et al., 1988). At the western side of the block, narrow and deep arc-parallel canyons such as Kresta Trough show expression of these faults. This western side of the block can be the eastern side of the sliver plate which is thought to be near the Bering Island. The Ingenstrom Depression is a narrow summit basin which is the northeast limit of the block. Block A encompasses Attu and Agattu Islands.

The second block is the Buldir Block (B) between the Near and Rat blocks. Its western limit is Heck Canyon and the eastern limit is Murray Canyon. The north boundary is the Buldir depression (Buldir Summit Basin). The southern edge of the block lies near the trench-slope break, as the lower most point which is an evidence of block rotation. The Buldir depression is a deep summit basin with active volcanism occurring at its base. The Pennant basin lies within the boundaries of the Buldir block and is thought to form by downflexure of the basement surface (Scholl et al., 1987). There are no volcanic islands in this block.

The third one, Rat Block (C), extends from the Murray Canyon in the west and Amchitka Pass in the east. There are several small summit basins separated by narrow horst blocks between the Rat Block and Bowers Ridge. Sunday Basin and Pratt Depression are two of them, very large well-known basins and they are the northern limit of the Rat Block.

The Delarof Block (D) is the fourth one and lies between Amchitka Pass and Adak Canyon. There are no summit basins bordering the northern limit of the Delarof Block, however, a narrow extensional valley borders the northern limit. At the south part of the block, several small transverse canyons cut the southern margin that suggest that the Delarof Block has been segmented into several small sub-blocks.

The last block, Andreanof Block (E) is bounded on the west side by the Adak Canyon and on the east side by a broad canyon extending off of Yunaska Island. The northeast boundary of the block is Amlia and Amukta basins which are two of the largest summit basins along the arc. The southern margin of the block is almost at the trench-slope break and located

as subparallel to the Aleutian Trench. The Andreanof Block encompasses Adak, Atka, and Amlia Islands.

1.4.3 Paleomagnetic Evaluation

Sparse paleomagnetic data taken from the volcanic arc shows that Aleutian Arc, which is dominated by an arc-parallel component of Pacific Plate motion, is separated into blocks and slivers which are rotating clockwise and travelling toward west along the curve (Krutikov et al., 2008).

Westward translation along the curved Aleutian Arc was recorded as a change in latitude indicated by inclination of the Paleomagnetic vector.

The paleomagnetic results from the Amchitka Island (in Block C) show clockwise rotation ($R=54.7^\circ \pm 8.0^\circ$) between 14 Ma and the present. On the other hand, Adak Island (in Block E) does not show any rotation for Quaternary age rocks.

Paleomagnetic data results from the Bering Island (at western side of the Near block) show that it was transported westward as a forearc sliver rather than rotated as forearc blocks. Lateral migration of Bering Island initiated by the arc-parallel component of the strain and facilitated by the Beringia and Steller strike-slip fault systems (Krutikov et al., 2008).

Rotation of Mendy Island is $70^\circ \pm 12^\circ$ and $23^\circ \pm 7^\circ$ of northward latitudinal displacement. It shows that not only translation but also block rotation occurs in this area. Mendy Island may have formed as a part of a rotating forearc block further east and south than Amchitka Island (Krutikov et al., 2008).

The entire Aleutian Arc is pivoting about a point near Unalaska Island. The majority of the paleomagnetic data show clockwise rotation about 30°.

2 DATA & METHOD, AND CALCULATIONS

To calculate the velocity and movement directions of the blocks at the Aleutian arc, Global Positioning System (GPS) data were used.

2.1 GLOBAL POSITIONING SYSTEM METHODS AND MEASUREMENTS

The Global Positioning System (GPS) data used in this study are taken from the Nevada Geodetic Laboratory System. There are 5 different GPS measurement stations which are fixed at different locations. Their positions are given in Table 2.1 from east to west, respectively. Reference frame for GPS measurements is the North America fixed frame, NA12. For station PETS, the frame is IGS08.

Table 2.1: Locations of GPS Stations

GPS Station	Latitude	Longitude	Island Name
AB01	52.210	-174.205	Atka Island
AB21	51.864	-176.663	Adak Island
AC66	51.378	179.301	Amchitka Island
AC60	52.715	174.076	Shemya Island
PETS	53.023	158.650	Russia

NA12 is a terrestrial reference frame for geodetic studies designed to be used in the North America. There are 299 stations in and around the North America included in this frame. This frame is based on the GPS measurements and they are presented in time series format. The unit of time series is one day. One of the design characteristics of NA12 frame is that there is no net rotation with respect to the interior North America tectonic plate. Another important property of this reference frame is that the vertical motion with respect to Earth-

system center of mass is $\pm 0.5\text{mm/yr}$. Data for a GPS station is tabulated including easting and northing with vertical position according to NA12 frame.

GPS measurements are taken by Nevada Geodetic Laboratory between 2004 and 2015. These data sets have the date, location, elevation measurements and error estimation of daily measurements. One measurement set represents the positional variation of the station within 24 hours.

There are other GPS locations at the east side of the Aleutian Arc towards Alaska, but they were not chosen because most of the displacement partitioning and arc-parallel extension occurs at the west side of the studied area. Moreover, there are no GPS stations on all islands, and therefore not on every block.

2.2 GLOBAL POSITIONING SYSTEM CALCULATIONS

GPS calculations are presented from east to west for stations AB01, AB21, AC66, AC60 and PETS.

In this study, two different displacement values were calculated. The first one, R_1 , represents daily (in one-time step) displacements. The second displacement is R_2 and it shows total displacement from the beginning of data set until each measurement day.

Based on the displacement data, there are two different movement direction angles calculated from the north. These are θ_1 for R_1 and θ_2 for R_2 .

θ_1 shows the direction of movement for one day; on the other hand, θ_2 represents the direction of total movement till each time step. Their configurations can be seen at Figure 2.2.1.

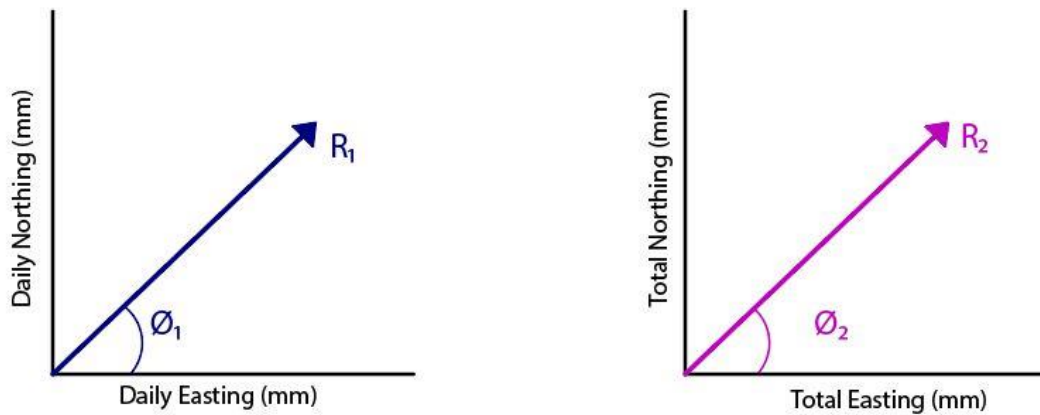


Figure 2.2.1. Displacement parameters configurations

Polar graphs show movement direction angle and movement amount together. With these graphs, daily and total movements with their orientations are given.

2.2.1 GPS Station AB01

GPS Station AB01 is located on Atka Island (52.210, -174.205), east side of the arc and its measurement data cover from May 2007 to April 2015. This station is on the Andreanof Block (Block E). Its reference frame is NA12.

Figure 2.2.2 shows the position of Station AB01 according to the north. Integer north amount (from the equator) is 5786655 meters. This plot shows that the position of Station AB01 moves toward the south.

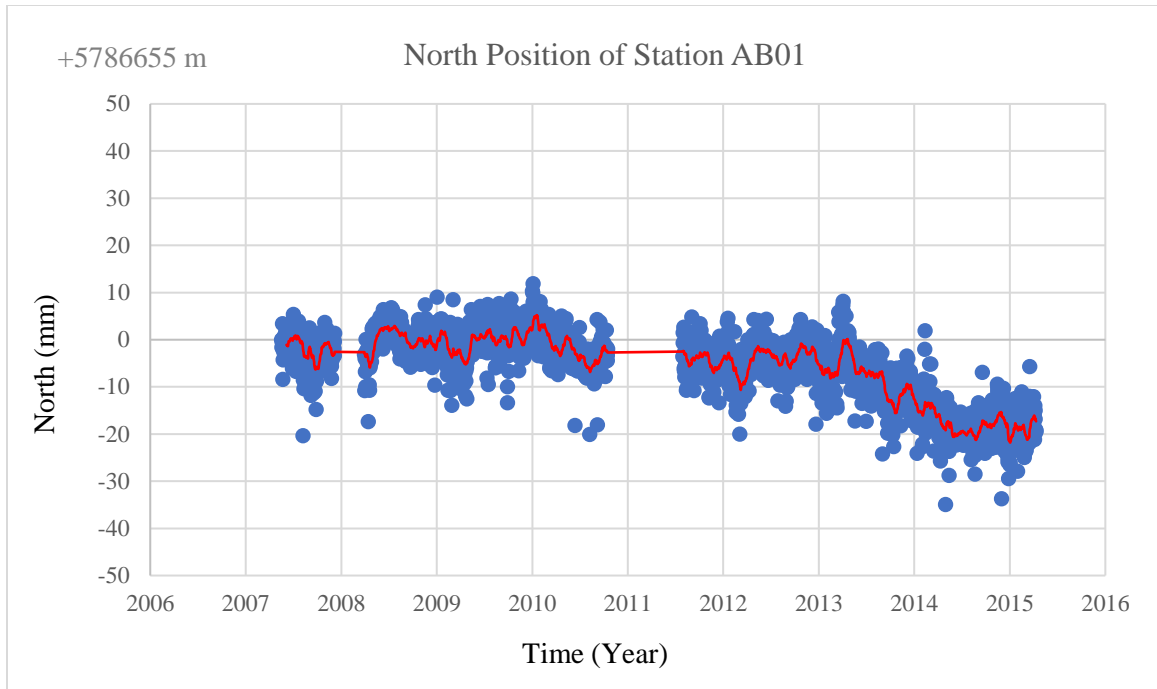


Figure 2.2.2. Position of Station AB01 at North Direction. Blue dots are measurements, red line is the average trend line.

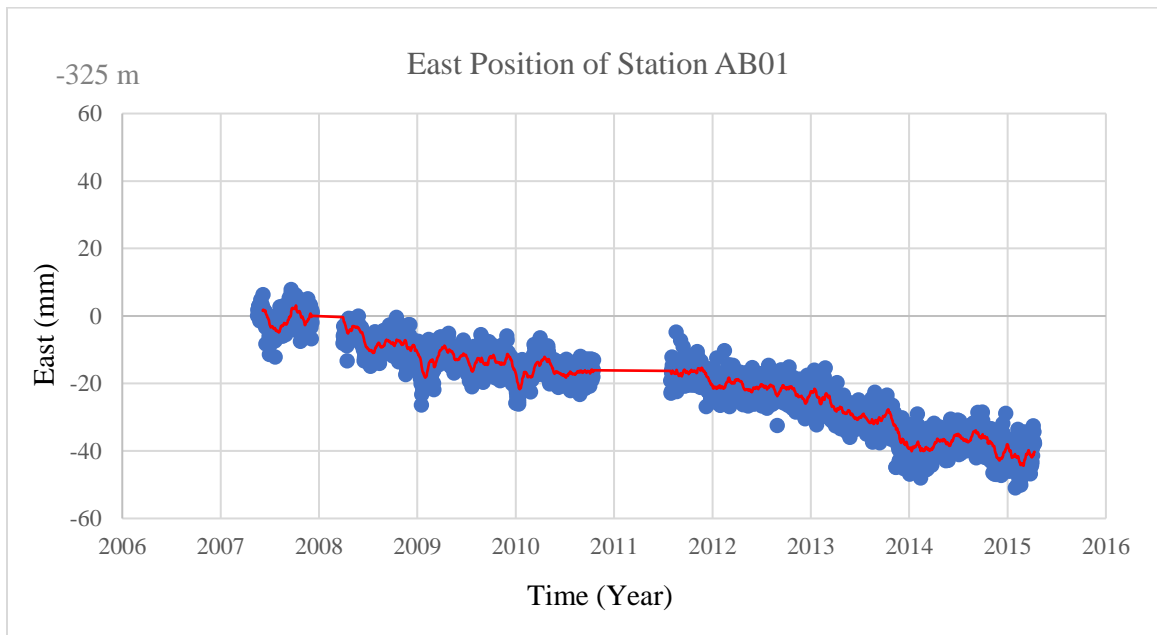


Figure 2.2.3. Position of Station AB01 at East Direction. Blue dots are measurements, red line is the average trend line.

Figure 2.2.3 shows the position of Station AB01 according to east direction. This plot shows that Station AB01 moves toward the west. Longitude (degrees) of its reference

meridian is -174.2 (W 172.5°) and integer portion of easting from reference meridian is -325 meters.

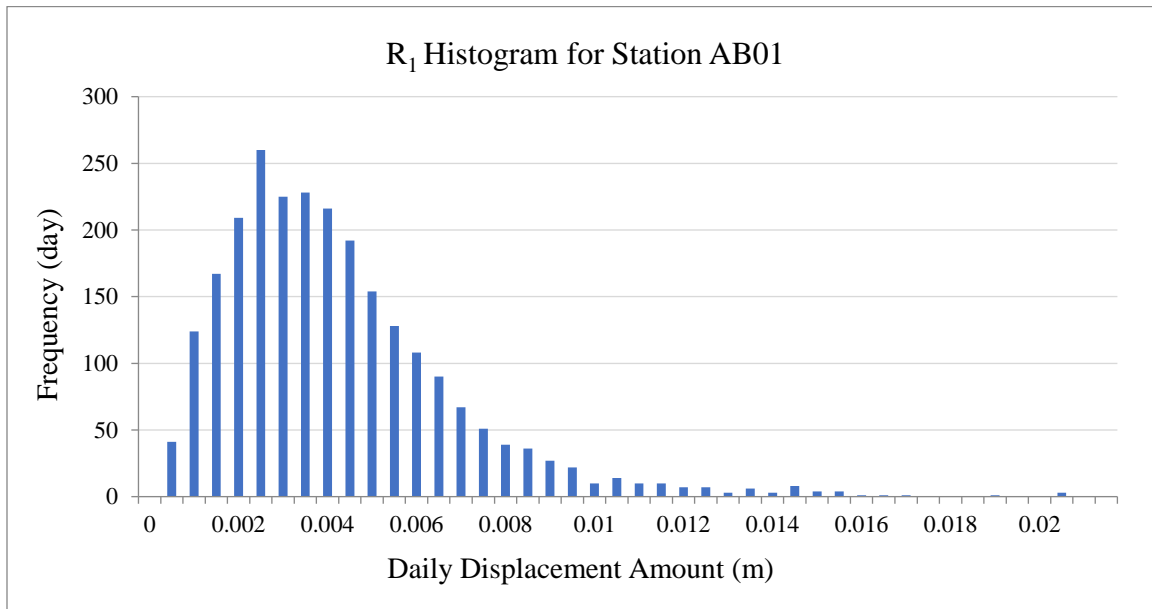


Figure 2.2.4. Frequency versus Amount of Daily Displacement Vector for Station AB01

Figure 2.2.4 shows frequency of daily displacement amount of Station AB01. It moves generally between 0.001 and 0.009 m/day (1-9 mm/day) towards different directions. Average daily movement amount is 3.98 mm/day for Station AB01.

Figure 2.2.5 shows that directions of daily displacement vectors of Station AB01 could take any value in the range. It moves almost all directions.

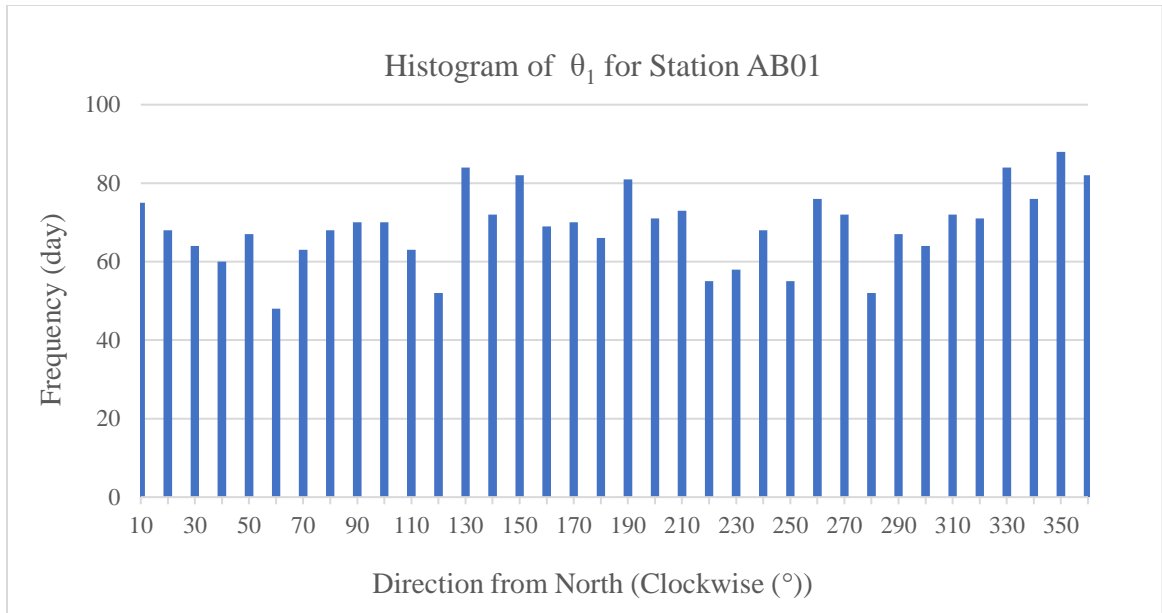


Figure 2.2.5. Frequency versus Direction of Daily Displacement Vector for Station AB01

Figure 2.2.6 shows the total displacement amount until each measurement moment of a day since the beginning of the dataset (May 2007). Since easting and northing values change from day to day indicating movements toward east or west and/or toward north or south, these total displacement value frequencies only show the direction-free distance of the station with respect to the first measurement day.

The velocity of the station should be computed from the final R_2 , which is calculated from the last data couple. Since it covers all the measurement levels which are affecting each other like going southwest and then northeast cumulatively. R_2 shows the overall movement amount.

R_2 for Station AB01 is 0.0425 m which is represented by 2478 measurement days. The velocity of the station is 6.26 mm/year.

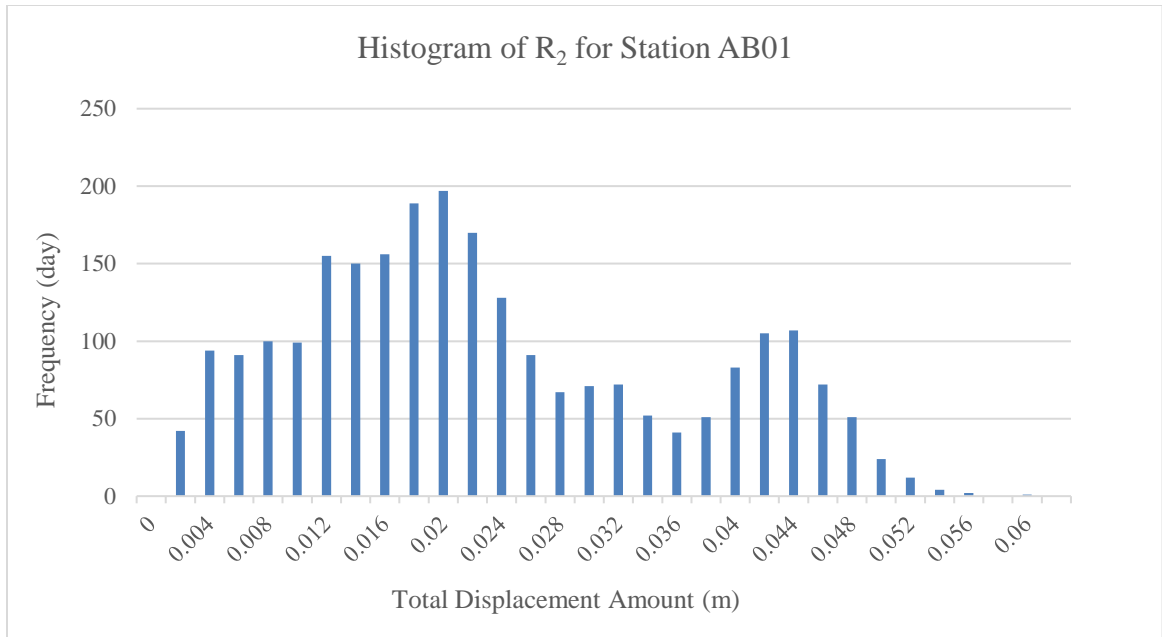


Figure 2.2.6. Frequency versus Amount of Total Displacement Vector for Station AB01

On the other hand, as it can be seen from Figure 2.2.7, Station AB01 has an overall preference for direction between 250° and 290° approximately. Its mean value is 253.182° and median value is 256.408° . These two directions amounts are very close to each other and all values seem accurate. Since mean and median values are close, histogram is symmetric. Standard deviation is 32.291° which indicates that the station's movement stays mostly within the vicinity of 32.3° of the major direction. This indicates that from 2007 to 2015, Station AB01 shows a maximum 32.3° deviation from its major movement direction. Moreover, the last calculated θ_2 represents the movement direction of the station. The movement direction of Station AB01 is 242.97° .

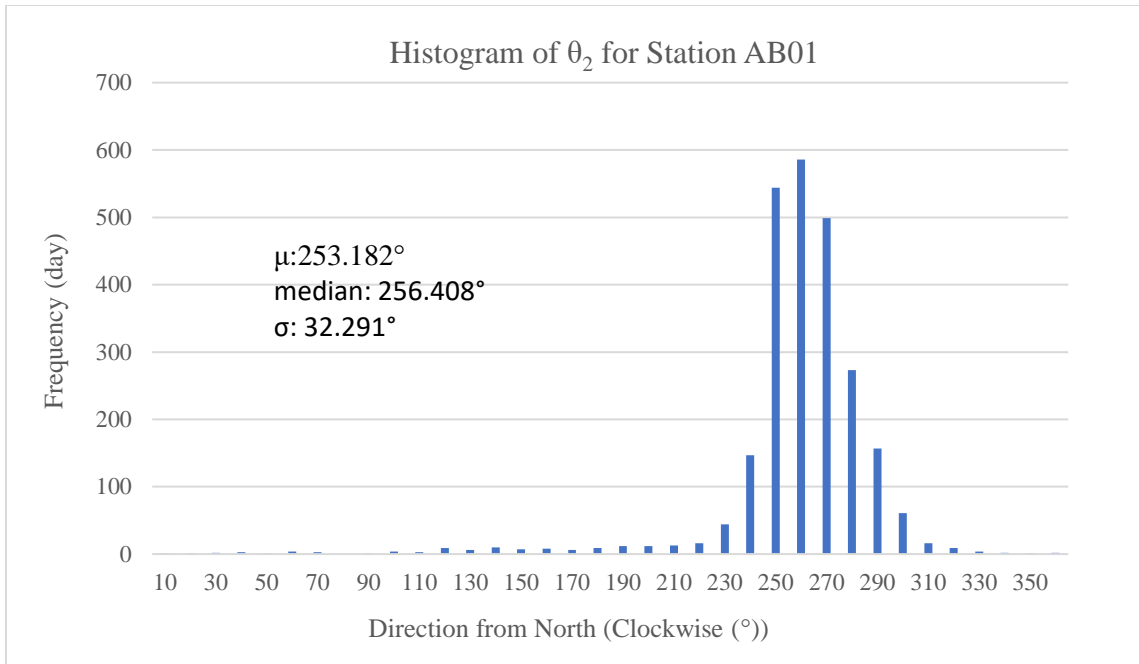


Figure 2.2.7. Frequency versus Direction of Total Displacement Vector for Station AB01

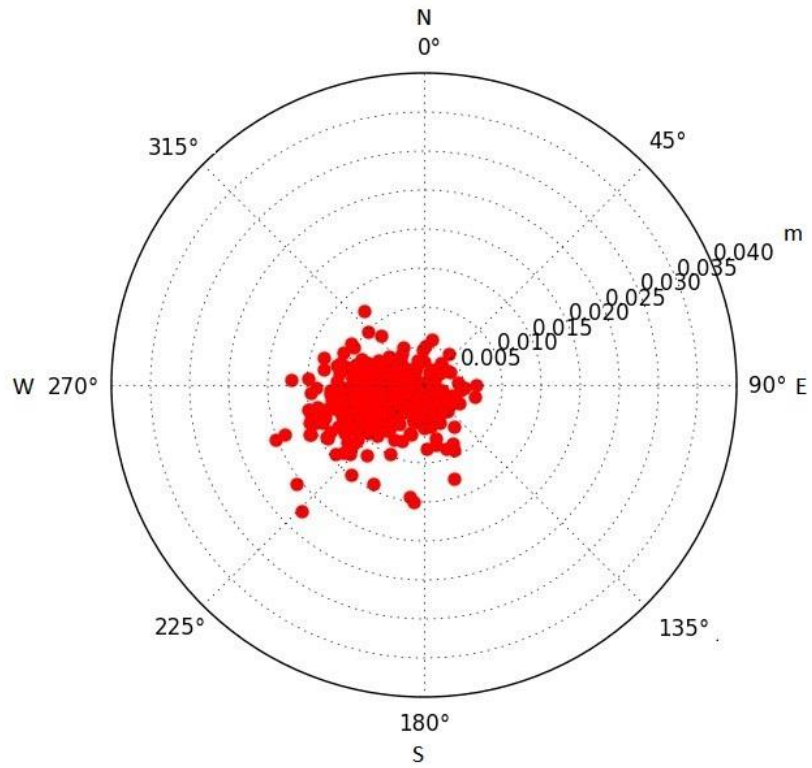


Figure 2.2.8. Polar Graph of Daily Displacement Vector for Station AB01

Figure 2.2.8 shows the daily displacement vector in a polar coordinate system. Here the distance from the origin is the daily displacement and the angle from the north is the direction angle in the horizontal plane. The main movement direction is towards the west-southwest but there are small steps towards all other directions as well. Furthermore, as it can be seen from Figure 2.2.9, minor changes (standard deviation of 32.3°) do not affect the major displacement preference. Polar graph of total displacement of Station AB01 shows that main movement direction is towards the west-southwest (Figure 2.2.9). This graph is plotted with R_2 and θ_2 .

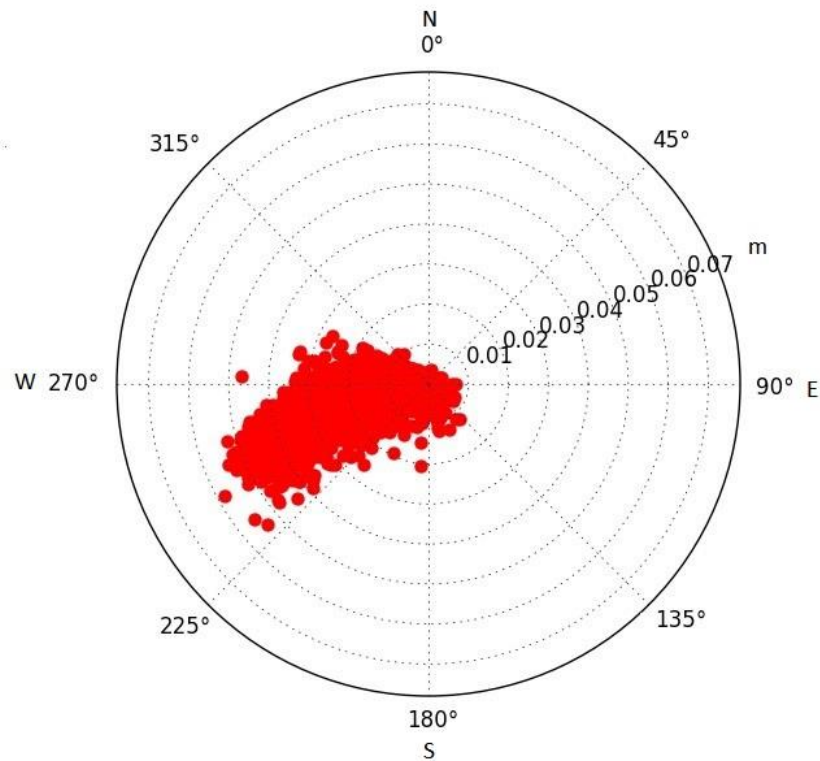


Figure 2.2.9. Polar Graph of Total Displacement Vector for Station AB01

Figure 2.2.10 shows daily elevation change for Station AB01.

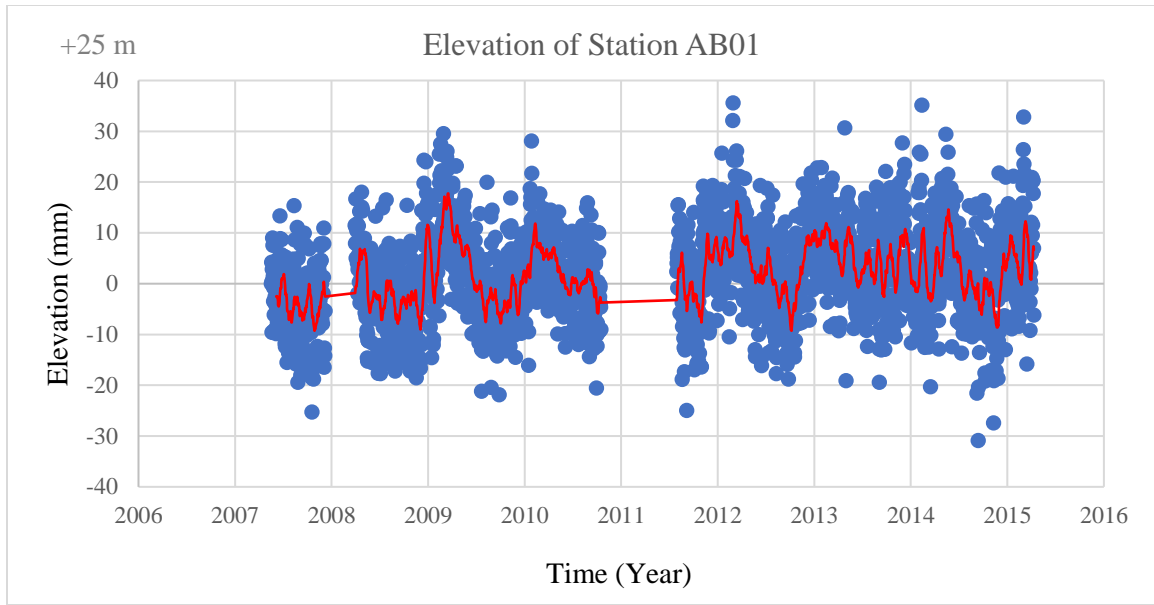


Figure 2.2.10. Elevation Graph for Station AB01. Blue dots are measurements, red line is the average trend line.

After all these calculations and evaluations, the velocity of Station AB01 is 6.26 mm/yr and its movement direction is towards west-southwest, 242.97°.

2.2.2 GPS Station AB21

GPS Station AB21 is located on Adak Island (51.864, -176.663), the second island from the east in the study area. Its measurement period covers from April 2006 to December 2014. It is located on Block E, at the northwestern corner. Its reference frame is NA12.

Figure 2.2.11 shows the position of Station AB21 according to the north. Integer north amount (from the equator) is 5748228 meters. This graph shows the position of Station AB21 moves toward the north daily.

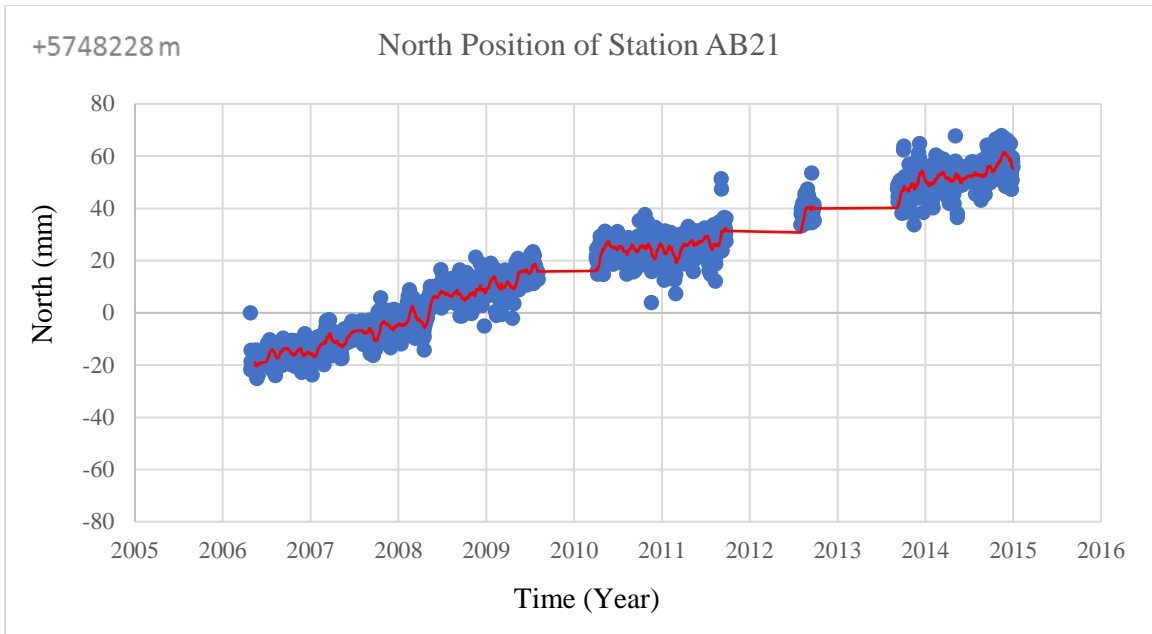


Figure 2.2.11. Position of Station AB21 at North Direction. Blue dots are measurements, red line is the average trend line.

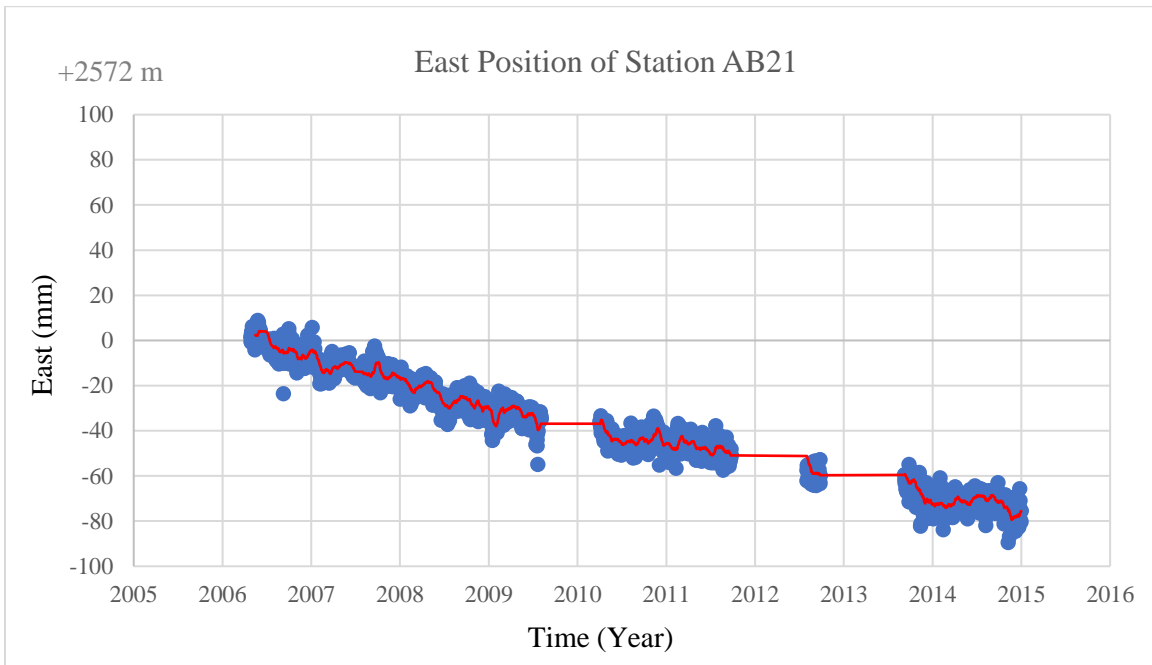


Figure 2.2.12. Position of Station AB21 at East Direction. Blue dots are measurements, red line is the average trend line.

Figure 2.2.12 shows the position of Station AB21 according to east direction. Station AB21 moves toward the west direction. Its longitude (degrees) of reference meridian is -176.7 (W 176.7°) and integer portion of easting from reference meridian is $+2572$ meters.

Figure 2.2.13 shows frequency of daily displacement amount of Station AB21. R_1 histograms of both Station AB01 and AB21 are very similar. They both have similar histogram shapes and frequency values.

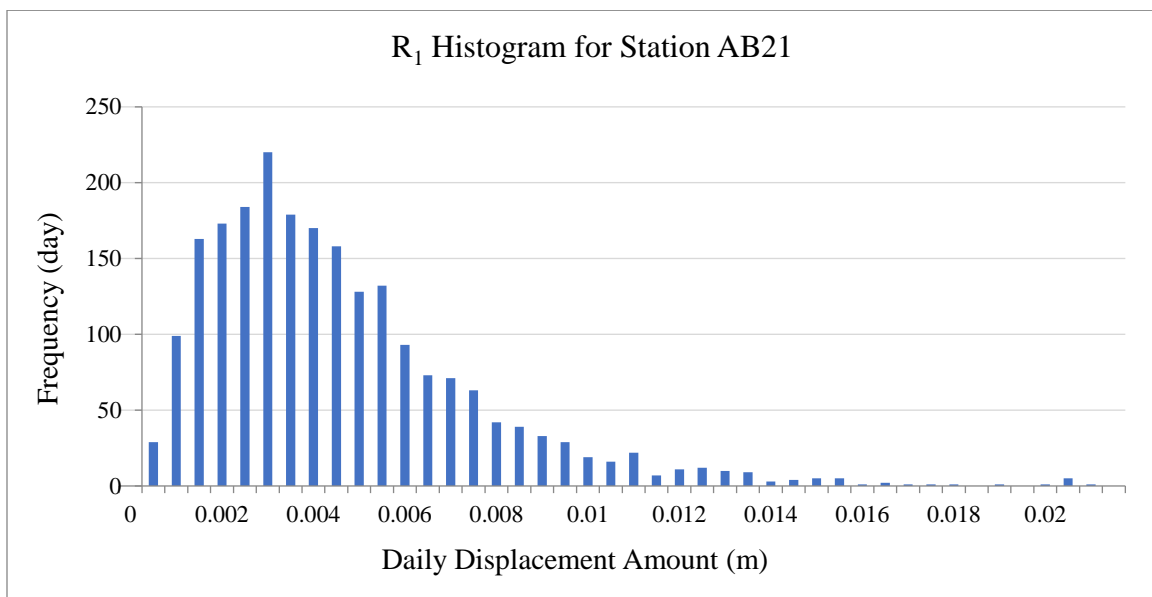


Figure 2.2.13. Frequency versus Amount of Daily Displacement Vector for Station AB21

Figure 2.2.14 shows the direction of the daily displacement vector of Station AB21.

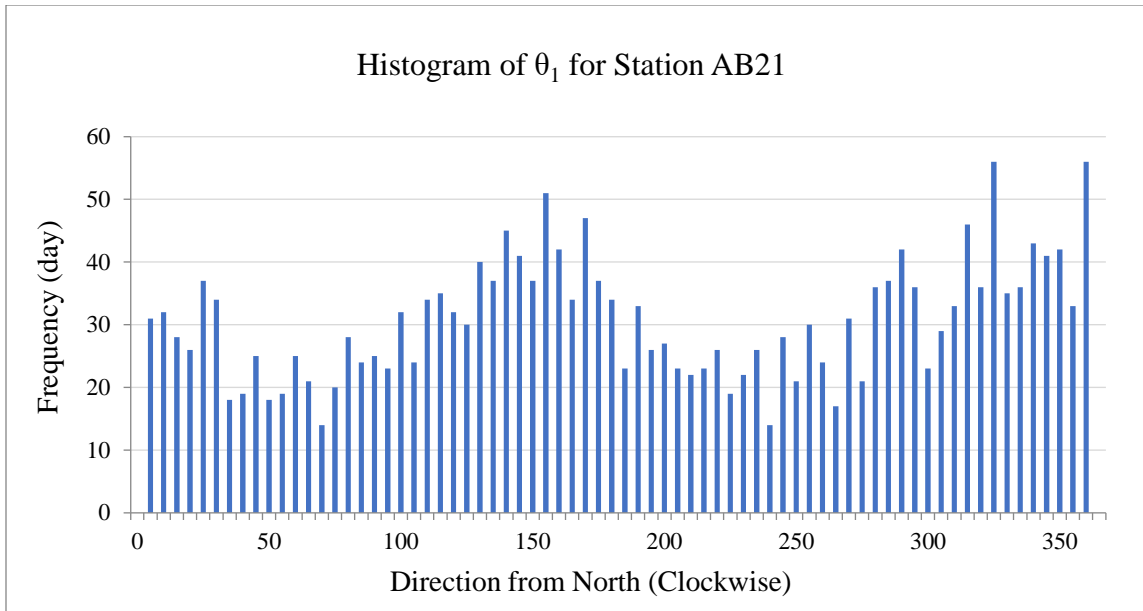


Figure 2.2.14. Frequency versus Direction of Daily Displacement Vector for Station AB21

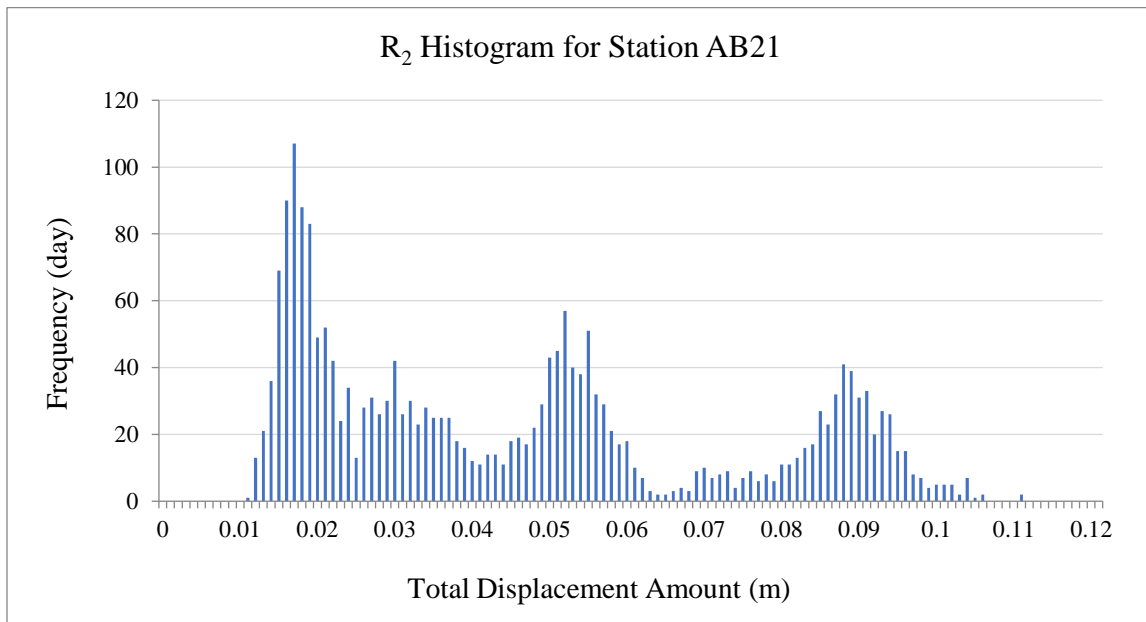


Figure 2.2.15. Frequency versus Amount of Total Displacement Vector for Station AB21

Figure 2.2.15 shows the total displacement amount until each measurement moment of a day since the beginning of the dataset (April 2006).

R_2 for Station AB21 is 0.09391 m which is represented by 2216 measurement days. The velocity of the station is 15.47 mm/year.

Figure 2.2.16, the histogram of θ_2 for Station AB21, shows that the major movement direction is between 150° and 310° . Its mean is 275.947° and the median value is 294.426° . These two direction amounts are not close to each other and the histogram is asymmetric. Moreover, the standard deviation is 37.876° . This value is larger than Station AB01's value which means Station AB21 moves with a wider range of directions. It is obvious that movements with a direction between 150° and 270° have minor effects on overall movement direction, however, displacements between 270° and 310° are responsible for the major movement. Most of the movements stay within the vicinity of 37.9° of the major direction.

Furthermore, the last calculated θ_2 represents the movement direction of the station. The movement direction of Station AB21 is 306.51° .

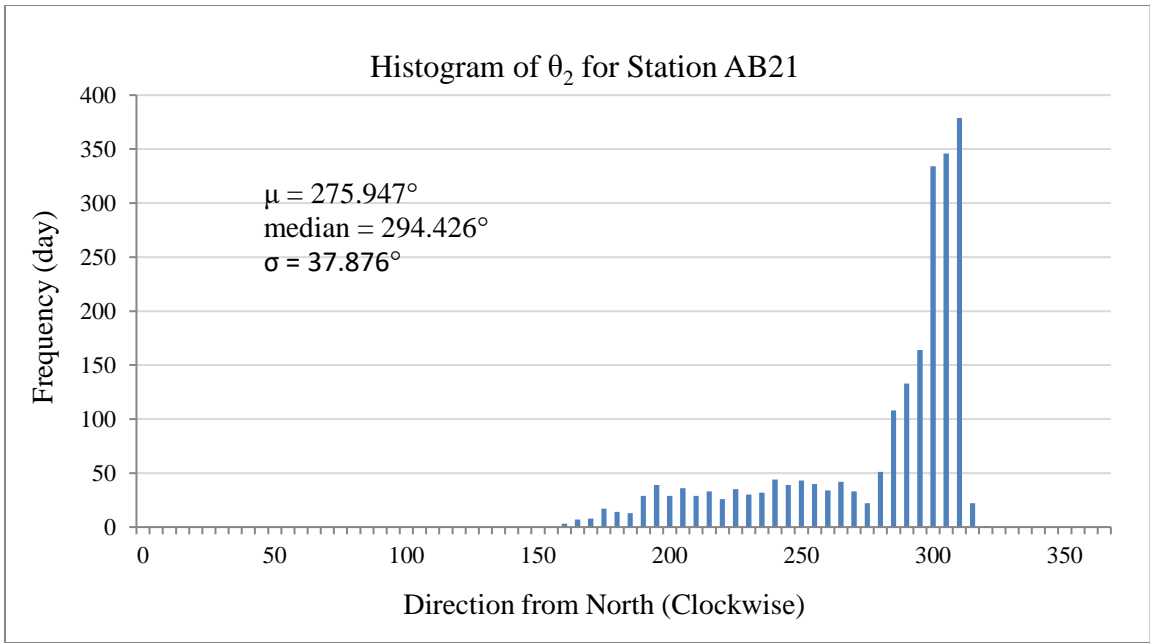


Figure 2.2.16. Frequency versus Direction of Total Displacement Vector for Station AB21

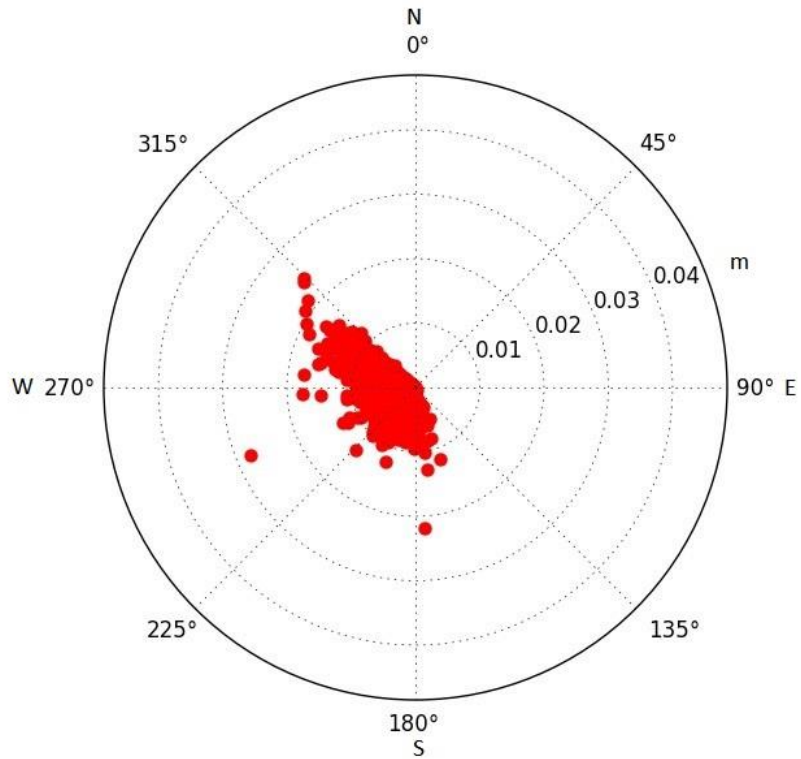


Figure 2.2.17. Polar Graph of Daily Displacement Vector for Station AB21

Figure 2.2.17 shows the daily displacement vector for Station AB21 in a polar coordinate system. The main movement direction is not very clear. But it is obvious that there is not any motion from 315° to 135° clockwise.

Figure 2.2.18 shows the polar graph of total displacement vectors day by day. The main direction of Station AB21 is towards the west-northwest, while Station AB01 is moving toward west-southwest. Since they are located on the same block and diagonal corners; this difference in movement directions supports the block rotation clearly.

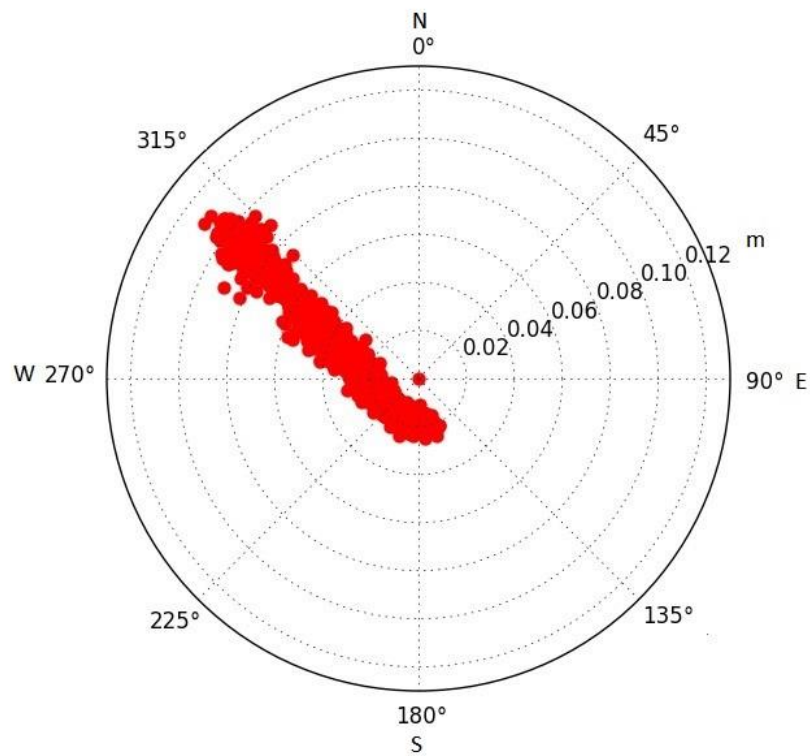


Figure 2.2.18. Polar Graph of Total Displacement Vector for Station AB21

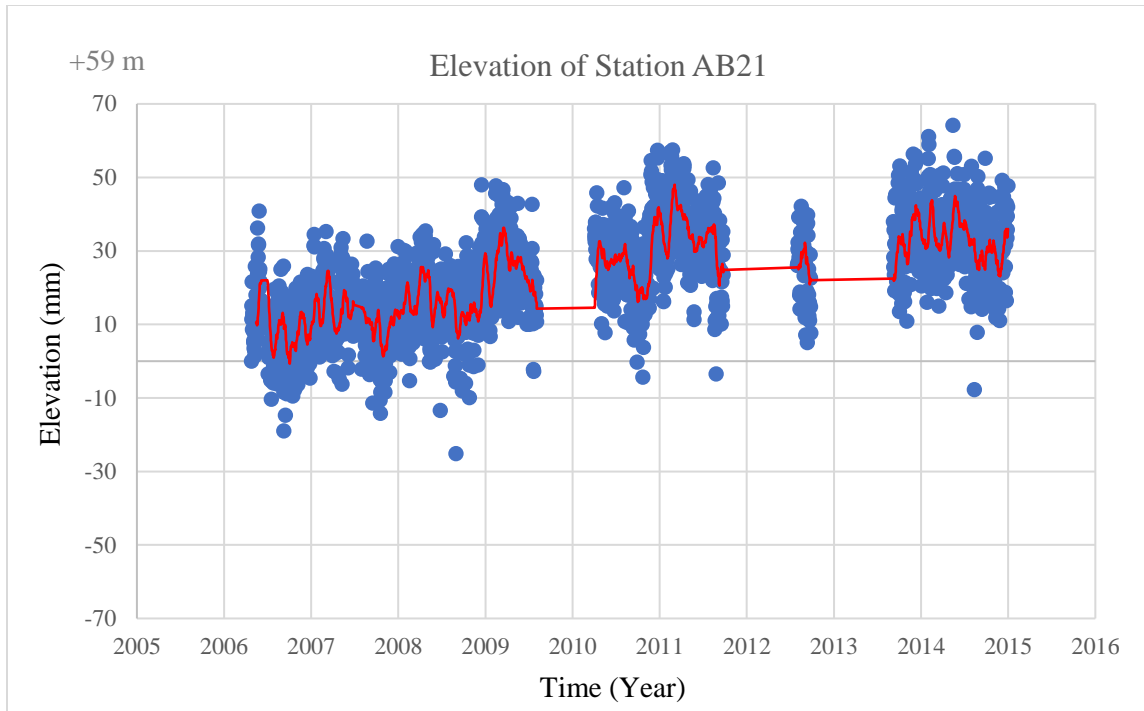


Figure 2.2.19. Elevation Graph for Station AB21. Blue dots are measurements, red line is the average trend line.

Figure 2.2.19 shows daily elevation change for Station AB21.

After all these calculations and evaluations, the velocity of Station AB21 is 15.47 mm/yr and its movement direction is towards west-northwest, 306.51°.

2.2.3 GPS Station AC66

GPS Station AC66 is located on Amchitka Island (51.378, 179.301), south limit of Bowers Ridge. Its measurement data cover from September 2005 to February 2015. It is located on Block C. Its reference frame is NA12.

Figure 2.2.20 shows the position of Station AC66 according to the north. Integer north amount (from the equator) is 5694153 meters. This plot shows that the position of Station AC66 moves firstly towards the south and then north.

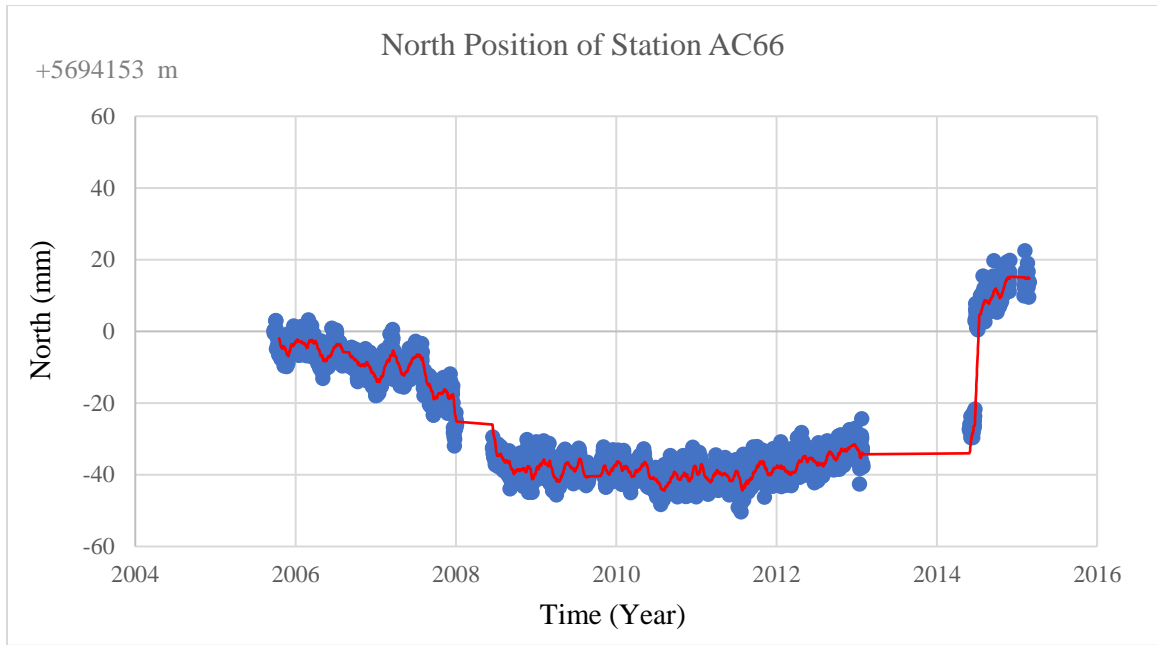


Figure 2.2.20. Position of Station AC66 at North Direction. Blue dots are measurements, red line is the average trend line.

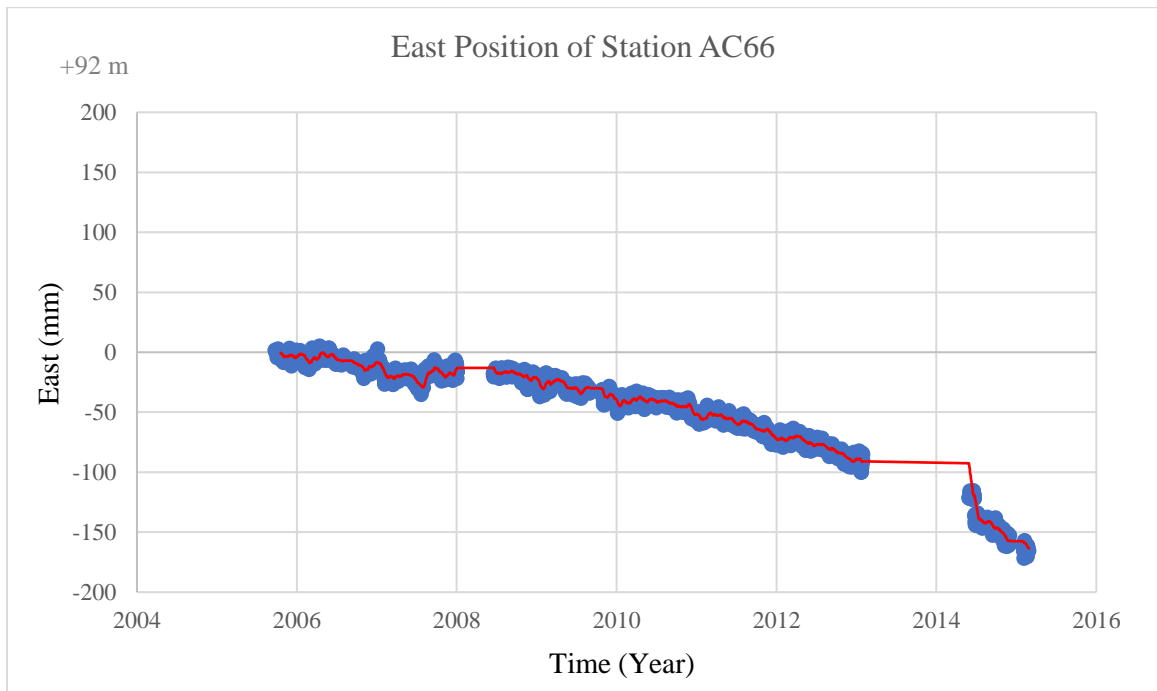


Figure 2.2.21. Position of Station AC66 at East Direction. Blue dots are measurements, red line is the average trend line.

Figure 2.2.21 shows the position of Station AC66 according to east direction. Station AC66 moves toward the west. Longitude (degrees) of its reference meridian is 179.3 and integer portion of easting from reference meridian is 92 meters.

Figure 2.2.22 shows frequency of daily displacement amount of Station AC66. This histogram is very similar with other two stations, AB01 and AB21.

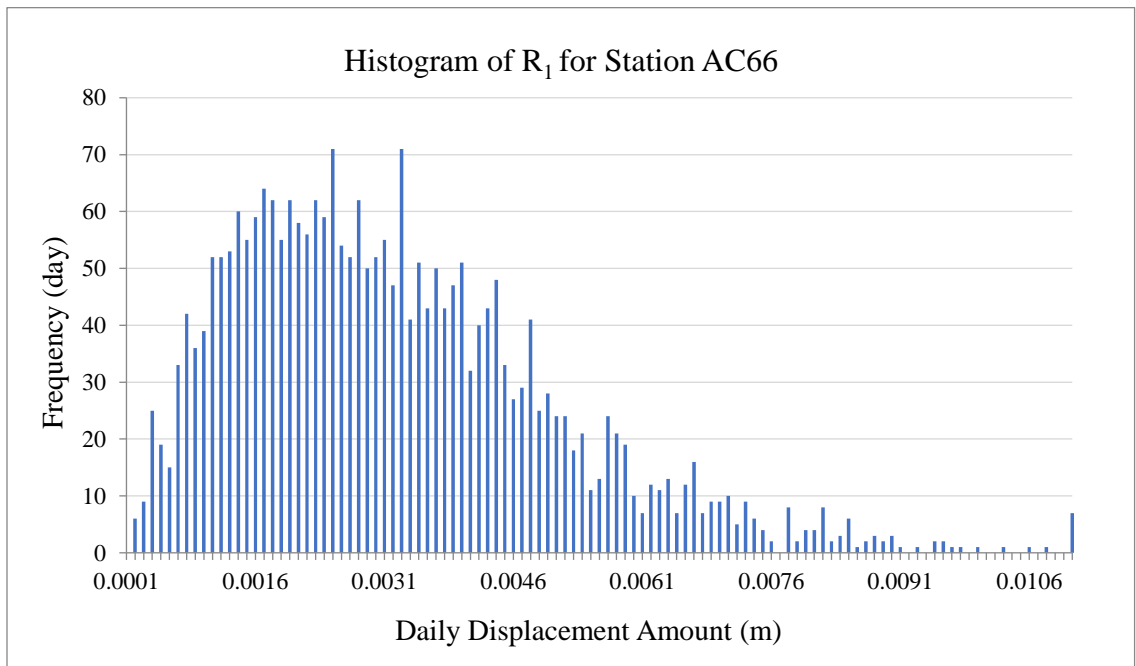


Figure 2.2.22. Frequency versus Amount of Daily Displacement Vector for Station AC66

Figure 2.2.23 shows the direction of daily displacement vectors for Station AC66. It has very similar results to Station AB21 in Figure 2.2.14.

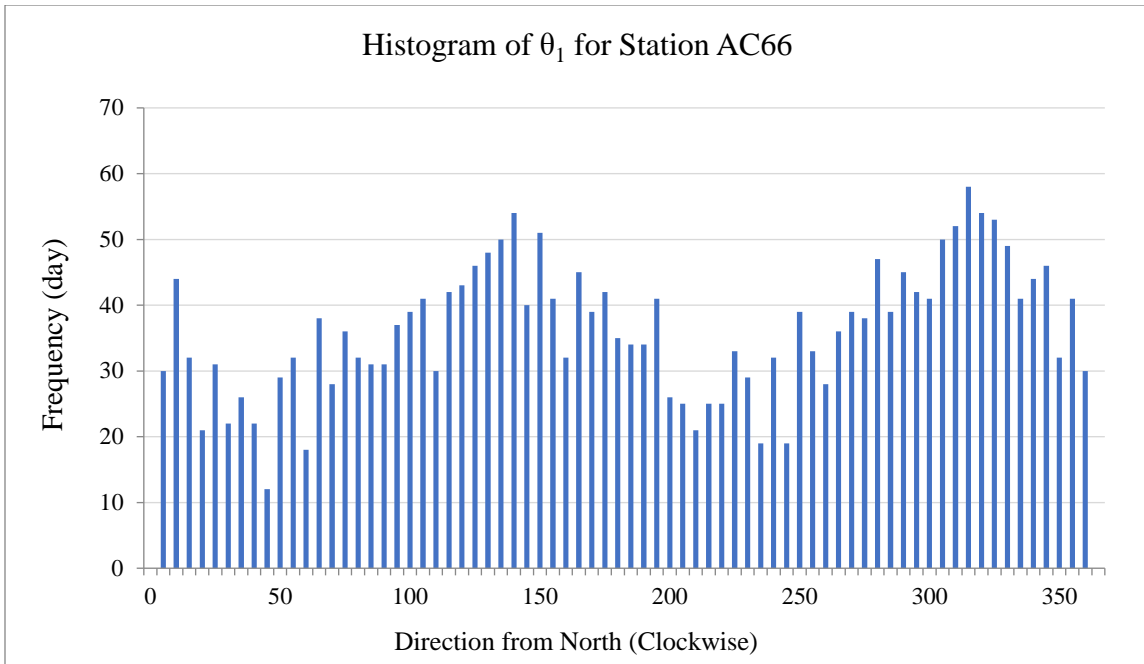


Figure 2.2.23. Frequency versus Direction of Daily Displacement Vector for Station AC66

Figure 2.2.24 shows the total displacement amount until each measurement moment of a day since the beginning of the dataset (September 2005). It has a similar appearance with the same graph for Station AB21.

R_2 for Station AC66 is 0.16627 m which is represented by 2611 measurement days. The velocity of the station is 23.25 mm/year.

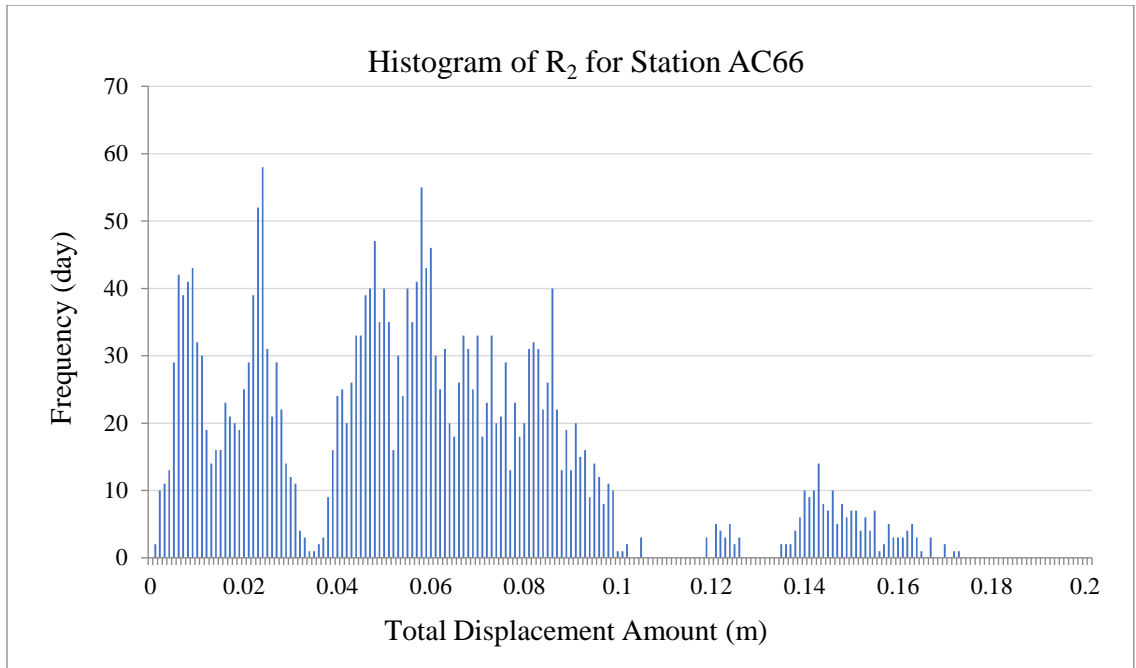


Figure 2.2.24. Frequency versus Amount of Total Displacement Vector for Station AC66

Figure 2.2.25 shows the histogram of the movement direction of Station AC66. The arithmetic average of data is 232.028° and the median value is 232.251° . These two direction amounts are almost the same. Standard deviation is 21.579° which shows the diversity in the movement direction is less than Station AB01 and AB21. This station is steady about the movement direction. Moreover, with this standard deviation, most of the movement directions stay within the vicinity of 21.6° of the major direction.

The last calculated θ_2 represents the movement direction of the station. The movement direction of Station AC66 is 274.74° .

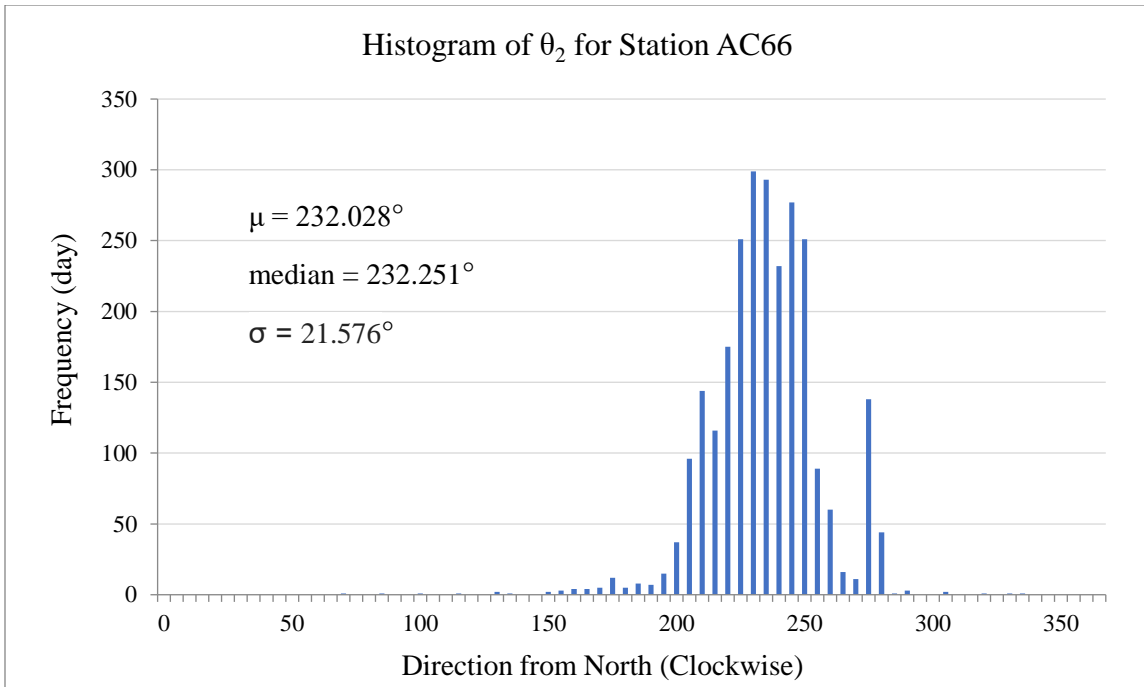


Figure 2.2.25. Frequency versus Direction of Total Displacement Vector for Station AC66

Figure 2.2.26 shows the daily the displacement vector in a polar coordinate system. Main movement direction is not clear, but it can be interpreted that movement directions and amounts are so close to each other.

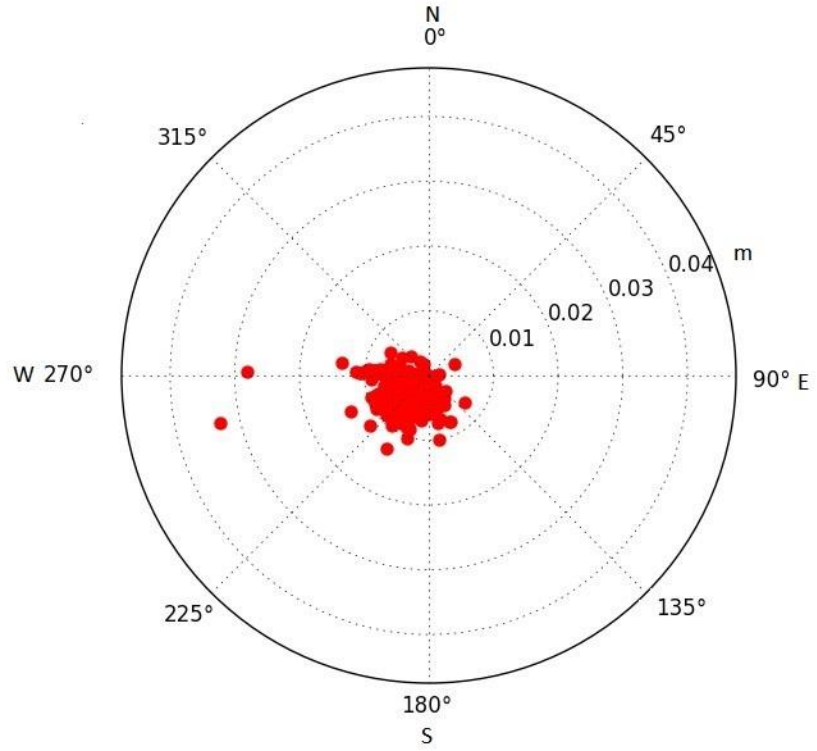


Figure 2.2.26. Polar Graph of Daily Displacement Vector for Station AC66

Figure 2.2.27 shows the total displacement vectors in a polar coordinate system. Main movement direction is firstly towards the southwest, then it turns towards the west-northwest.

This change in the movement direction can be caused by volcanic activity and/or possible earthquake event where the epicenter is within 10° of the Station AC66. It shows the local change in direction, not the rotation of the block it is located on.

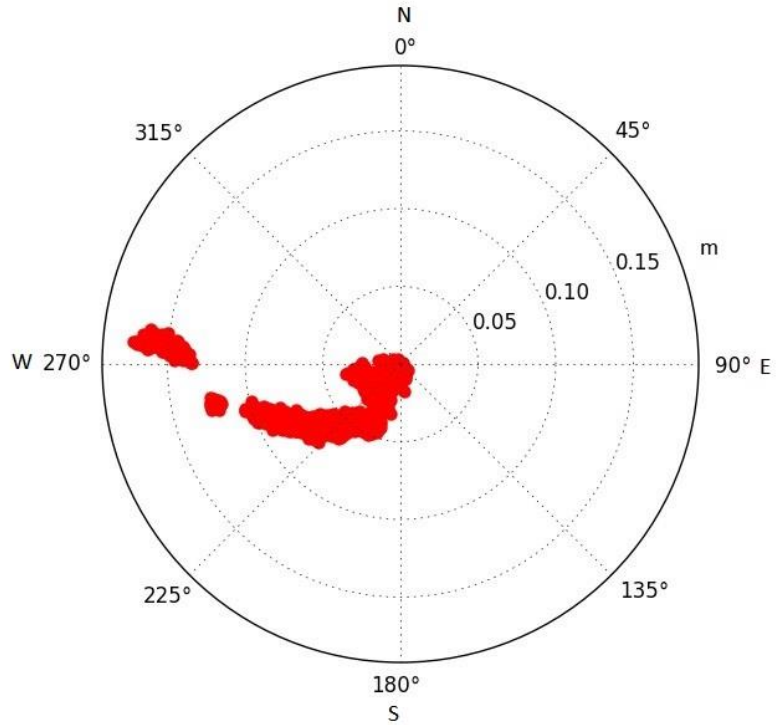


Figure 2.2.27. Polar Graph of Total Displacement Vector for Station AC66

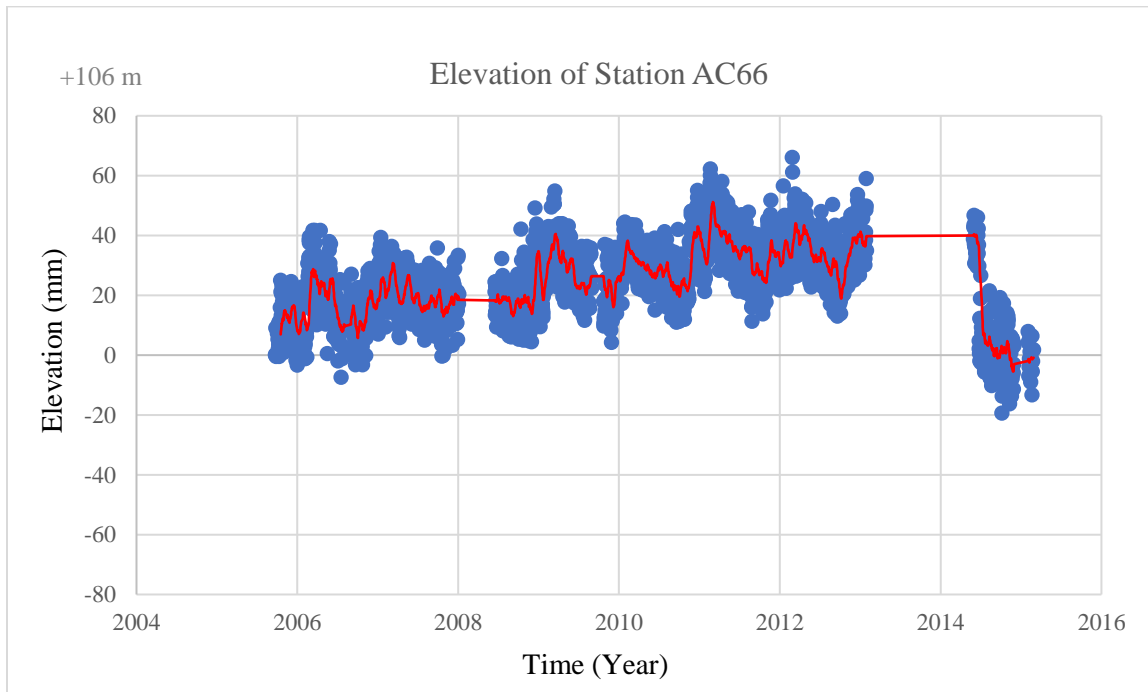


Figure 2.2.28. Elevation Graph for Station AC66. Blue dots are measurements, red line is the average trend line.

Figure 2.2.28 shows daily elevation change for Station AC66. As can be seen from the graph, there is an abrupt elevation decrease when the station changed its movement from southwest to north-northwest.

The velocity of Station AC66 is 23.25 mm/yr and its movement direction is towards the west, 274.74° .

2.2.4 GPS Station AC60

GPS Station AC60 is located on Shemya Island (52.715, 174.076), on the west side of the island arc. The recorded data cover from October 2008 to April 2015. It is located on Block A. Its reference frame is NA12.

Figure 2.2.29 shows the position of Station AC66 according to north direction. Integer north amount (from the equator) is 5842862 meters. Figure 2.2.29 shows the Station AC60 moves towards the north.

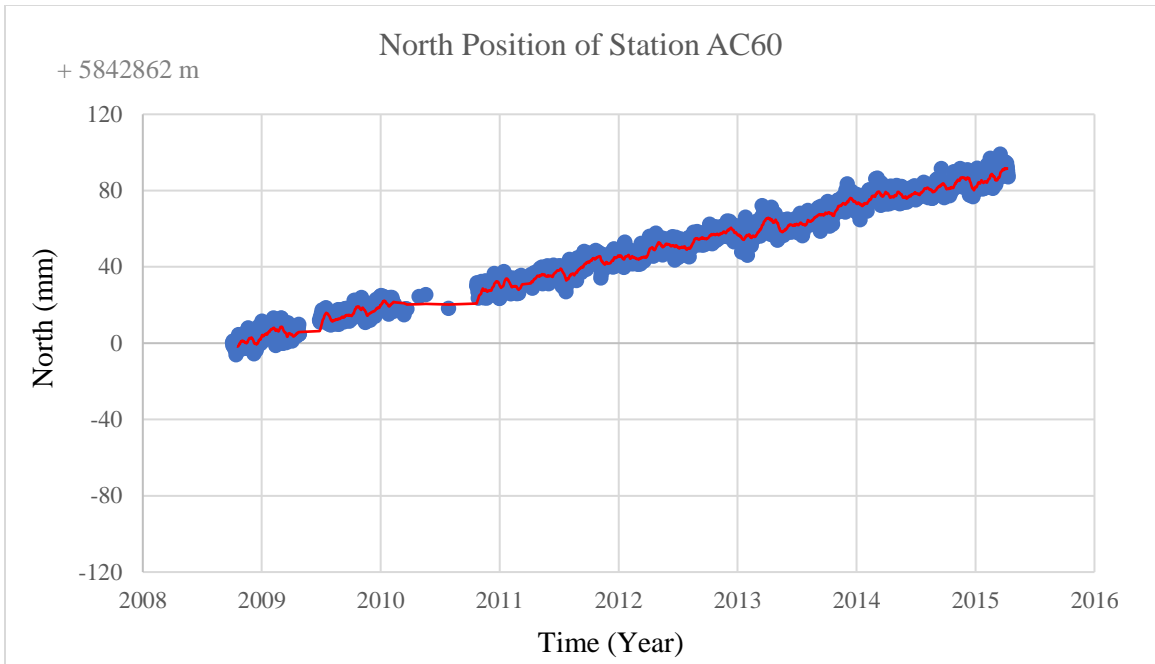


Figure 2.2.29. Position of Station AC60 at North Direction. Blue dots are measurements, red line is the average trend line.

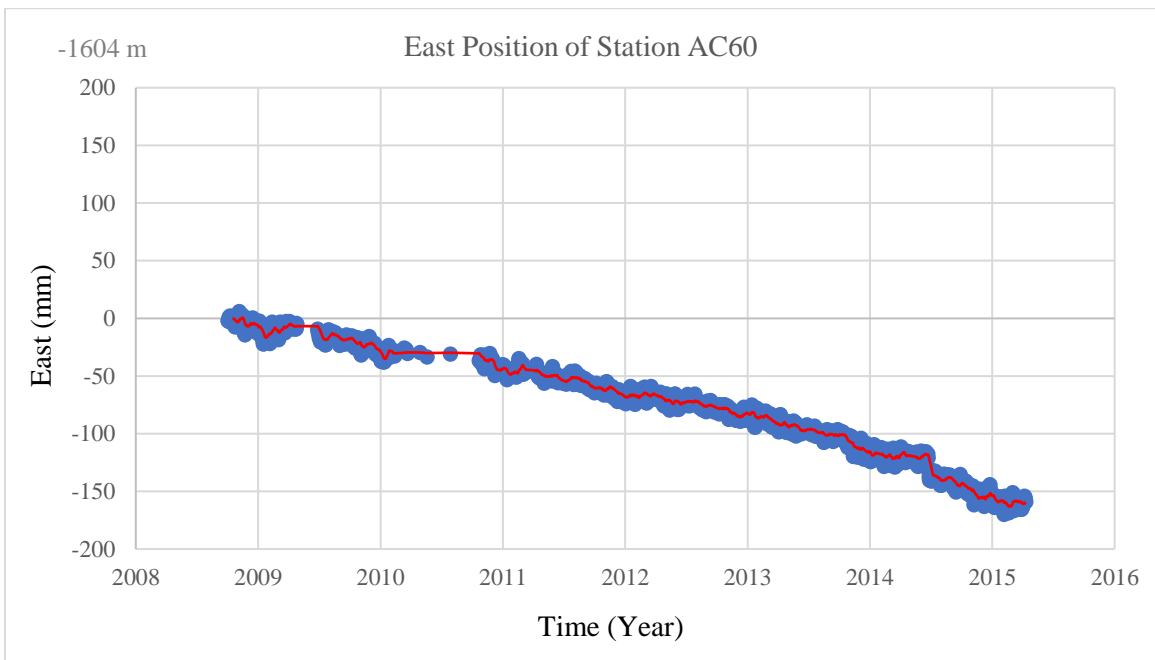


Figure 2.2.30. Position of Station AC60 at East Direction. Blue dots are measurements, red line is the average trend line.

Figure 2.2.30 shows the position of Station AC60 according to east direction. This station moves towards west. Longitude (degrees) of its reference meridian is 174.1 and integer portion of easting from reference meridian is -1604 meters.

Figure 2.2.31 shows the frequency of daily displacement of Station AC60. Its daily movement is similar to stations, AB01, AB21, AC66.

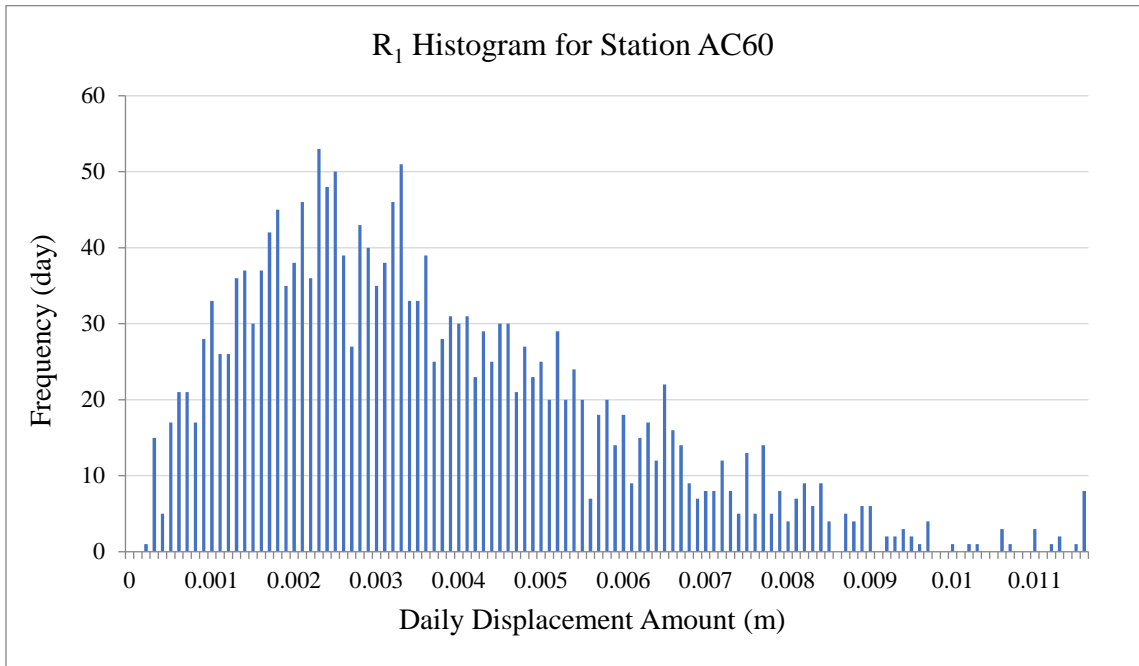


Figure 2.2.31. Frequency versus Amount of Daily Displacement Vector for Station AC60

Figure 2.2.32 shows the directions of daily displacement vectors of Station AC60 that could take any value in the range. It moves almost in all directions.

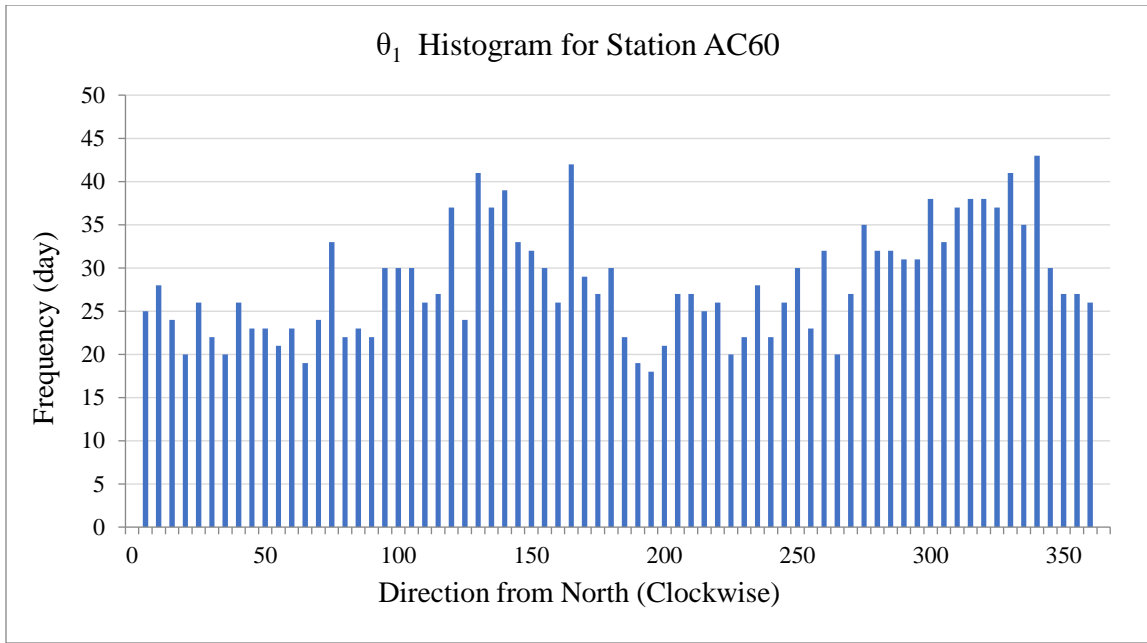


Figure 2.2.32. Frequency versus Direction of Daily Displacement Vector for Station AC60

Figure 2.2.33 shows the total displacement amount until each measurement moment of a day since the beginning of the dataset (October 2008).

R_2 for Station AC60 is 0.18152 m which is represented by 2041 measurement days. The velocity of the station is 32.48 mm/year.

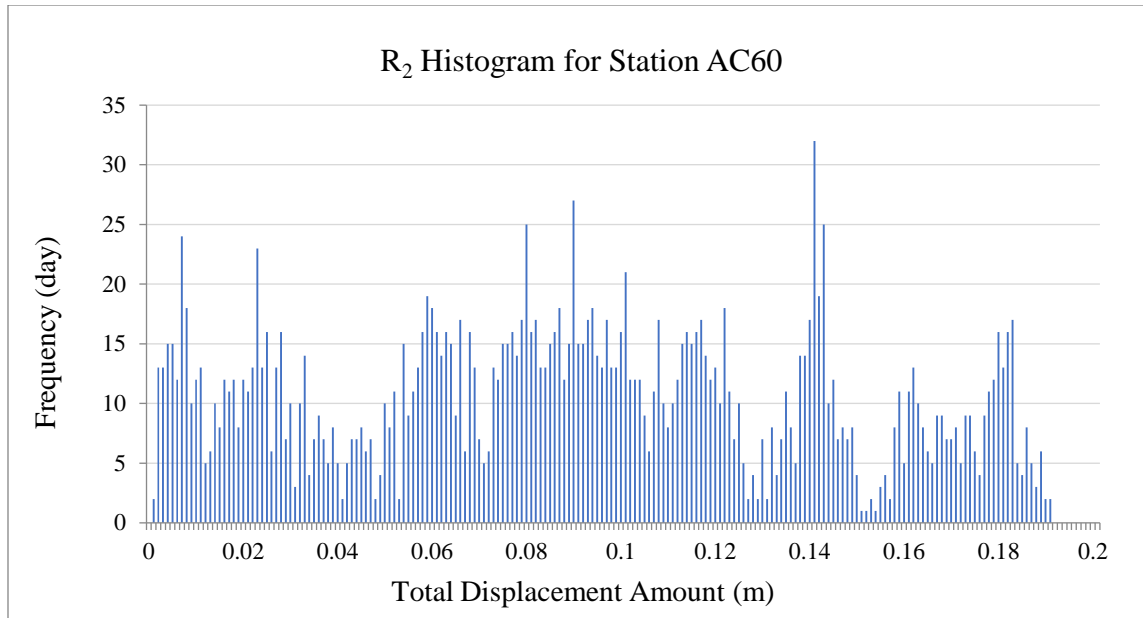


Figure 2.2.33. Frequency versus Amount of Total Displacement Vector for Station AC60

Figure 2.2.34 shows the Station AC60 has an overall preference of direction between 295° and 315° approximately. Its mean is 301.202° and median value is 303.806° . These two directions are very close to each other and all values seem accurate according to each other. Standard deviation is 19.93° , which indicates movement of station stays mostly within the vicinity of 19.93° of the major direction. This value is smaller than the other three stations indicating that the movement of Station AC60 almost follows a straight line (does not deviate from the main path as in AB01, AB21, and AC66).

Furthermore, the last calculated θ_2 represents the movement direction of the station. The movement direction of Station AC60 is 298.72° .

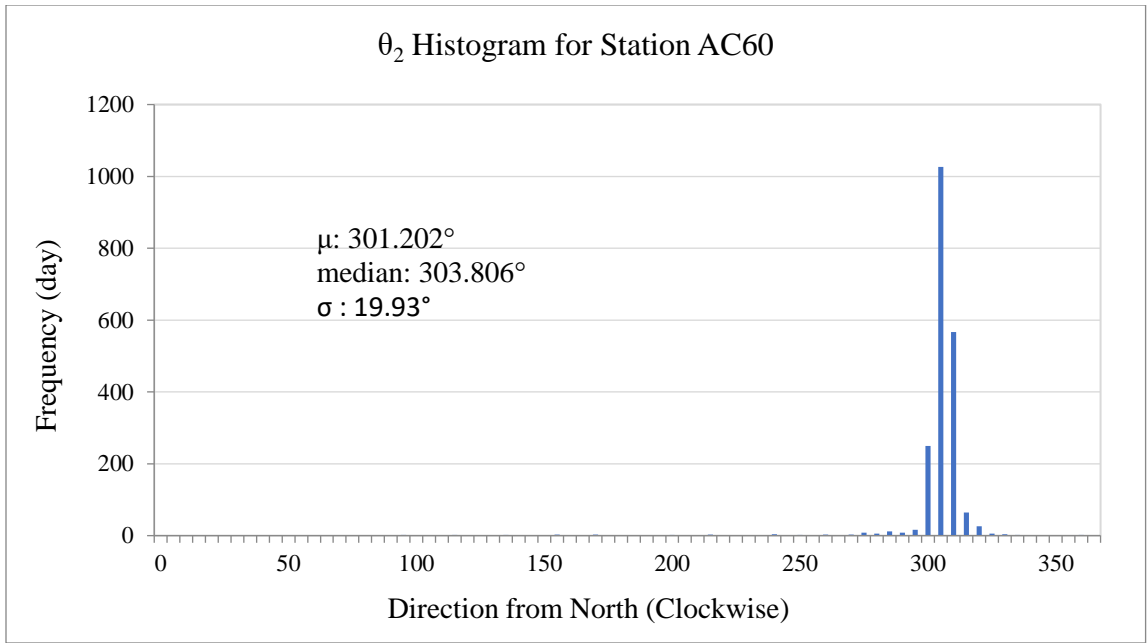


Figure 2.2.34. Frequency versus Direction of Total Displacement Vector for Station AC60

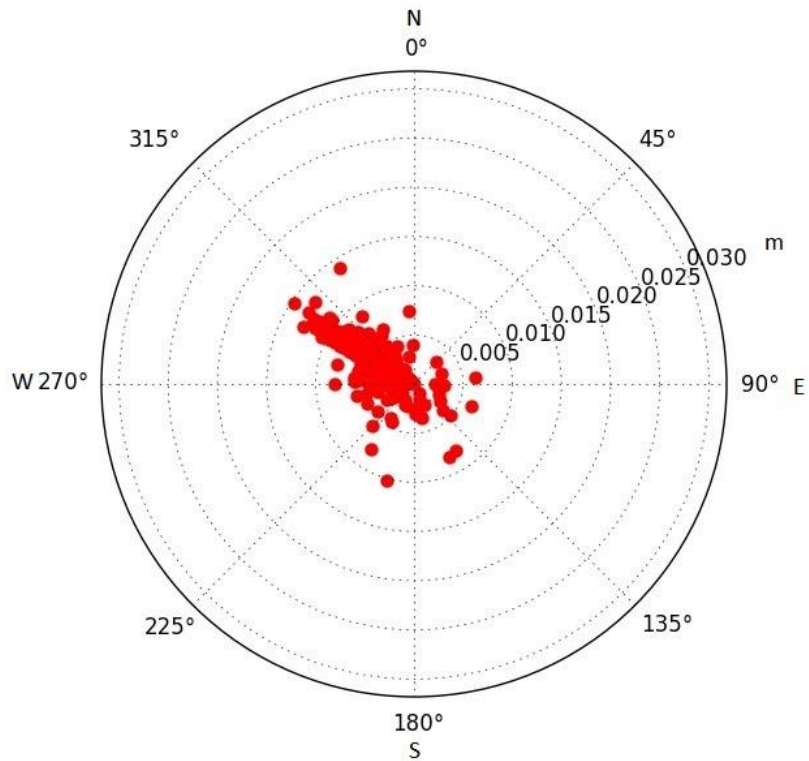


Figure 2.2.35. Polar Graph of Daily Displacement Vector for Station AC60

Figure 2.2.35 shows the polar graph of daily displacement vector in polar coordinate system. Major movement direction is not clear depends on daily data. On the other hand, the main movement direction is very clear in Figure 2.2.36 and it is west-northwest. This plot shows a linear movement.

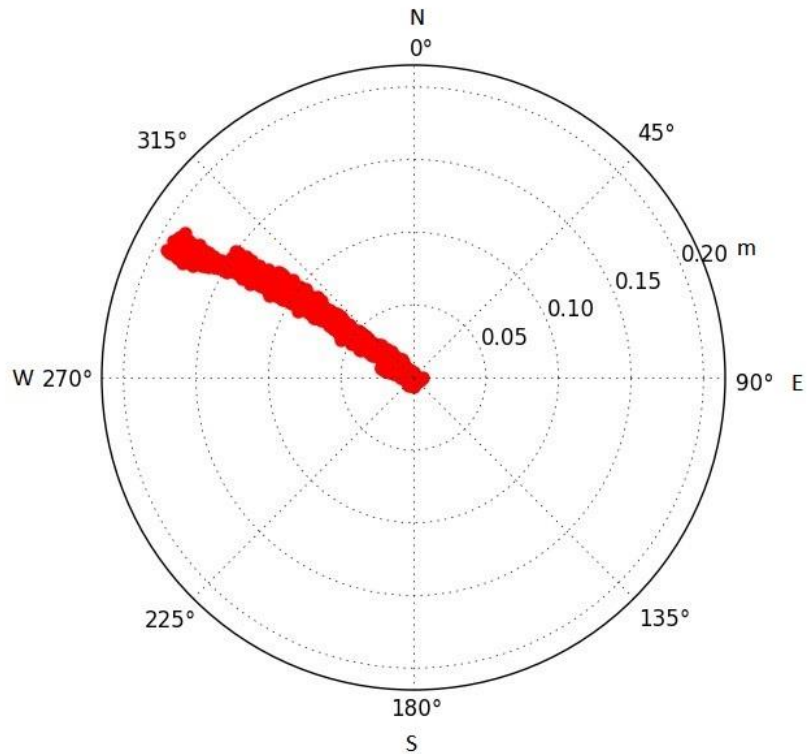


Figure 2.2.36. Polar Graph of Total Displacement Vector for Station AC60

Figure 2.2.37 shows the daily elevation change for Station AC60. There is no significant elevation change for measurement time for Station AC60.

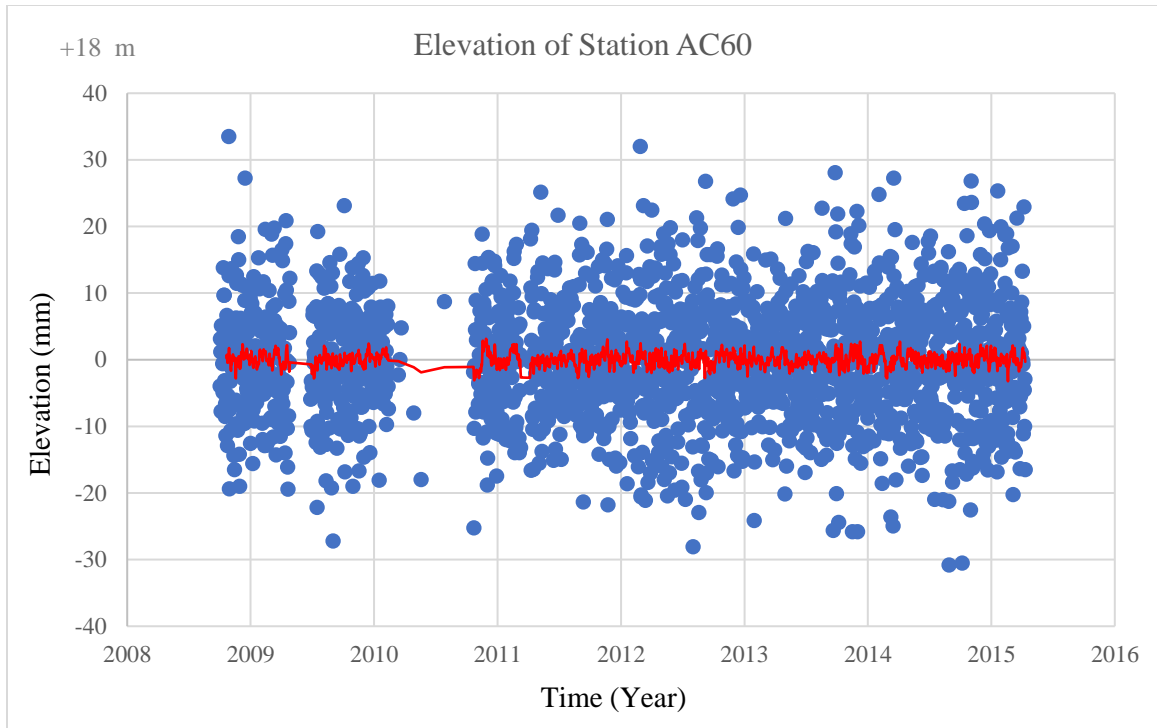


Figure 2.2.37. Elevation Graph for Station AC60. Blue dots are measurements, red line is the average trend line.

The velocity of Station AC60 is 32.48 mm/yr and the movement direction is west-northwest, 298.72°.

2.2.5 GPS Station PETS

GPS Station PETS is located at Russian part, Kamchatka Peninsula (53.023, 158.650). Its measurements cover dates from June 2004 to April 2011. Its reference frame is IGS08.

Figure 2.2.38 shows the position of Station PETS according to north direction. Integer north amount (from the equator) is 5877213 meters. This plot shows that Station PETS moves through south direction year by year.

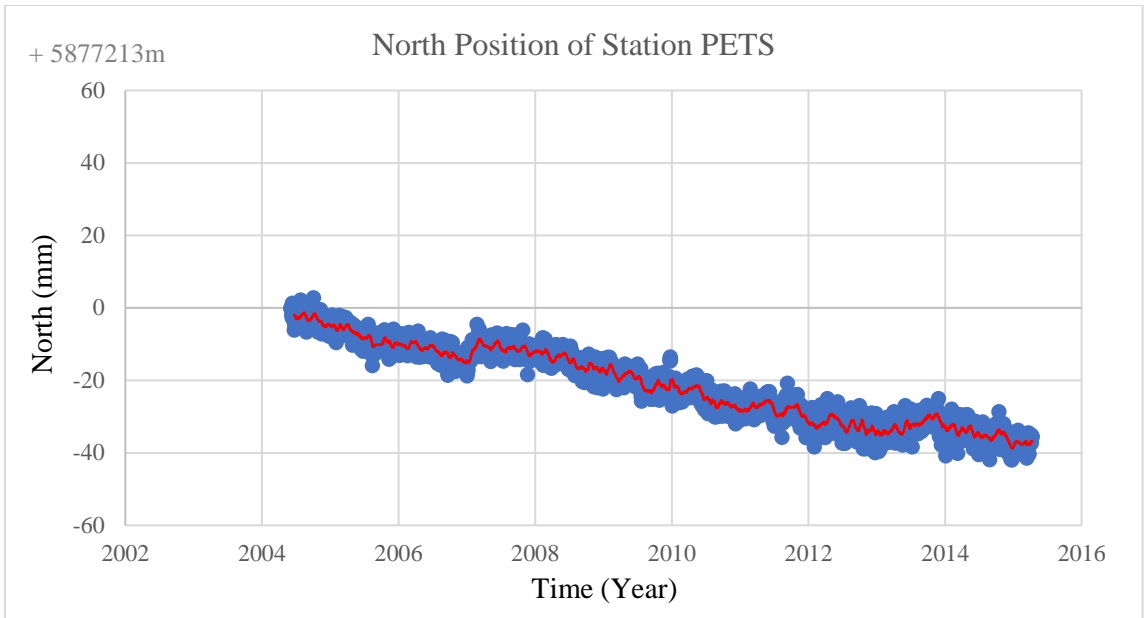


Figure 2.2.38. Position of Station PETS at North Direction. Blue dots are measurements, red line is the average trend line.

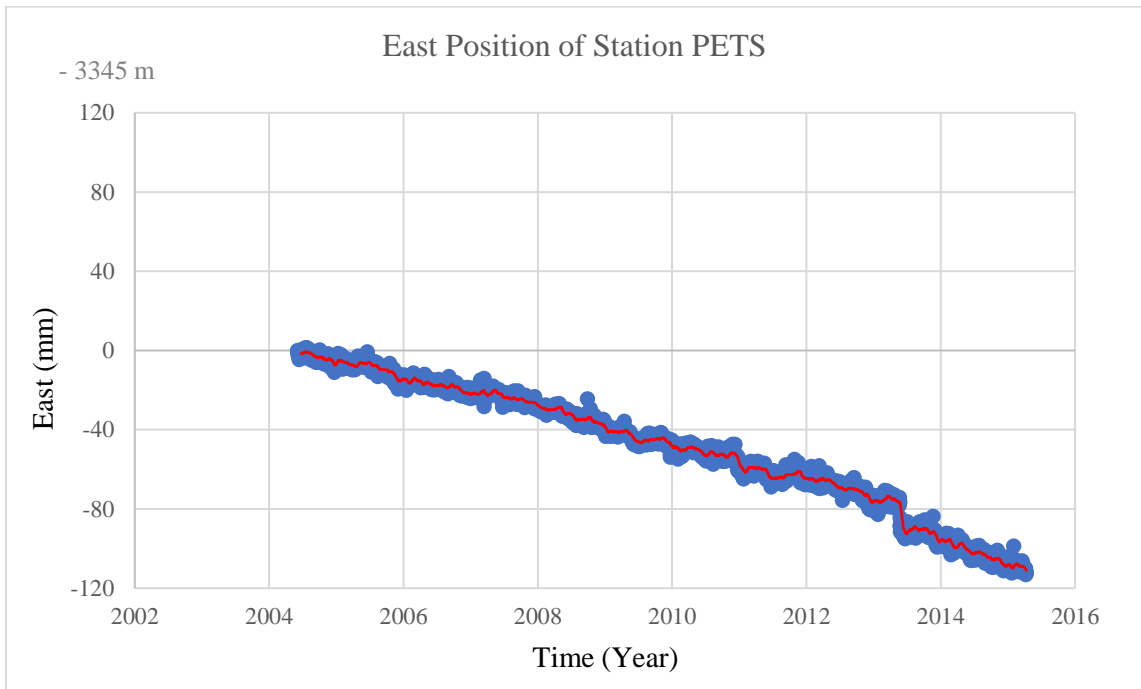


Figure 2.2.39. Position of Station PETS at East Direction. Blue dots are measurements, red line is the average trend line.

Figure 2.2.39 shows the position of Station PETS according to east direction. Movement of this station is directly toward the west. Its longitude (degrees) of reference meridian is 158.7 and integer easting portion from reference meridian is -3345 meters.

Figure 2.2.40 shows the frequency of daily displacement amount of Station PETS. Its daily movement amounts are similar with other stations.

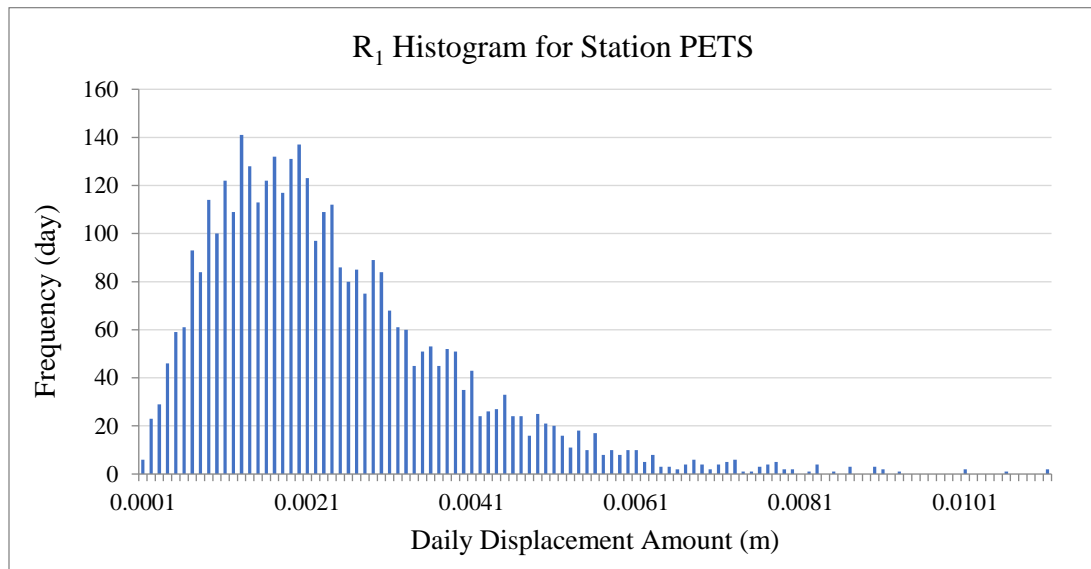


Figure 2.2.40. Frequency versus Amount of Daily Displacement Vector for Station PETS

Figure 2.2.41 shows the directions of daily displacement vectors of Station PETS which could take any value in the range. It moves almost in all directions.

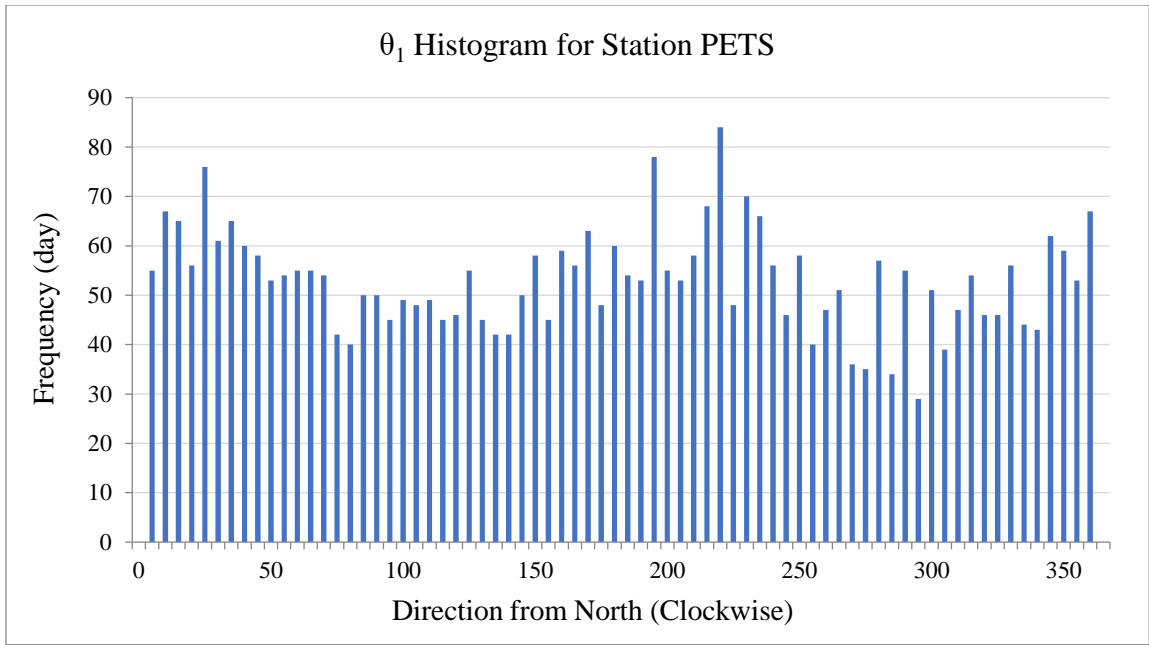


Figure 2.2.41. Frequency versus Direction of Daily Displacement Vector for Station PETS

Figure 2.2.42 shows the total displacement amount until each measurement moment of a day since the beginning of the dataset (June 2004).

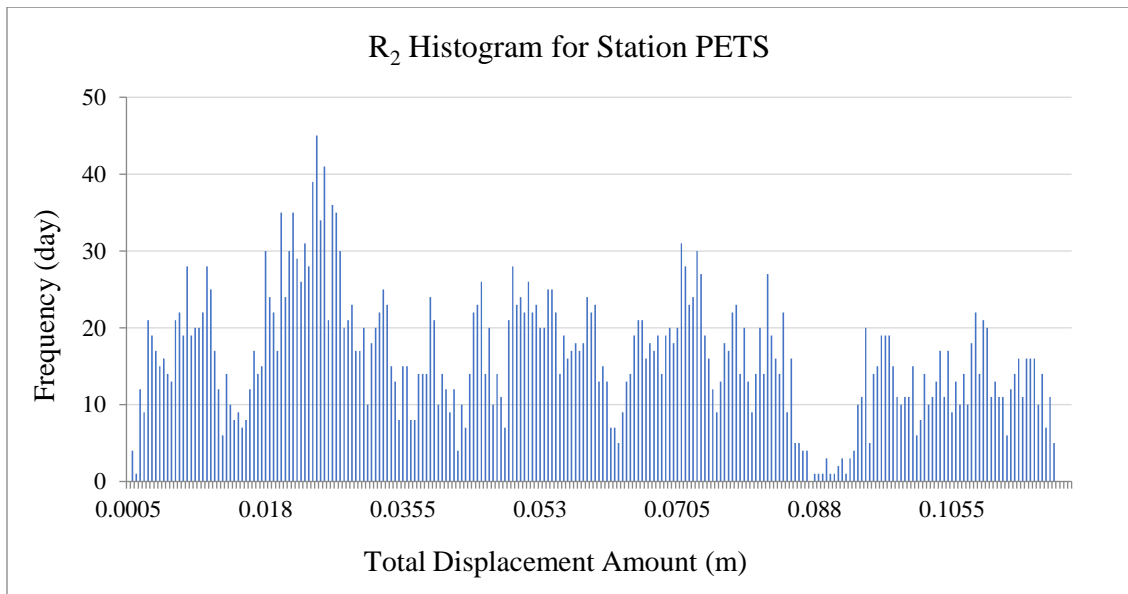


Figure 2.2.42. Frequency versus Amount of Total Displacement Vector for Station PETS

Figure 2.2.43 shows that Station PETS has an overall preference for direction between 245° and 255° approximately. Its mean is 242.853° and the median value is 245.029° . These two directions values are very close to each other. Standard deviation is 10.34° which means movement of station stays mostly within the vicinity of 10.34° of the major direction. This value is smaller than the all other stations. That shows the movement of Station PETS follows a straight line. But at this point, making a comparison is not convenient since the stress distribution and so movement path is different than other four stations which are in the Aleutian Arc convergence system.

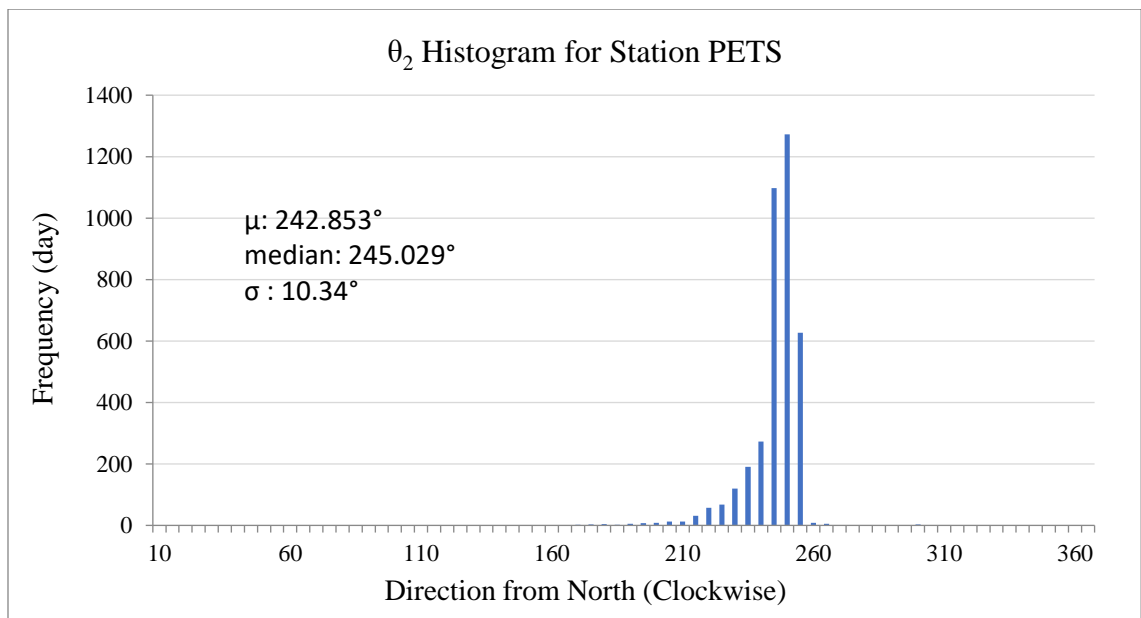


Figure 2.2.43. Frequency versus Direction of Total Displacement Vector for Station PETS

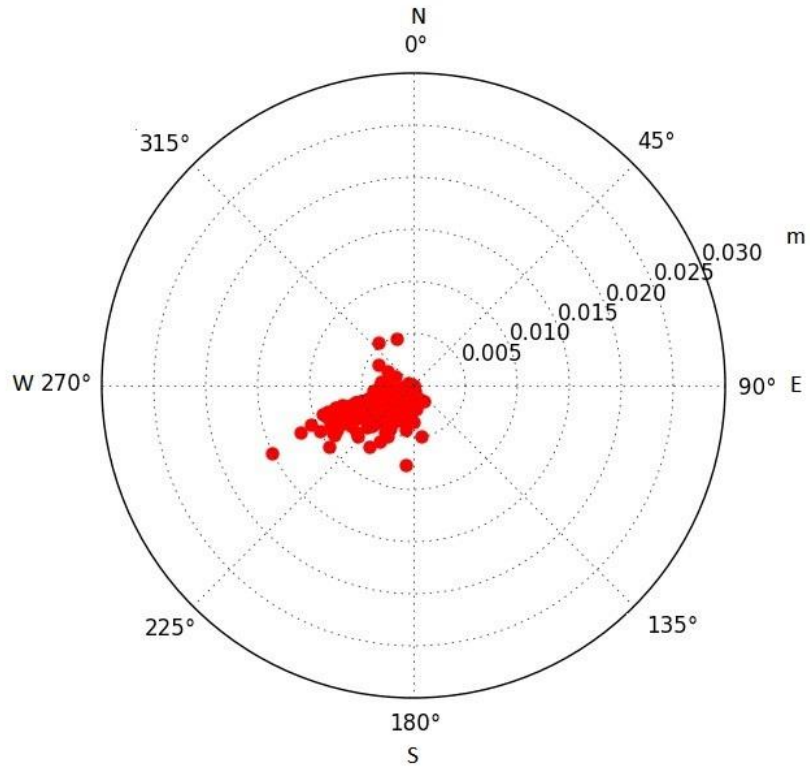


Figure 2.2.44. Polar Graph of Daily Displacement Vector for Station PETS

Figure 2.2.44 shows the polar graph of daily displacement vector in the polar coordinate system of Station PETS. The major movement direction is west-southwest but it is constant over the time measured. On the other hand, the movement direction is very clear at Figure 2.2.45 as west-southwest. It shows exactly linear movement.

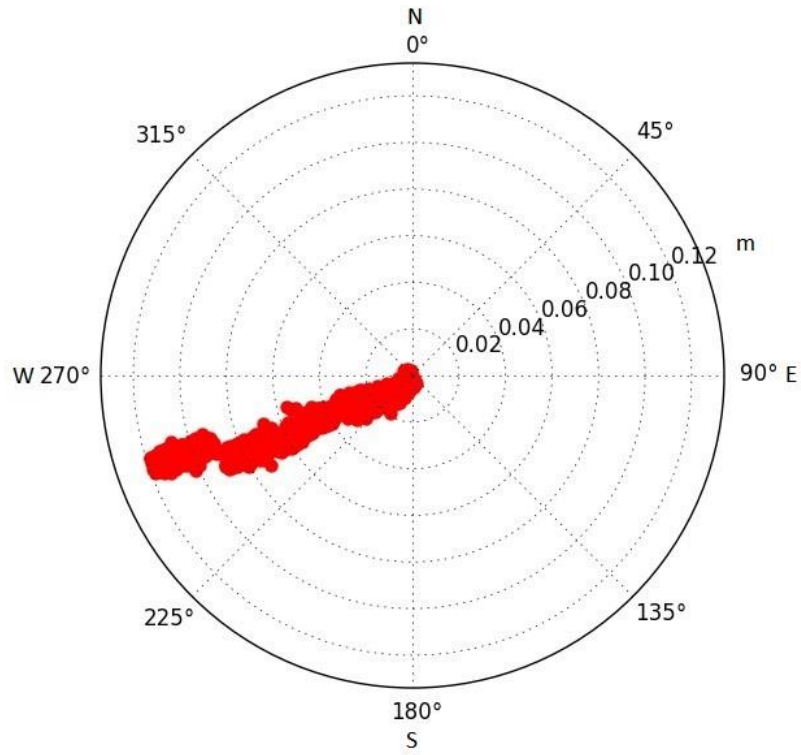


Figure 2.2.45. Polar Graph of Total Displacement Vector for Station PETS

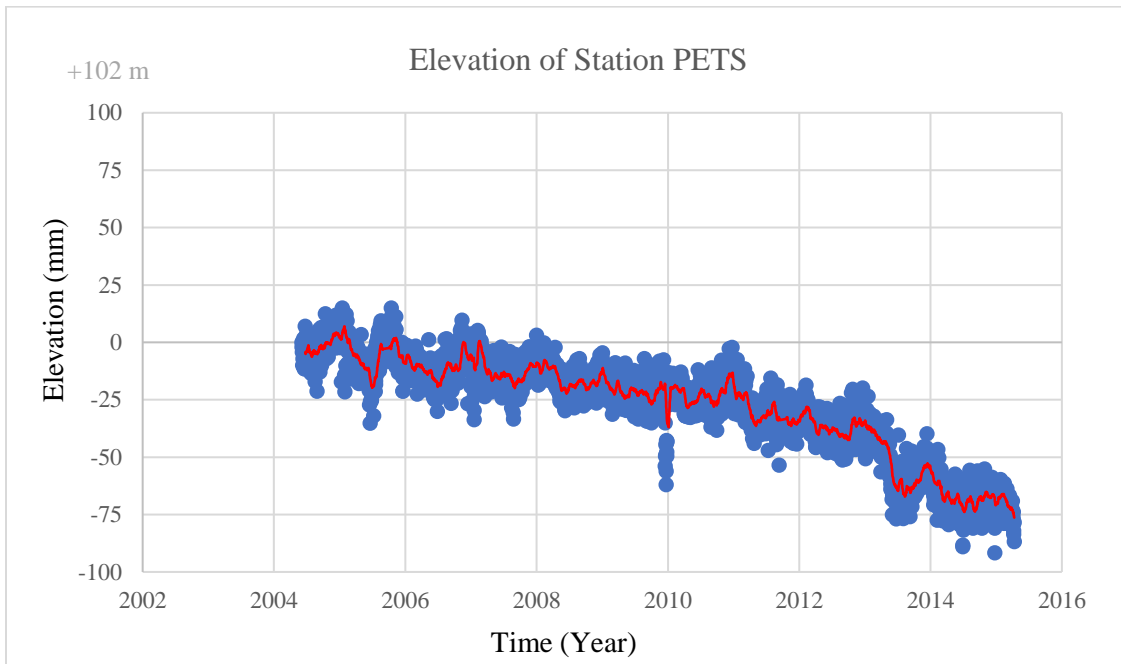


Figure 2.2.46. Elevation Graph for Station PETS. Blue dots are measurements, red line is the average trend line.

Figure 2.2.46 shows daily elevation change for Station PETS.

As a conclusion, the velocity of Station PETS is 27.82 mm/yr and its movement direction is towards west-northwest.

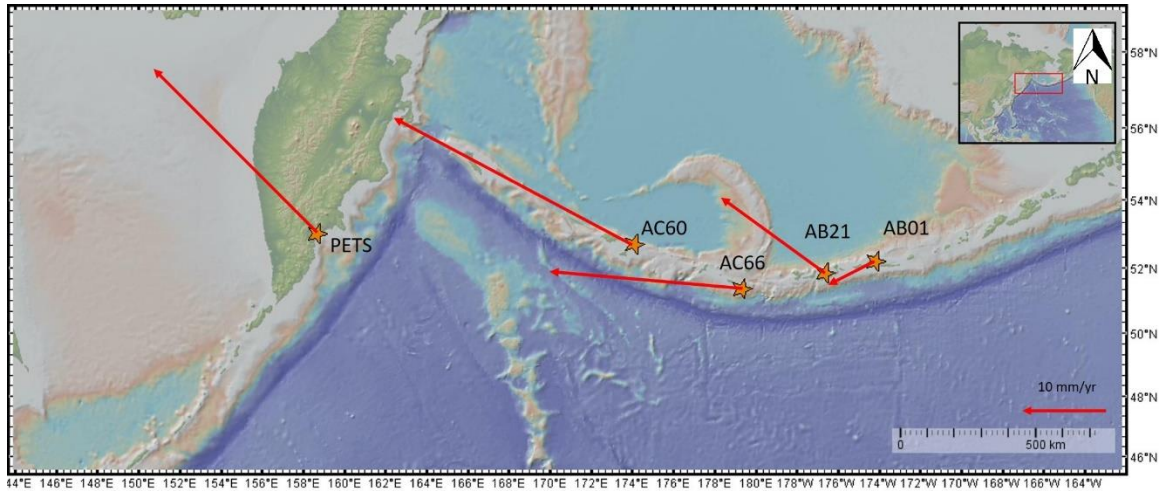


Figure 2.2.47. Velocity and Directions of GPS Stations

Figure 2.2.47 shows all velocity of GPS stations with respect to NA12 and IGS08 (for Station PETS) reference frames along the arc. Velocity amounts are increasing from east to west with changing movement directions.

2.3 GPS STATIONS HORIZONTAL VELOCITY CALCULATIONS ACCORDING TO REFERENCE STATIONS

There are 5 discrete blocks which interact with each other while undergoing clockwise rotation. There are 4 GPS Stations located on different islands. Two of them are on the same block and the others are on different blocks.

Relative horizontal velocities of each GPS stations are calculated to understand block motion. To calculate these relative horizontal velocities, several reference stations are

chosen. Firstly, all GPS stations are represented as a fixed reference station. Then, common measurement days between chosen reference station and the GPS station whose horizontal velocity is to be calculated are determined. After that, horizontal relative velocities are calculated according to that chosen reference station.

Moreover, after each GPS station had been chosen as fixed reference station and their relative horizontal velocities calculated; PETS and AB02 were chosen as the fixed reference station, too. These two GPS stations are not in the Aleutian blocking system. Station PETS is located on Kamchatka Peninsula and its subduction system is different than Aleutian. Station AB02 is located east of Station AB01, on Nikolski Island. It is not located on any rotating block.

2.3.1 AB01 FIXED

Station AB01 is located on Block E. It is the first chosen reference GPS station.

The common measurement period of reference Station AB01 and Station AB21 is between May 2007 and December 2014. They have 1445 measurement days in common.

Station AB21 is on the west side of reference Station AB01. Figure 2.3.1 shows, it is moving toward the west side with some undulations according to Station AB01. Depending on the common measurement days, horizontal velocity of Station AB21 according to Station AB01 is moving westward at 3.08 mm/year.

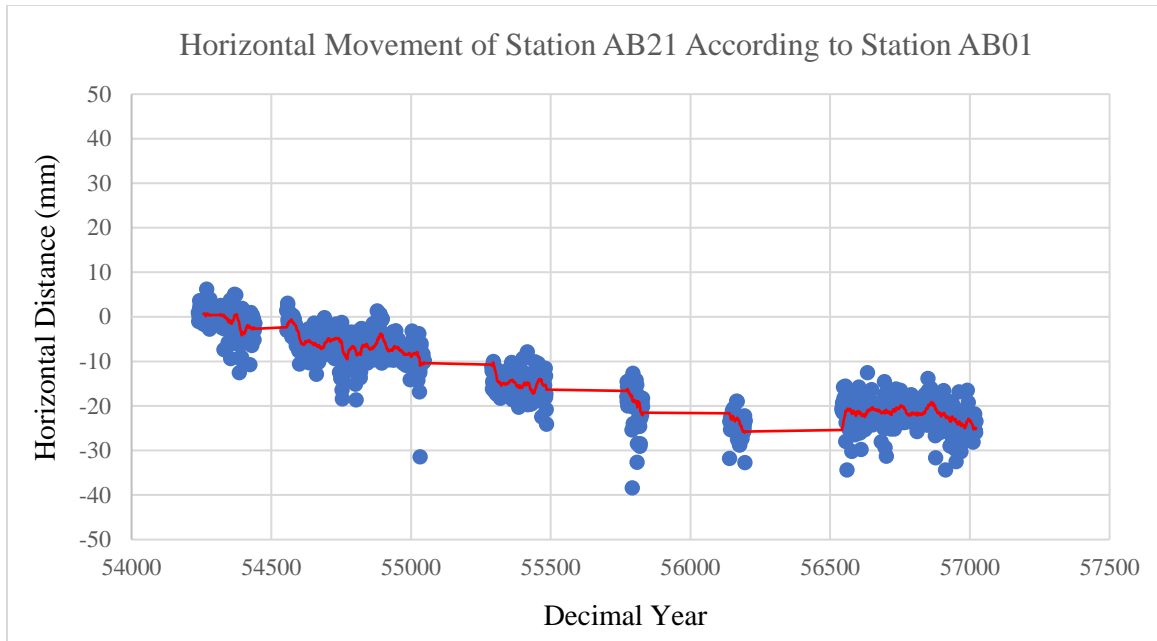


Figure 2.3.1. Horizontal Movement of Station AB21 According to Station AB01. Blue dots are measurements, red line is the average trend line.

Station AC66 is on the west side of the reference Station AB01. Their common measurement days are between May 2007 and February 2015 with 1731 days.

This station first moves eastward then moves westward (Figure 2.3.2). It has fewer undulations than Station AB21. This eastward movement shows that the reference station AB01 is faster than station AC66 during those shared measurement days. Depending on the common measurement days, horizontal velocity of Station AC66 according to Station AB01 is 12.56 mm/year towards west.

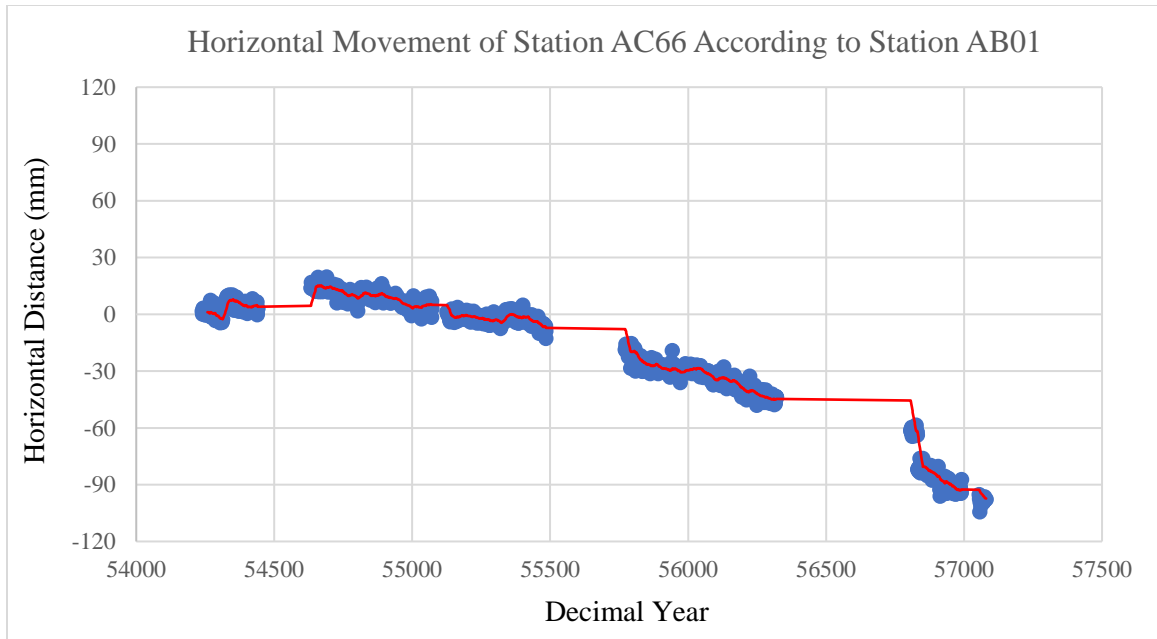


Figure 2.3.2. Horizontal Movement of Station AC66 According to Station AB01. Blue dots are measurements, red line is the average trend line.

Station AC60 is on the west part of the Aleutian Arc. The common measurement period of the reference Station AB01 and Station AC60 is between October 2008 and April 2015. They have 1788 measurement days in common.

Station AC60 is moving directly toward the west (Figure2.3.3) according to Station AB01. It has some undulations but not like other two stations.

Depending on the common measurement days, horizontal velocity of Station AC60 according to Station AB01 is 20.17 mm/year towards the west.

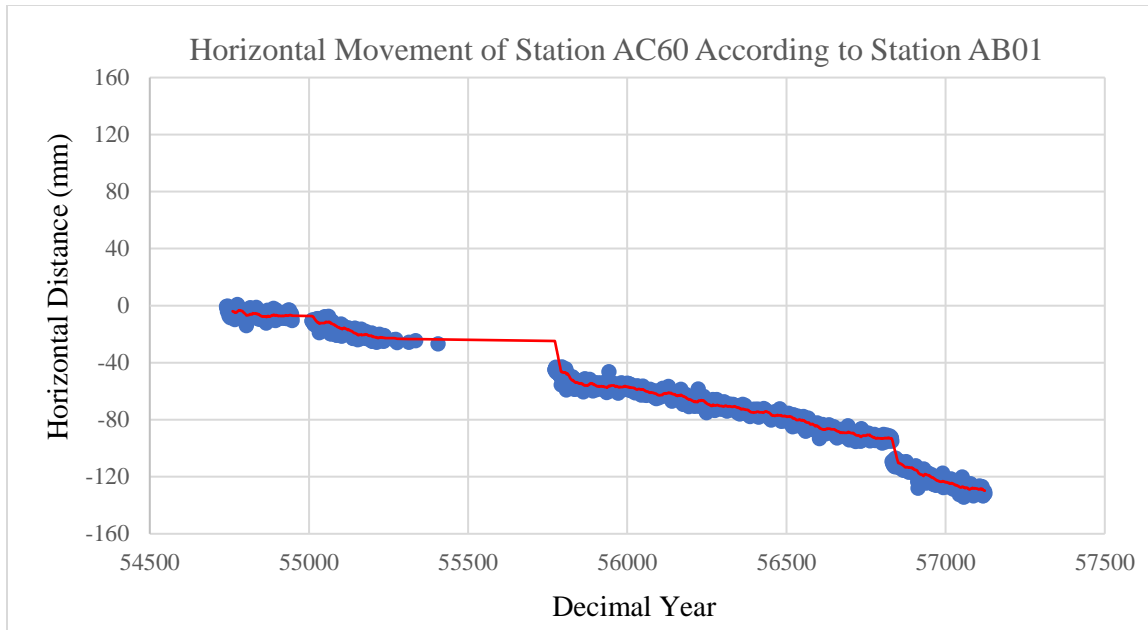


Figure 2.3.3. Horizontal Movement of Station AC60 According to Station AB01. Blue dots are measurements, red line is the average trend line.

2.3.2 AB21 FIXED

Station AB21 is located at the east part of the Aleutian Arc, on the Block E. Station AB01 is located west of Station AB21. It is the second chosen reference GPS station.

The common measurement period of the reference Station AB21 and Station AB01 is between May 2007 and December 2014. They have 1445 measurement days in common.

Station AB01 is at the east of reference Station AB21. Figure 2.3.4 shows it is moving toward the east with some undulations according to Station AB21. Depending on the common measurement days, horizontal velocity of Station AB01 according to Station AB21 is 3.08 mm/year, moving eastward.

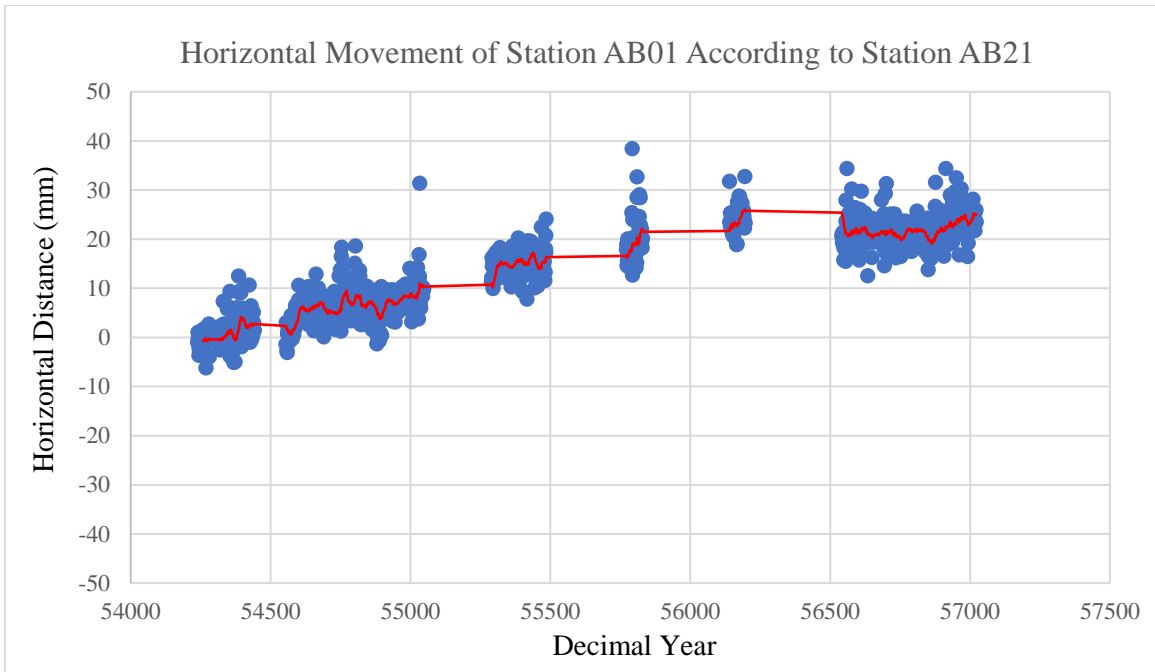


Figure 2.3.4. Horizontal Movement of Station AB01 According to Station AB21. Blue dots are measurements, red line is the average trend line.

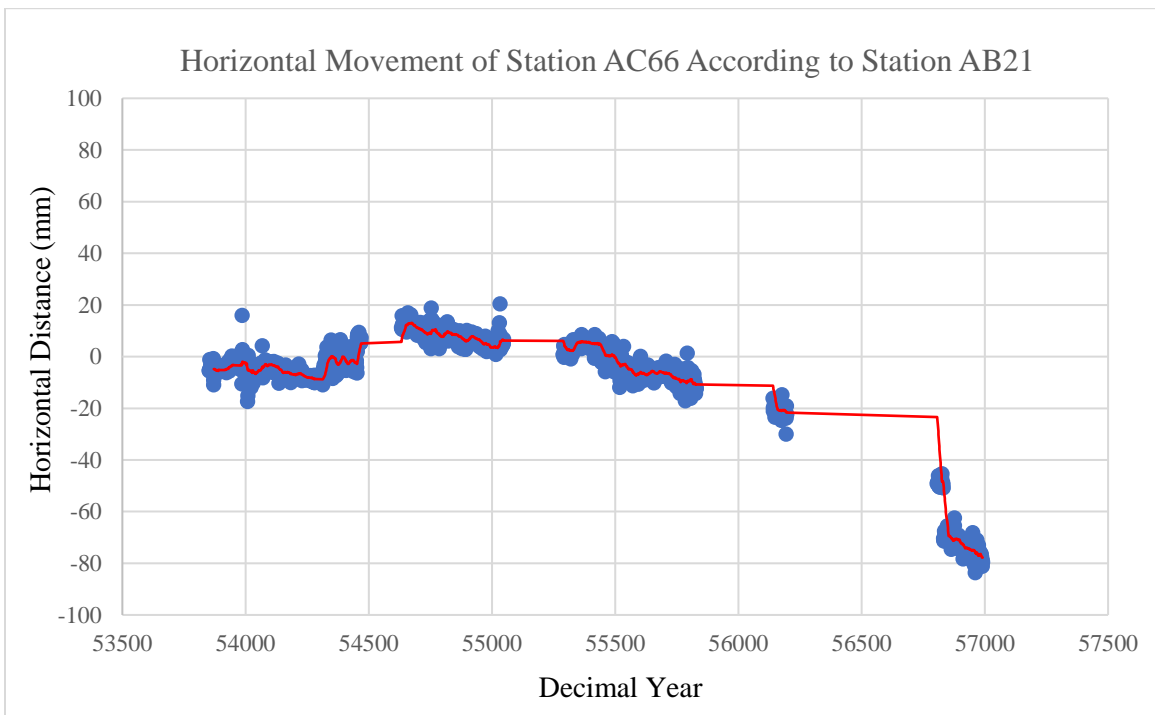


Figure 2.3.5. Horizontal Movement of Station AC66 According to Station AB21. Blue dots are measurements, red line is the average trend line.

Station AC66 is on the west side of the reference Station AB21. Their common measurement days are between April 2006 and November 2014 with 1727 days.

This station firstly moves eastward then moves westward (Figure 2.3.5). It has fewer undulations than Station AB01. This eastward movement shows that reference Station AB21 is faster than Station AC66 during those shared measurement days. Depending on the common measurement days, horizontal velocity of Station AC66 according to Station AB21 is 9.25 mm/year toward the west.

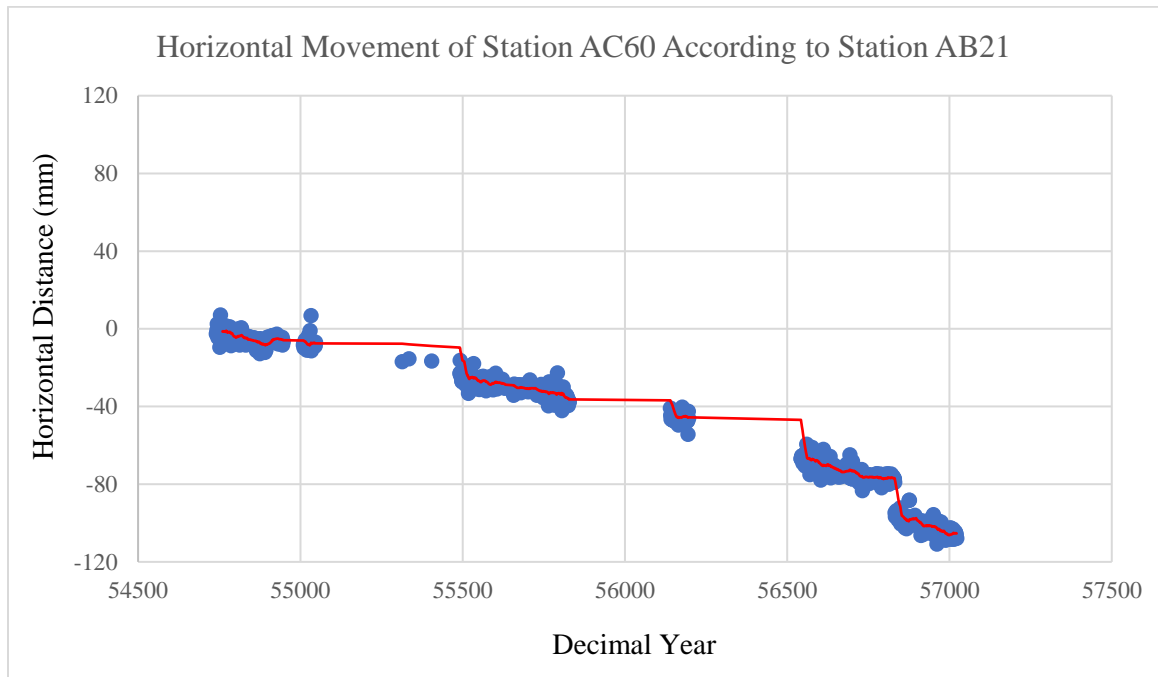


Figure 2.3.6. Horizontal Movement of Station AC60 According to Station AB21. Blue dots are measurements, red line is the average trend line.

Station AC60 is on the west side of the Aleutian Arc. The common measurement period of the reference Station AB21 and Station AC60 is between October 2008 and December 2014. They have 1087 measurement days in common. These two GPS stations have less common measurement days than other two stations.

Figure 2.3.6 shows Station AC60 is moving westward with some undulations but not affecting the main movement direction. Depending on the common measurement days, horizontal velocity of Station AC60 according to Station AB21 is 17.24 mm/year toward the west.

2.3.3 AC66 FIXED

Station AC66 is located at the center part of the Aleutian Arc, on Block C. It is chosen as the third reference GPS station.

The common measurement period of reference Station AC66 and Station AB01 is between May 2007 and February 2015. They have 1731 measurement days in common.

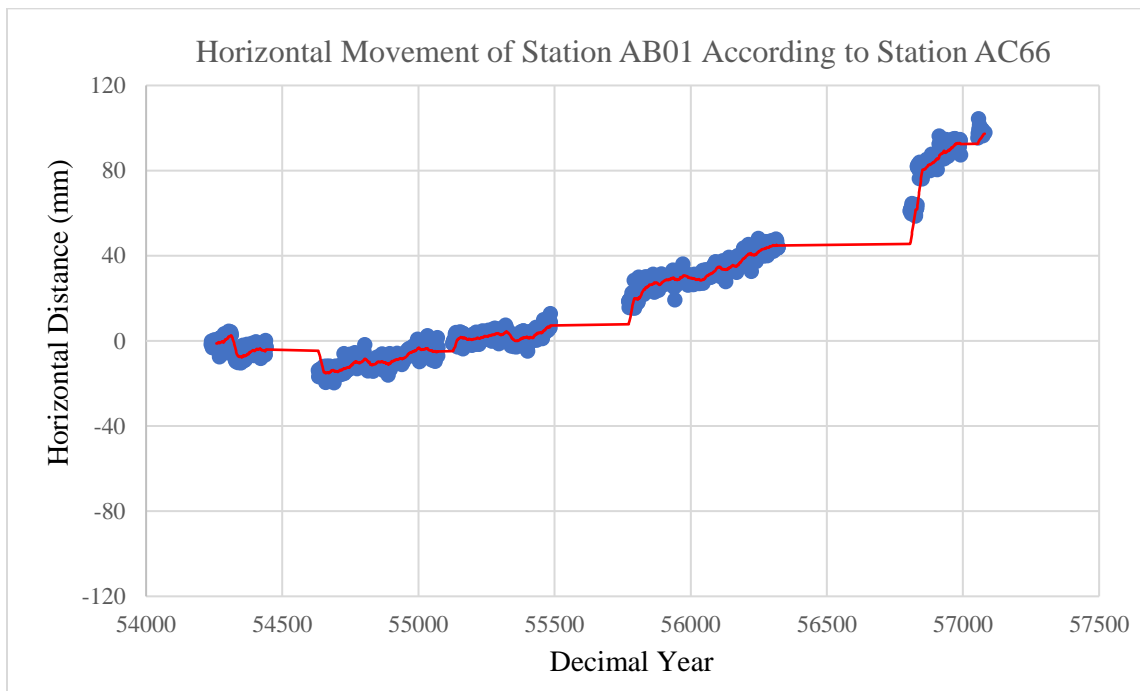


Figure 2.3.7. Horizontal Movement of Station AB01 According to Station AC66. Blue dots are measurements, red line is the average trend line.

Station AB01 is on the east side of Station AC66. Figure 2.3.7 shows it is moving toward the west and then east with some undulations according to Station AC66. Depending on the common measurement days, horizontal velocity of Station AB01 according to Station AC66 is 12.56 mm/year toward the east.

Station AB21 is on the east side of the reference Station AC66. The common measurement period of the reference Station AC66 and Station AB21 is between April 2006 and November 2014. They have 1727 measurement days in common.

Station AB21 is firstly moving west and then changing direction toward east according to reference Station AC66 (Figure 2.3.8). It has more undulations than Station AB01 since it is closer to reference station than Station AB01.

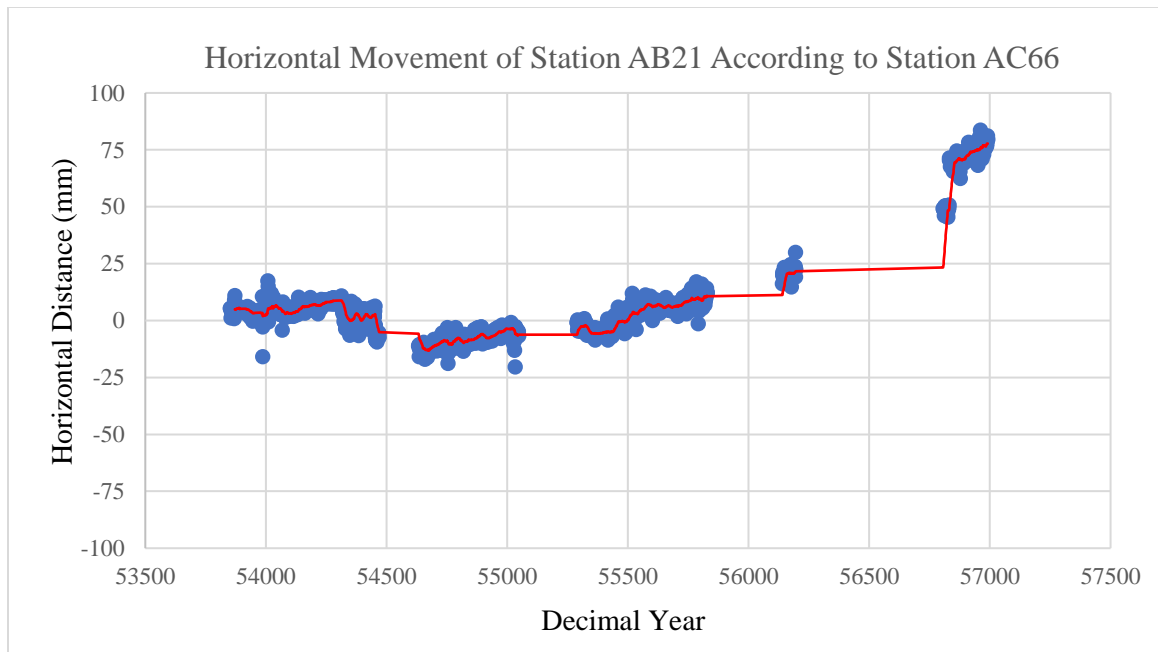


Figure 2.3.8. Horizontal Movement of Station AB21 According to Station AC66. Blue dots are measurements, red line is the average trend line.

Depending on the common measurement days, horizontal velocity of Station AB21 according to Station AC66 is 9.25 mm/year toward the east.

Station AC60 is on the west of reference Station AC66. Their common measurement days are between October 2008 and February 2015. They have 1374 measurement days in common.

Figure 2.3.9 shows this station is moving toward the west with some undulations. The reason for many undulation is that these two GPS stations are very close to each other rather than other ones. However, Station AC60 shows totally westward movement as predicted without a doubt.

Depending on the common measurement days, horizontal velocity of Station AC60 according to Station AC66 is 2.52 mm/year toward the west.

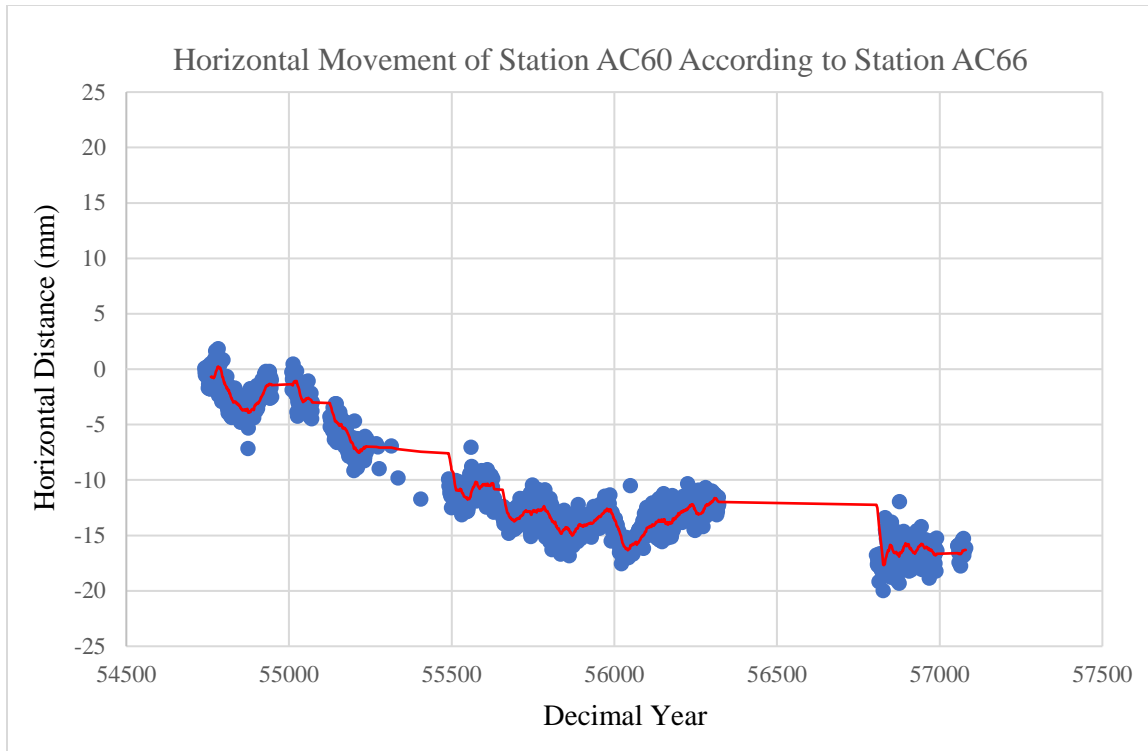


Figure 2.3.9. Horizontal Movement of Station AC60 According to Station AC66. Blue dots are measurements, red line is the average trend line.

2.3.4 AC60 FIXED

Station AC60 is located on Block A, east of Station AC60. It is the fourth chosen reference GPS station.

The common measurement period of the reference Station AC60 and Station AB01 is between October 2008 and April 2015. They have 1788 measurement days in common.

Figure 2.3.10 shows Station AB01 is moving directly east according to Station AC60. Depending on the common measurement days, horizontal velocity of Station AB01 according to Station AC60 is 20.17 mm/year toward the east.

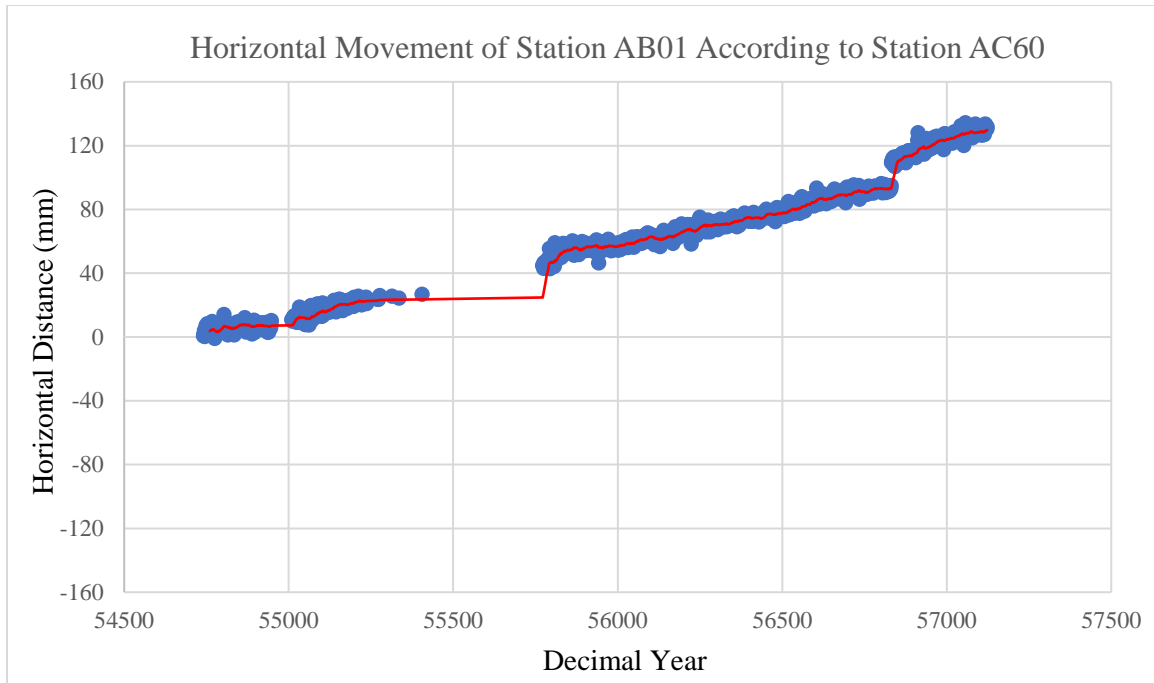


Figure 2.3.10. Horizontal Movement of Station AB01 According to Station AC60. Blue dots are measurements, red line is the average trend line.

Station AB21 is on the east side of the reference Station AC60. The common measurement period of reference Station AC60 and Station AB21 is between April 2008 and December 2014. They have 1087 measurement days in common.

Station AB21 shows directly eastward movement with some undulations (Figure 2.3.11).

It has more undulations than Station AB01 but its path is so similar.

Depending on the common measurement days, horizontal velocity of Station AB21 according to Station AC60 is 17.24 mm/year toward the east.

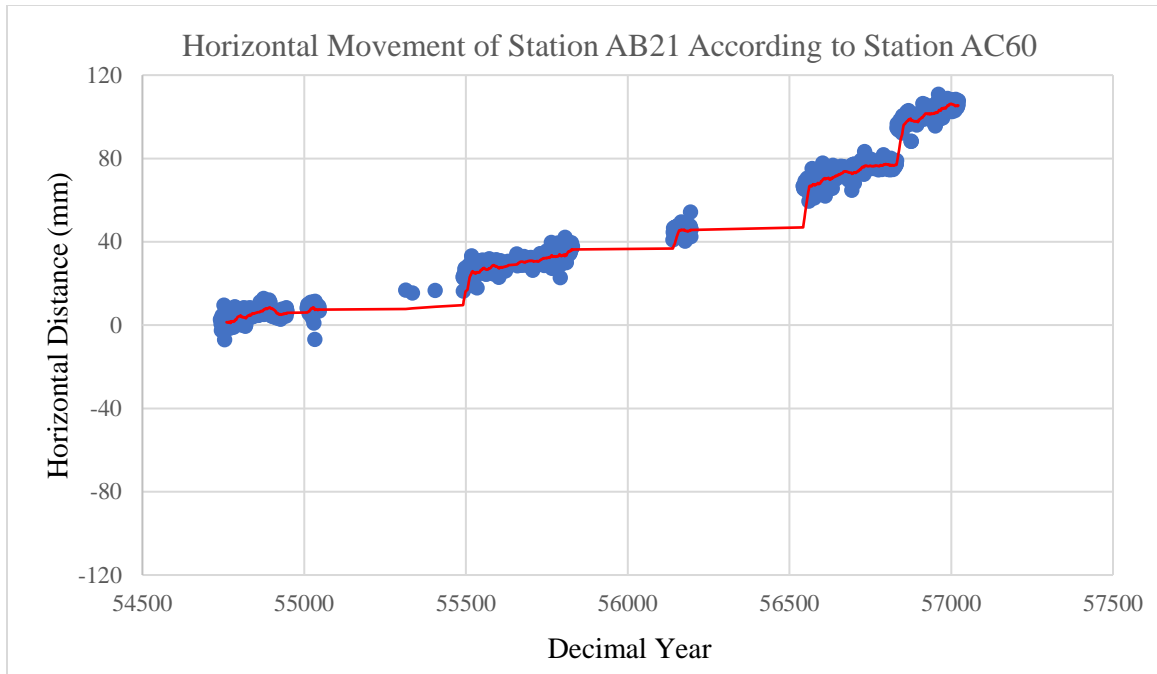


Figure 2.3.11. Horizontal Movement of Station AB21 According to Station AC60. Blue dots are measurements, red line is the average trend line.

Station AC66 is on the west side of the reference Station AC60. The common measurement period of the reference Station AC60 and Station AC66 is between October 2008 and February 2015. They have 1375 measurement days in common.

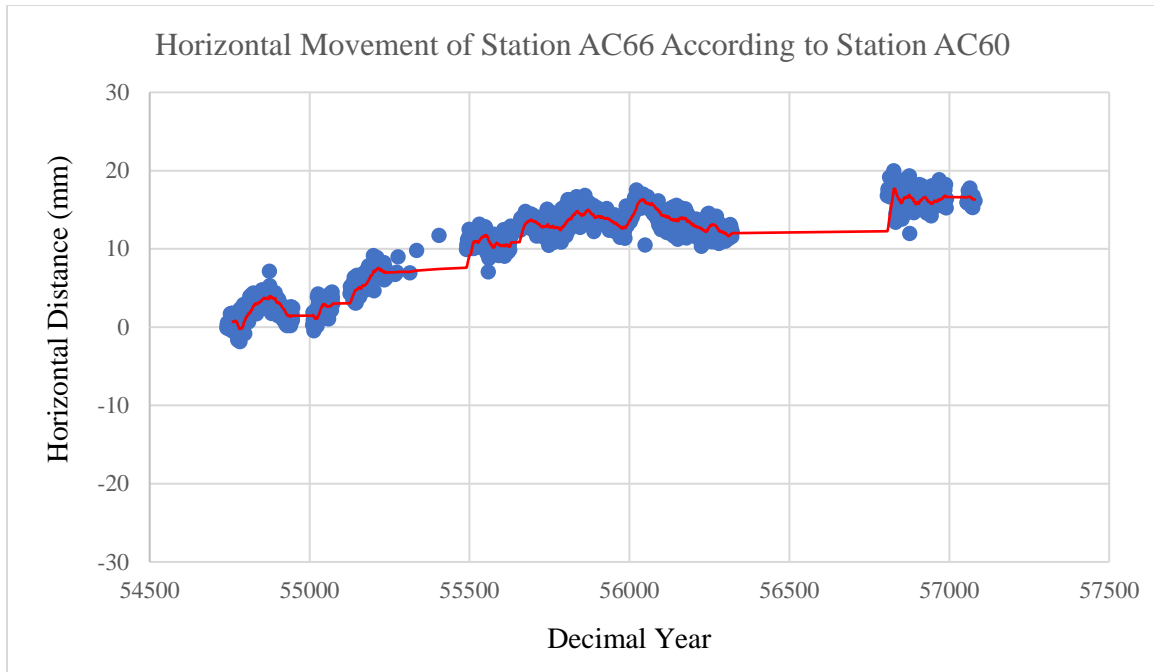


Figure 2.3.12. Horizontal Movement of Station AC66 According to Station AC60. Blue dots are measurements, red line is the average trend line.

Figure 2.3.12 shows Station AC66 has more undulations than other stations depending on horizontal movements according to reference Station AC60. But it has overall eastward movement.

Depending on the common measurement days, horizontal velocity of Station AC66 according to Station AC60 is 2.52 mm/year toward the east.

2.3.5 PETS FIXED

Station PETS is located on the Russian side, Kamchatka Peninsula. All Aleutian Arc stations are located on the east of the reference Station PETS. Station PETS is the fifth chosen reference station in this study.

The common measurement period of reference Station PETS and Station AB01 is between May 2007 and April 2015. They have 2403 measurement days in common.

Figure 2.3.13 shows Station AB01 is moving toward the east with some undulations according to Station PETS. Depending on the common measurement days, horizontal velocity of Station AB01 according to Station PETS is 6.54 mm/year towards east.

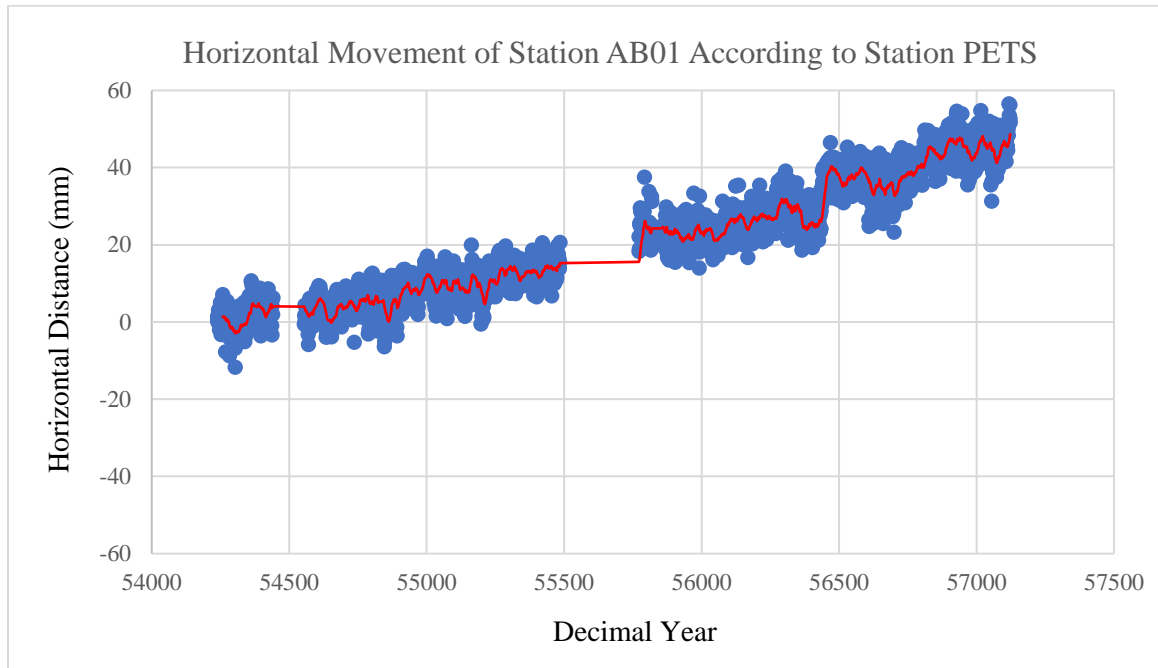


Figure 2.3.13. Horizontal Movement of Station AB01 According to Station PETS. Blue dots are measurements, red line is the average trend line.

Station AB21 is on east of the reference Station PETS. The common measurement period of reference Station PETS and Station AB21 is between April 2006 and December 2014. They have 2172 measurement days in common.

Station AB21 is firstly moving west and then moving toward the east (Figure 2.3.14). Since movement mechanism of reference Station PETS is different than Aleutian Arc; clearly, it can be said that Station AB21 shows a change in the movement direction.

Depending on the common measurement days, horizontal velocity of Station AB21 according to Station PETS is 2.57 mm/year toward the east. This horizontal velocity is less than AB01's one according to the reference Station PETS. Because Station AB21 has some rotation affecting the horizontal velocity according to the reference Station PETS.

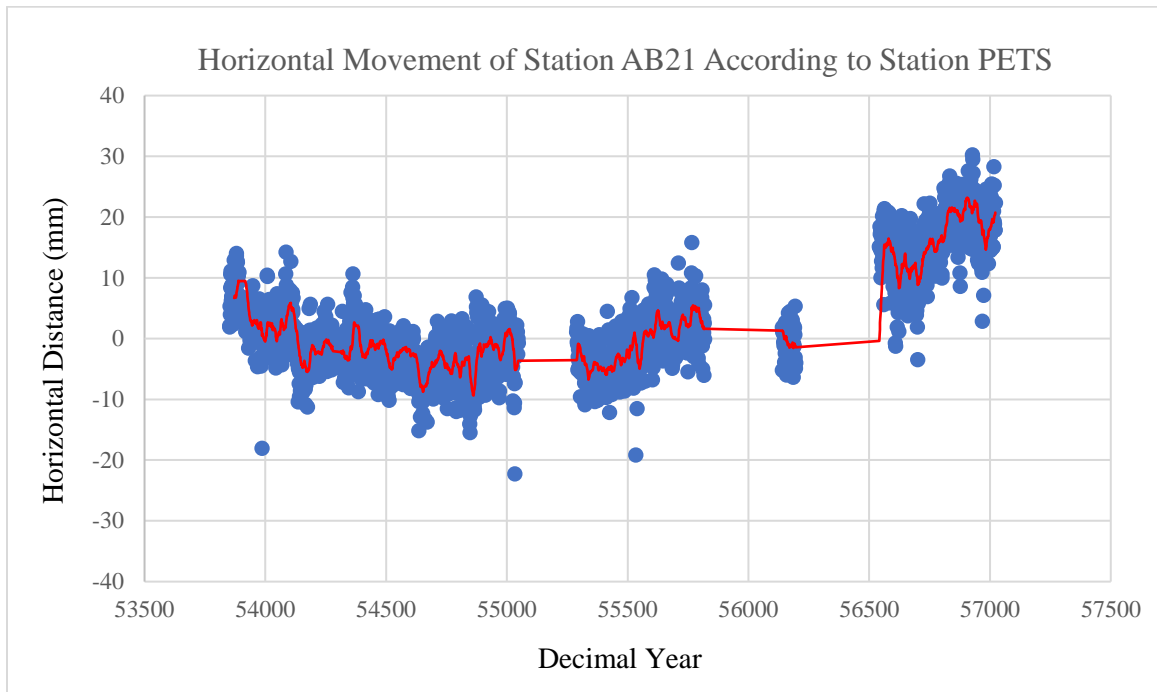


Figure 2.3.14. Horizontal Movement of Station AB21 According to Station PETS. Blue dots are measurements, red line is the average trend line.

Station AC66 is on the east side of the reference Station PETS. The common measurement period of reference Station PETS and Station AC66 is between October 2005 and February 2015. They have 2523 measurement days in common.

Station AC66 has some undulations at the horizontal movement like other stations. Figure 2.3.15 shows horizontal motion of Station AC66 has some change in movement direction.

Motion direction of Station AC66 according to the reference Station PETS is toward west. That means, Station AC66 is faster than reference Station PETS. Since the movement direction of Station PETS is toward the west, also.

Depending on the common measurement days, horizontal velocity of Station AC66 according to Station PETS is 7.58 mm/year toward the west.

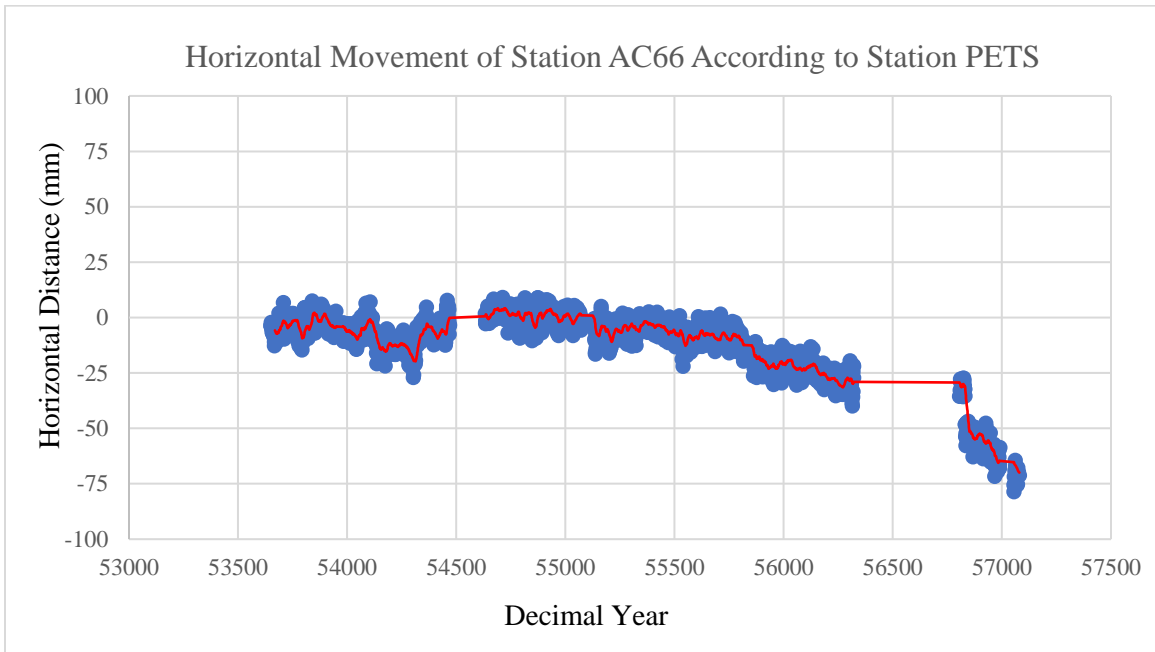


Figure 2.3.15. Horizontal Movement of Station AC66 According to Station PETS. Blue dots are measurements, red line is the average trend line.

Station AC60 is on the east side of the reference Station PETS. Their common measurement days are between October 2008 and April 2015 and they have 1974 measurement days in common. These two GPS stations have less common measurement days than other three stations. But this is not an obstacle to see the movement direction of Station AC60 according to the reference station. Figure 2.3.16 shows Station AC60 is

moving towards west. It has some undulations but not affecting the main movement direction.

Depending on the common measurement days, horizontal velocity of Station AC60 according to Station PETS is 12.67 mm/year toward the west.

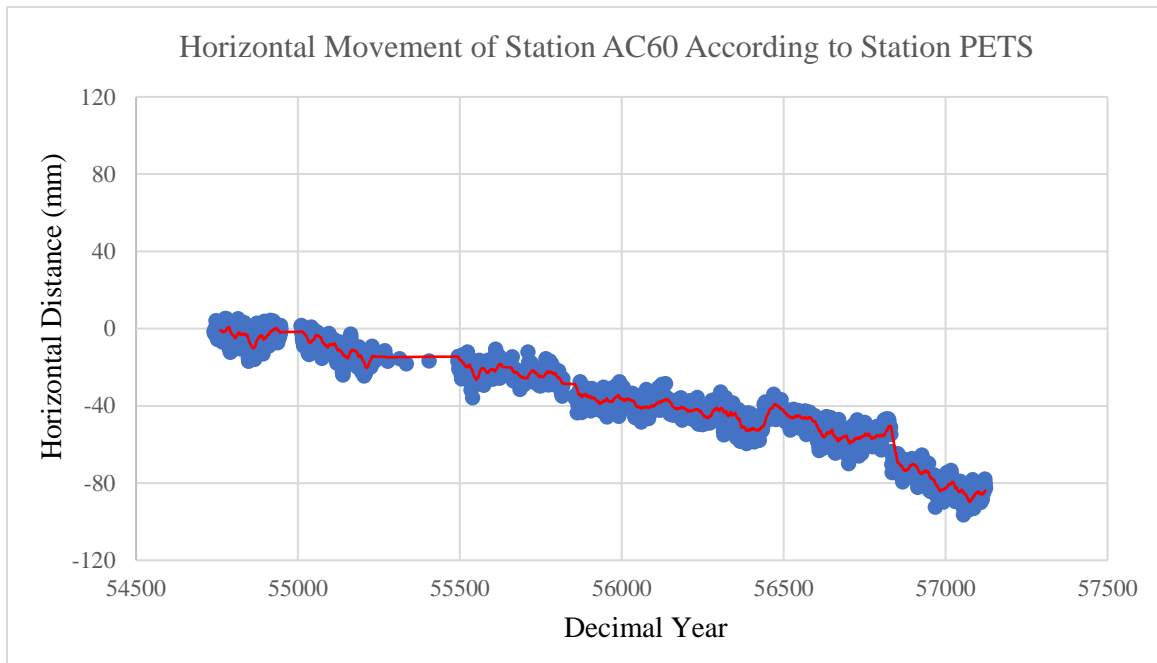


Figure 2.3.16. Horizontal Movement of Station AC60 According to Station PETS. Blue dots are measurements, red line is the average trend line.

2.3.6 AB02 FIXED

Station AB02 is in the east part of the Aleutian Arc and not on any block. It is located on east side of the Station AB01.

The common measurement period of reference Station AB02 and Station AB01 is between May 2007 and April 2015. They have 2211 measurement days in common.

Figure 2.3.17 shows Station AB01 is moving toward west with some undulations according to Station AB02. Since they are so closed to each other, their horizontal velocities can change according to each other so rapidly. Depending on the common measurement days, horizontal velocity of Station AB01 according to Station AB02 is 3.37 mm/year towards the west.

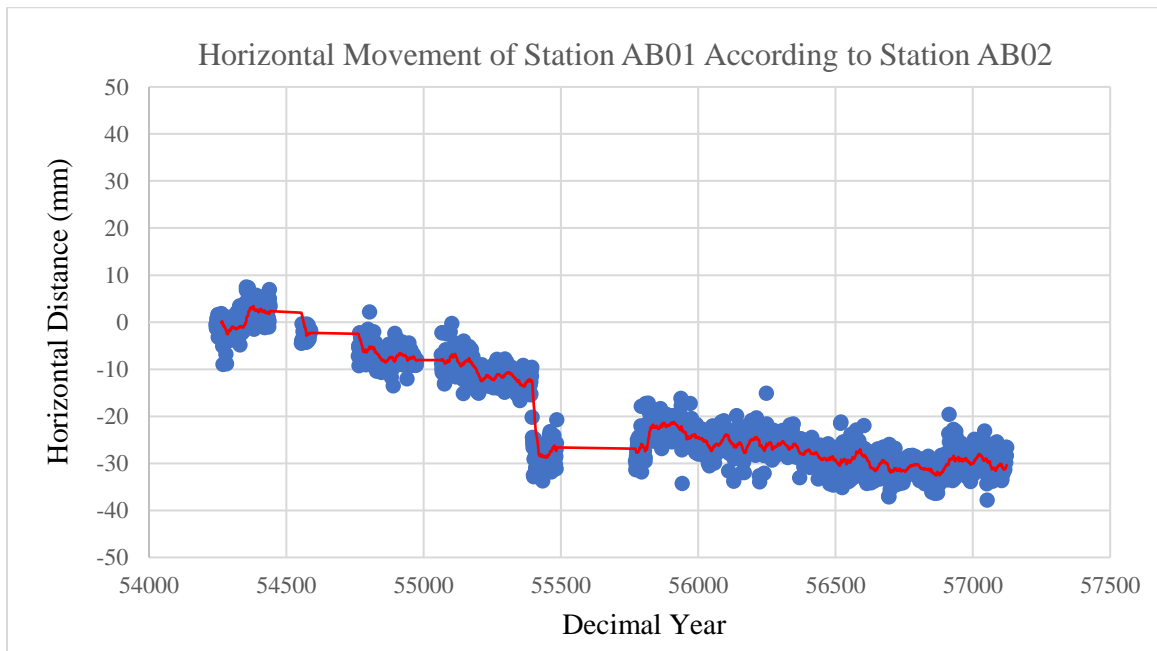


Figure 2.3.17. Horizontal Movement of Station AB01 According to Station AB02. Blue dots are measurements, red line is the average trend line.

Station AB21 is on the west of the reference Station AB02. The common measurement period between reference Station AB02 and AB21 is between May 2007 and December 2014. They have 1600 measurement days in common.

Station AB21 also has some undulations at horizontal velocity according to reference Station AB02 but not that much as Station AB01. Figure 2.3.18 shows Station AB21 is moving toward west according to reference Station AB02.

Depending on the common measurement days, horizontal velocity of Station AB21 according to Station AB02 is 7.48 mm/year toward the west.

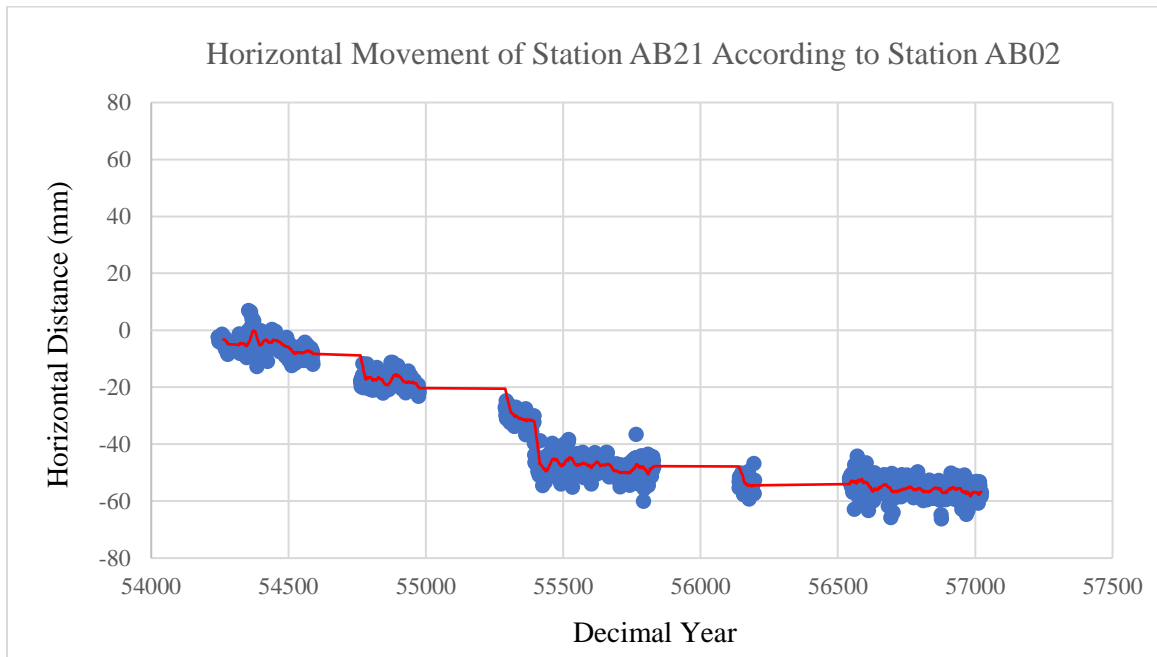


Figure 2.3.18. Horizontal Movement of Station AB21 According to Station AB02. Blue dots are measurements, red line is the average trend line.

Station AC66 is on the west side of the reference Station AB02. The common measurement period of reference Station AB02 and Station AC66 is between May 2007 and February 2015 and they have 1832 measurement days in common.

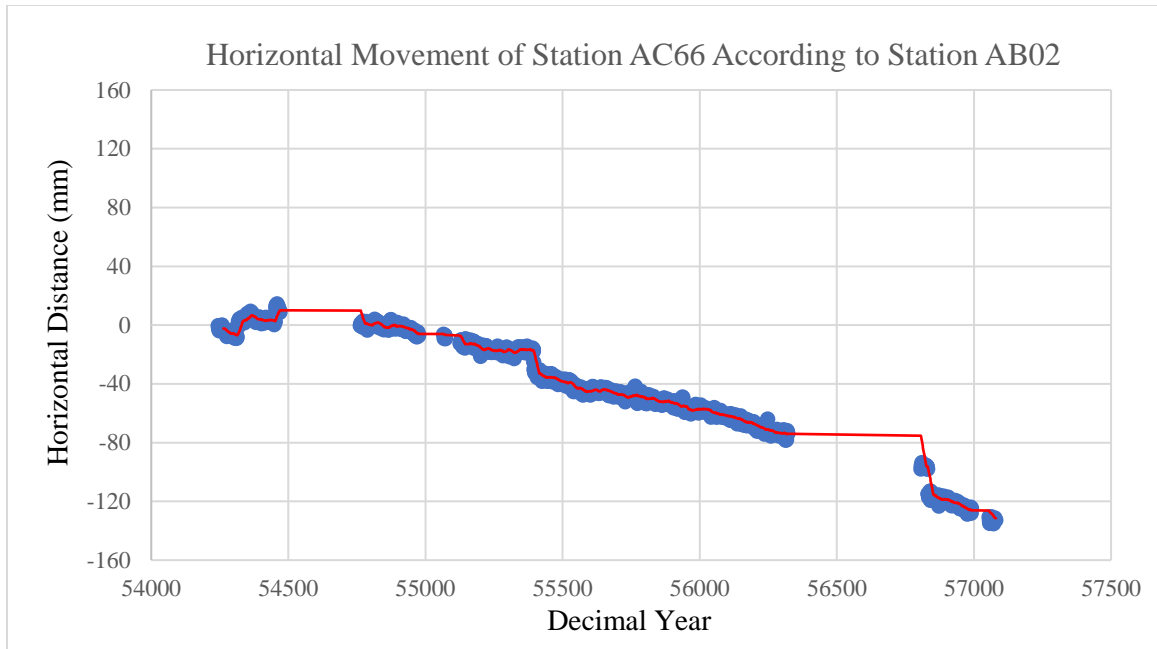


Figure 2.3.19. Horizontal Movement of Station AC66 According to Station AB02. Blue dots are measurements, red line is the average trend line.

Figure 2.3.19 shows Station AC66 is moving toward the east a little but then it turns completely toward the west.

Depending on the common measurement days, horizontal velocity of Station AC66 according to Station AB02 is 17.10 mm/year toward the west.

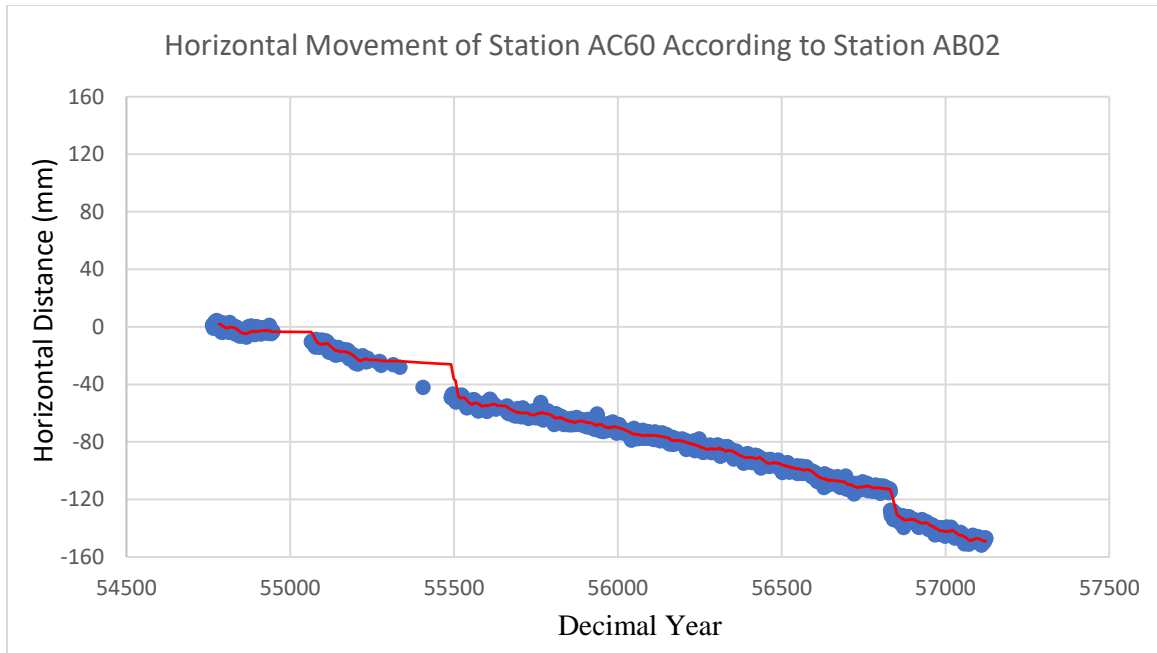


Figure 2.3.20. Horizontal Movement of Station AC60 According to Station AB02. Blue dots are measurements, red line is the average trend line.

Station AC60 is on the west side of the Aleutian Arc. The common measurement days of the reference Station AB02 and Station AC60 is between October 2008 and April 2015. They have 1961 days in common. Station AC60 is moving directly toward the west. It has some minor undulations but not affecting the main movement direction (Figure 2.3.20).

Depending on the common measurement days, horizontal velocity of Station AC60 according to Station AB02 is 22.72 mm/year toward the west.

Based on horizontal movement direction calculations, it can be said that the pivot point of the arc should be at the east side of Station AB21.

2.4 GPS STATIONS MOVEMENT DIRECTION CALCULATIONS ACCORDING TO REFERENCE STATIONS TO PREDICT PIVOT LOCATION

Horizontal-velocity calculations show the possible pivot point side of the arc but not the actual point. To be more accurate for the pivot point of the Aleutian Arc, velocities of each GPS stations calculated according to possible pivot point locations. To determine the rotation direction of the blocks, each GPS stations is assumed as fixed station and predicted as a pivot point. Then velocity and movement direction of other GPS stations were calculated. Depending on these relative movement parameters, some results are established about pivot point location and rotation and/or translation of the blocks.

2.4.1 Station AB01 Fixed

First predicted pivot location for block rotation is Station AB01. The relative movement direction of Station AB21, AC66 and AC60 is calculated according to Station AB01, respectively.

The movement direction of Station AB21 according to reference Station AB01 is shown in the Figure 2.4.1. Station AB21 is moving towards the northwest with an unstable rate. Since these two stations are located on the same block, linear motion is not expected.

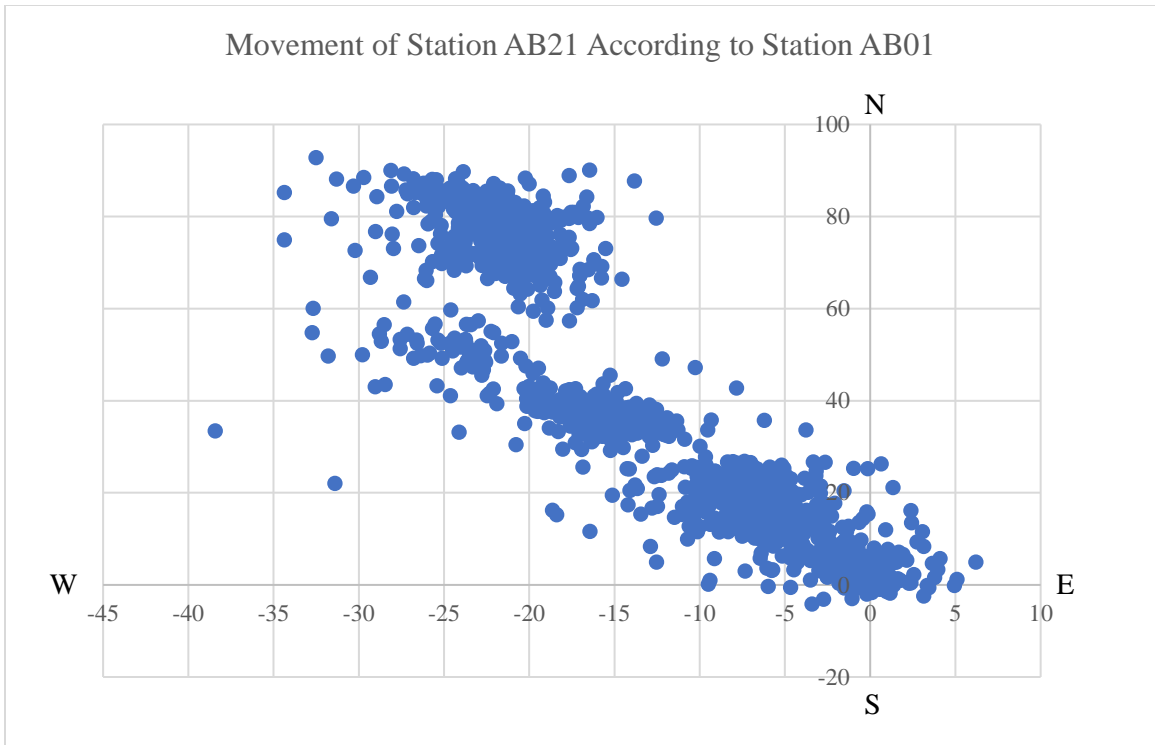


Figure 2.4.1. Movement Direction of Station AB21 According to Station AB01. Scale of the values is mm/day

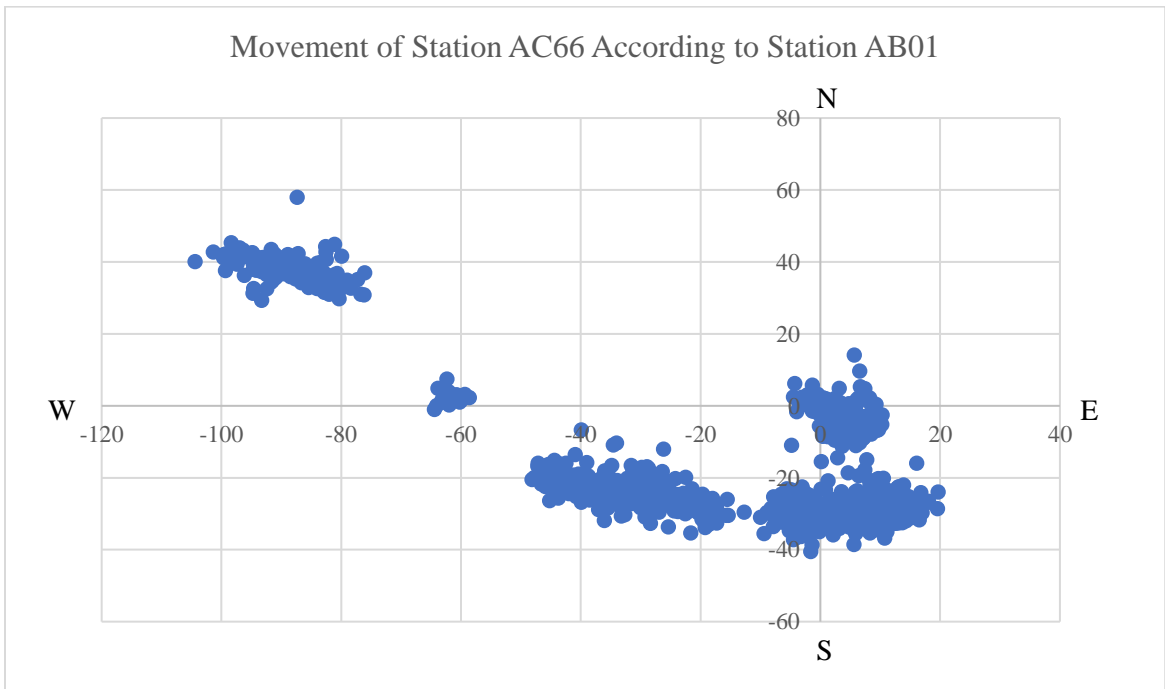


Figure 2.4.2. Movement Direction of Station AC66 According to Station AB01. Scale of the values is mm/day

The movement direction of Station AC66 according to reference Station AB01 is shown in the Figure 2.4.2. Station AC66 is moving first towards the southeast and then changed its direction toward the northwest. It shows a clockwise rotation in the data set. This clockwise rotation is consistent with previous studies.

The movement direction of Station AC60 according to reference Station AB01 is shown in the Figure 2.4.3. Station AC60 is moving towards the northwest. Its movement direction does not undulate like Station AB21. This is the predicted result for Station AC60 because it is located on the Block A where the convergence obliquity is low. At this location, plate movement is almost parallel to the trench.

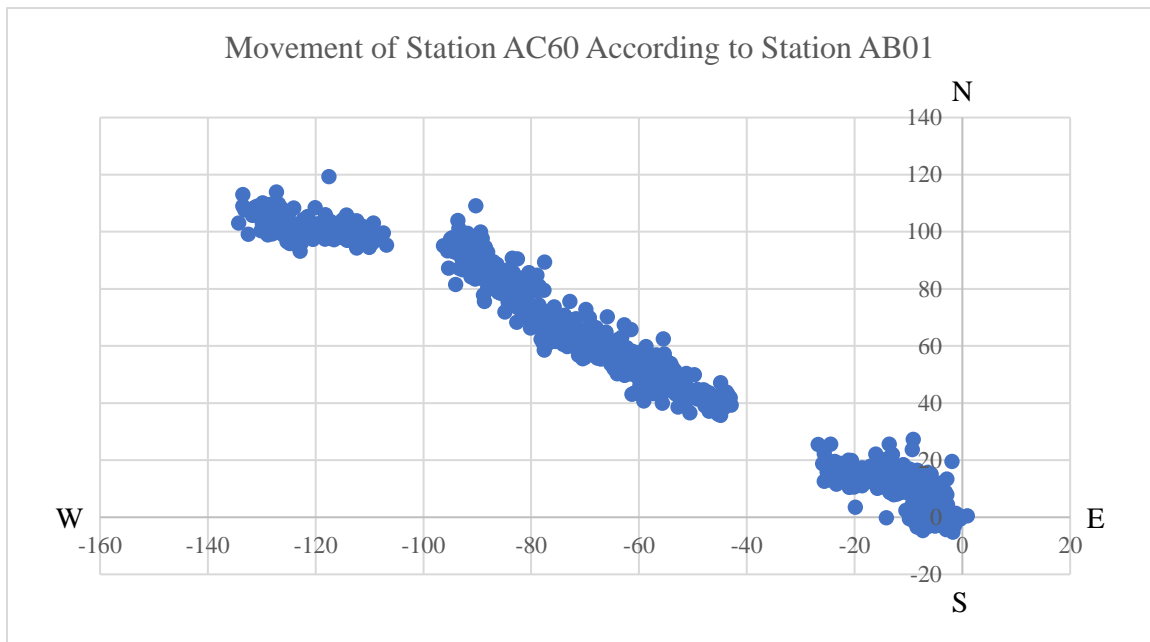


Figure 2.4.3. Movement Direction of Station AC60 According to Station AB01. Scale of the values is mm/day

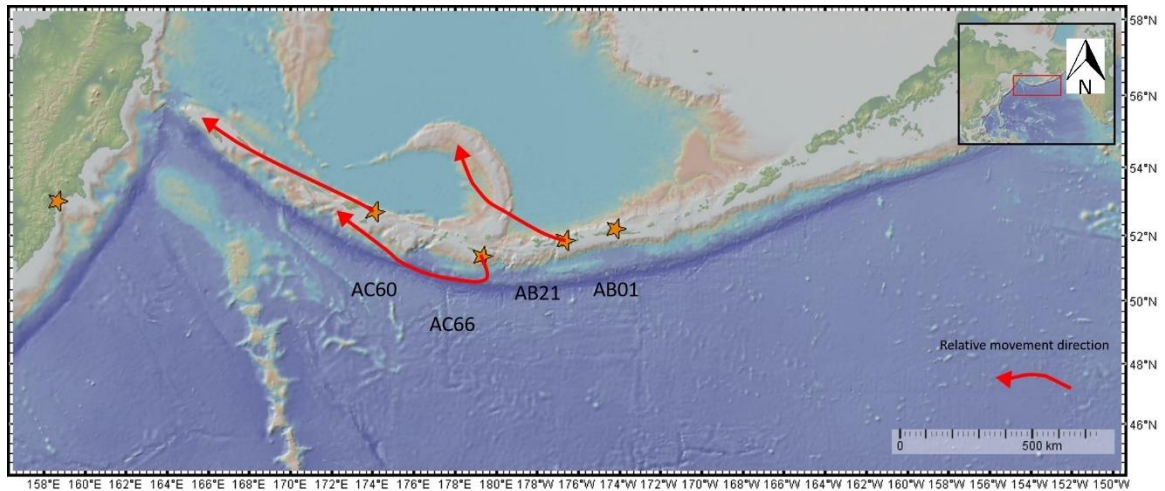


Figure 2.4.4. Relative Movement Directions When Station AB01 is Fixed

Figure 2.4.4 shows relative movement behavior of Station AB21, AC66, and AC60 when Station AB01 is chosen as fixed. This map shows comparable results for individual velocities of the stations.

2.4.2 Station AB21 Fixed

The second station predicted as pivot location for block rotation is Station AB21. Relative movement direction of Station AB01, AC66, and AC60 is calculated according to Station AB21.

The movement direction of Station AB01 according to reference Station AB21 is shown in the Figure 2.4.5. Station AB01 is moving towards the southeast. Its movement direction has undulations just as expected since they are located on the same block which means they have been affected in a similar way by the convergence system.

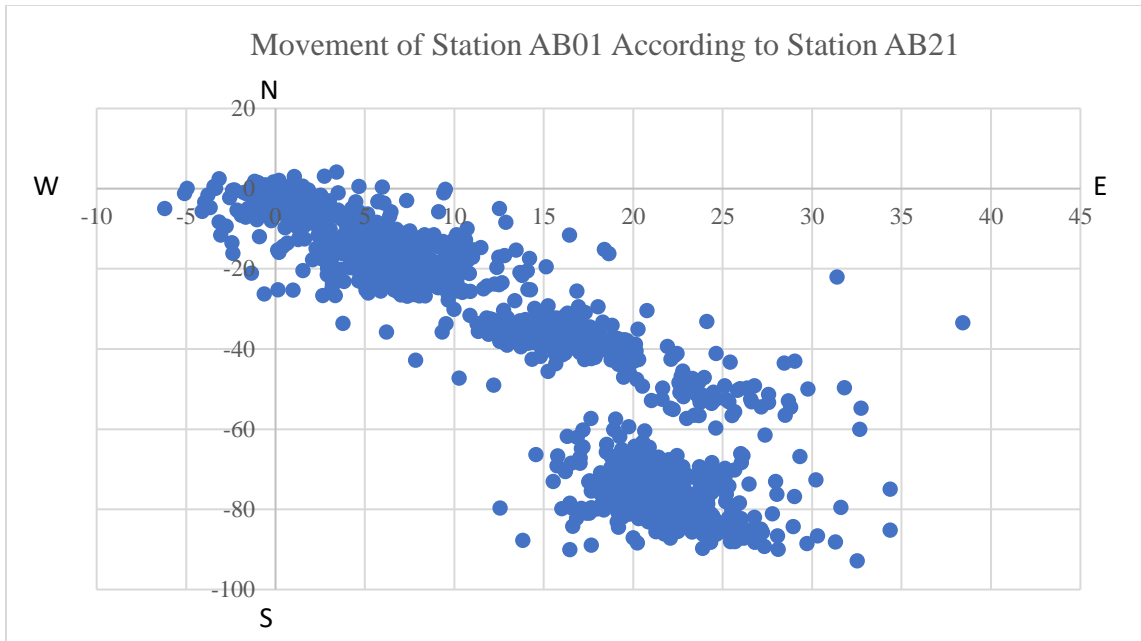


Figure 2.4.5. Movement Direction of Station AB01 According to Station AB21. Scale of the values is mm/day

The movement direction of Station AC66 according to reference Station AB21 is shown in the Figure 2.4.6. Station AC66 is firstly moving towards the southeast then turns towards the northwest. Its movement stays at south direction according to Station AB21. This indicates that Station AB21 is moving faster north than Station AB01 and AC66. This is also the found result from their calculated velocities.

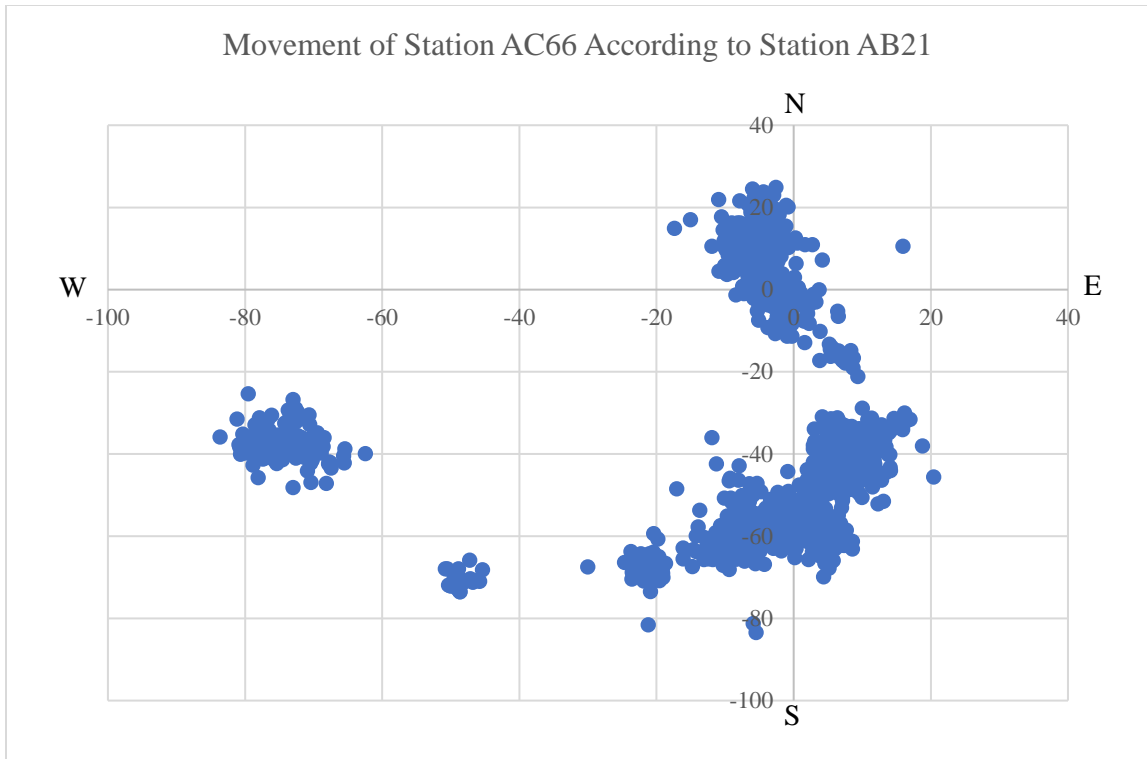


Figure 2.4.6. Movement Direction of Station AC66 According to Station AB21. Scale of the values is mm/day

The movement direction of Station AC60 according to reference Station AB21 is shown in the Figure 2.4.7. Station AC60 is moving towards the northwest. The general tendency of the movement is expected but it shows some curvature towards the south with this reference station. This is not the predicted result for movement direction of Station AC60.

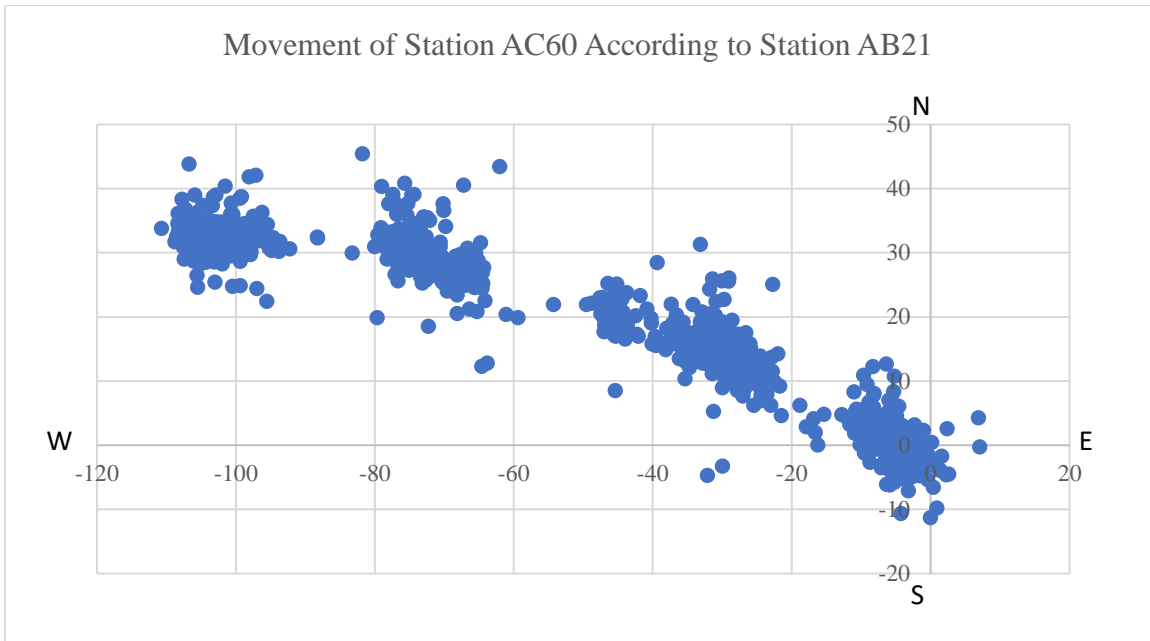


Figure 2.4.7. Movement Direction of Station AC60 According to Station AB21

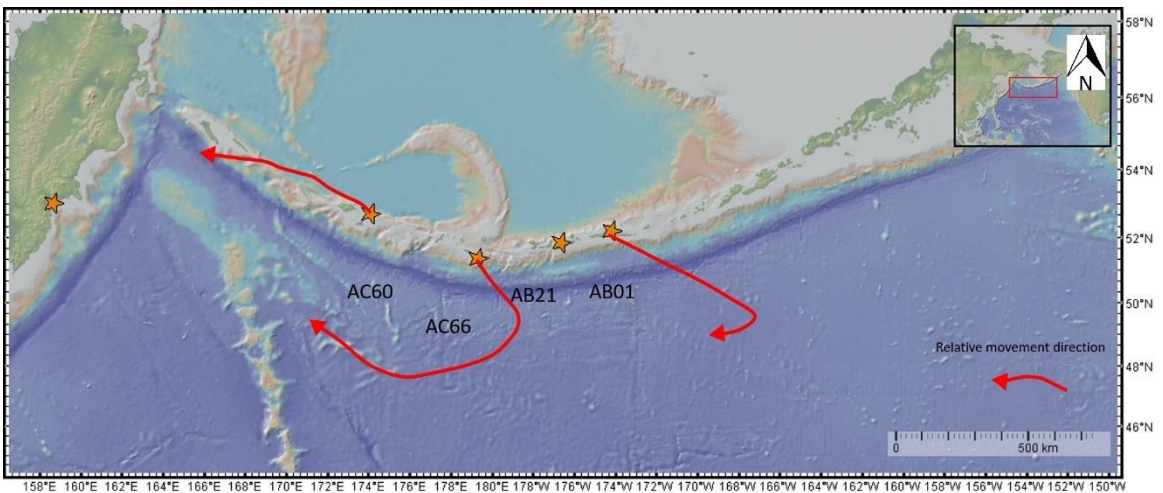


Figure 2.4.8. Relative Movement Directions When Station AB21 is Fixed

Figure 2.4.8 shows relative movement behavior of Station AB01, AC66, and AC60 when Station AB21 is chosen as fixed station. The movement directions of Station AB01, AC66, and AC60 is not convenient with their velocity directions according to this map. That means the pivot point cannot be the Station AB21.

2.4.3 Station AB02 Fixed

The last station chosen as pivot location is Station AB02. This GPS station is not located on any of the blocks. It is chosen according to Krutikov et al., (2008) since Krutikov says that there should be a pivot point located on Umnak Island. The relative movement direction of Station AB01, AB21, AC66 and AC60 is calculated according to Station AB02.

The movement direction of Station AB01 according to reference Station AB02 is shown in Figure 2.4.9. Station AB01 does not show a clear movement direction. General movement is towards the southwest with minor undulations. Although these two stations are not located on the same block, they are closer to each other than other stations.

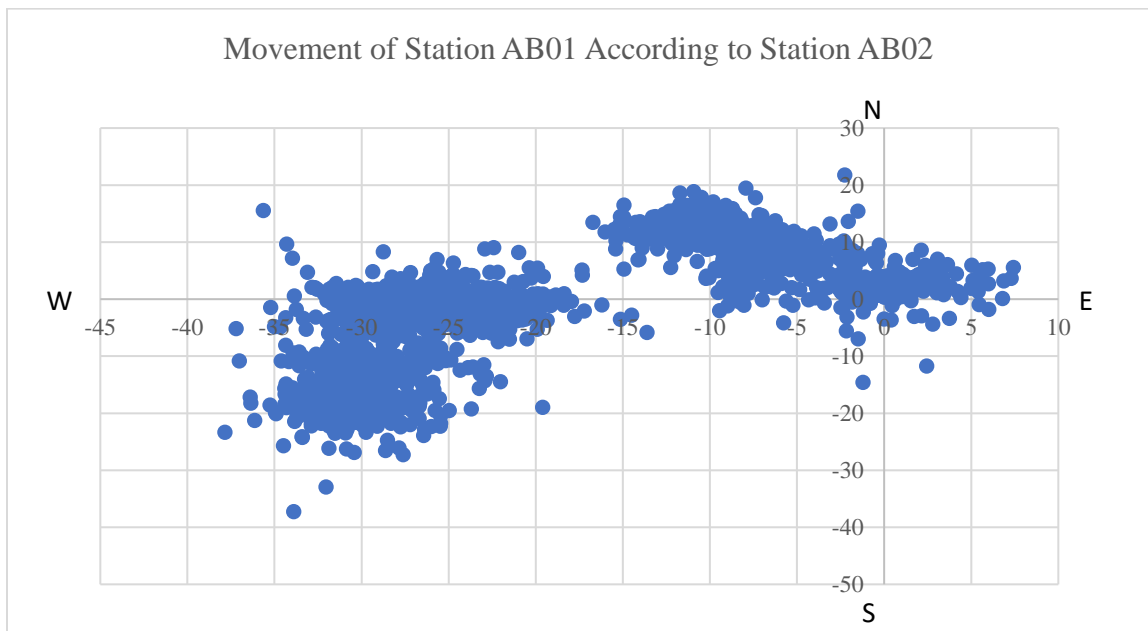


Figure 2.4.9. Movement Direction of Station AB01 According to Station AB02. Scale of the values is mm/day

The movement direction of Station AB21 according to reference Station AB02 is shown in the Figure 2.4.10. Station AB21 shows movement toward northwest direction. It has some curvature as predicted showing clockwise rotation.

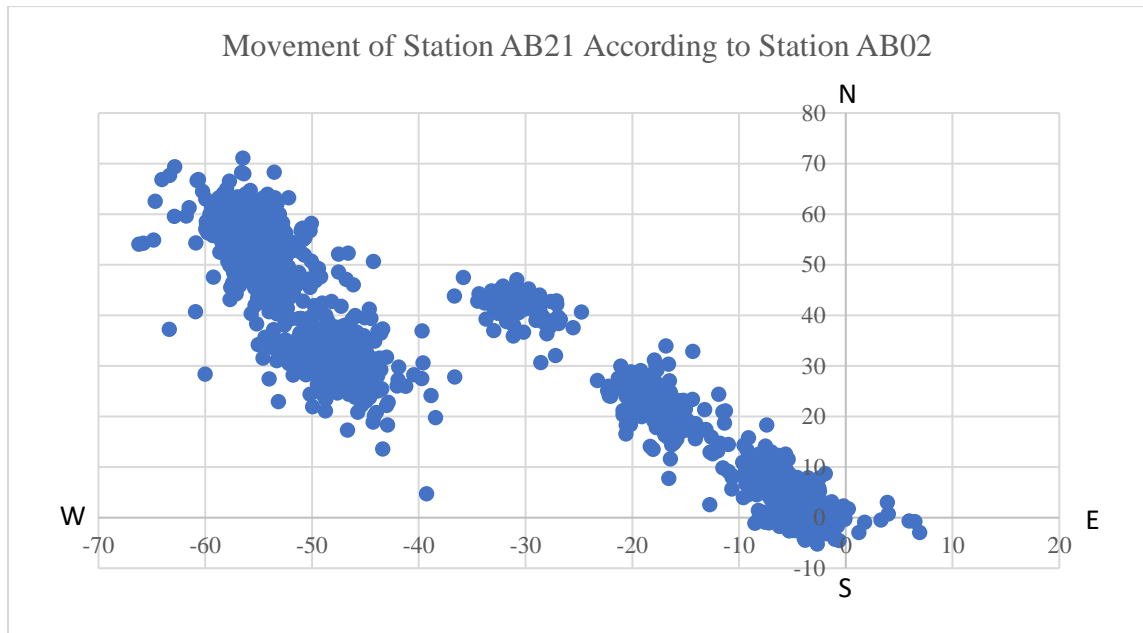


Figure 2.4.10. Movement Direction of Station AB11 According to Station AB02. Scale of the values is mm/day

The movement direction of Station AC66 according to reference Station AB02 is shown in the Figure 2.4.11. Station AC66 is moving first towards the southeast then turns towards the northwest. This movement direction indicates rotation of Station AC66 according to Station AB02.

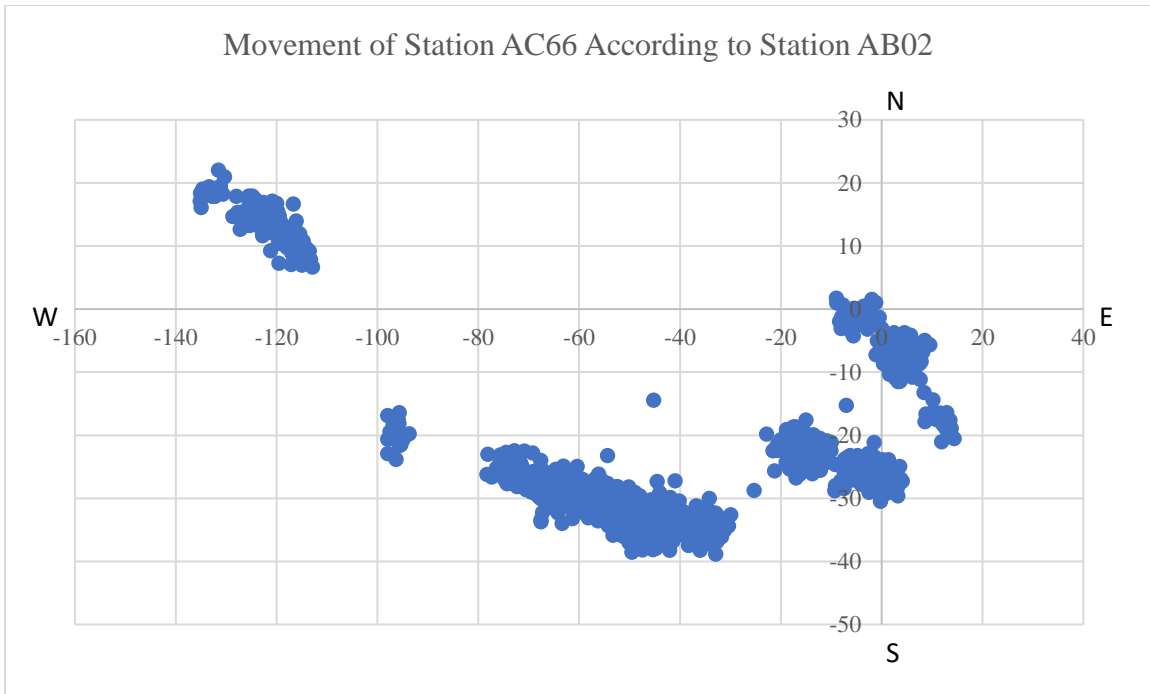


Figure 2.4.11. Movement Direction of Station AC66 According to Station AB02. Scale of the values is mm/day

The movement direction of Station AC60 according to reference Station AB02 is shown in the Figure 2.4.12. Station AC60 is moving towards the northwest, directly. This is the predicted result for the movement direction of Station AC60.

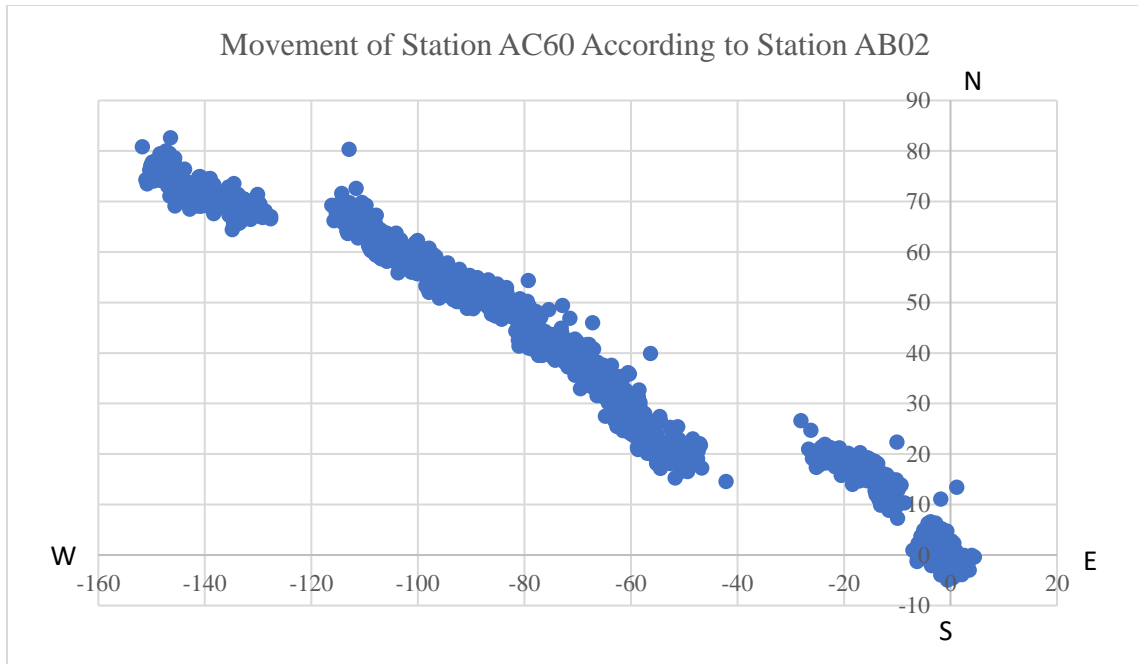


Figure 2.4.12. Movement Direction of Station AC60 According to Station AB02. Scale of the values is mm/day

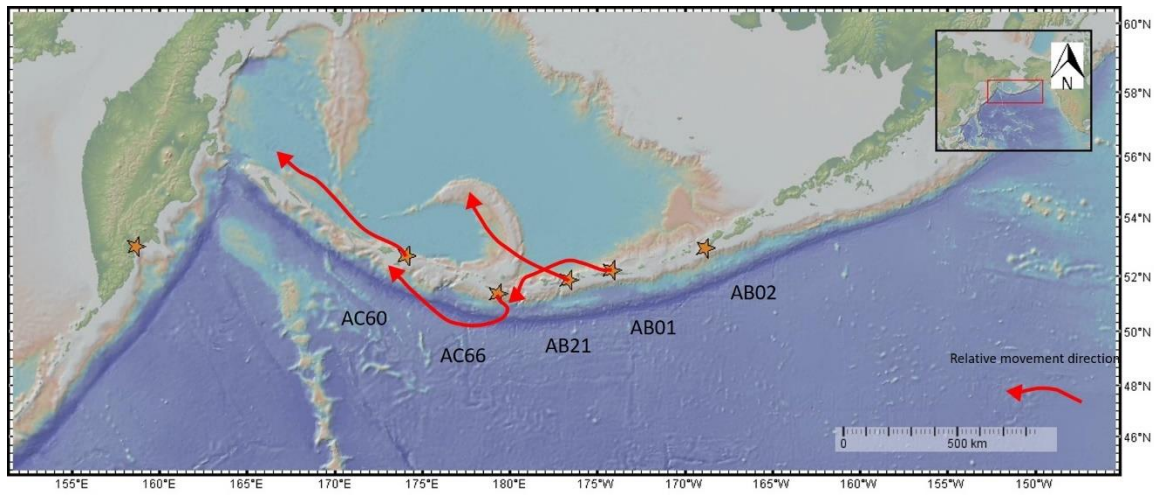


Figure 2.4.13. Relative Movement Directions When Station AB21 is Fixed

Figure 2.4.13 shows relative movement behavior of Station AB01, AB21, AC66, and AC60 when Station AB02 is chosen as the pivot station. The relative movement directions of all stations are the same with their velocity directions according to this map. That means the pivot point for the Aleutian Arc is the Station AB02.

3 EARTHQUAKE DEPTHS AND MAGNITUDES

Earthquake depths have important information about the structure and tectonic regime of the crust; mostly, at the subduction zones since the determination of depth and location of earthquakes provide information about subduction zone's structures like steepness of the subducting slab.

Earthquake data used in this research are taken from Global Centroid-Moment-Tensor (CMT) Project. Time range covers from January 1976 to April 2015. There are 1798 earthquake data with their location, date, time, depth and magnitude. Based on these data, earthquake depth maps of Aleutian Arc can be seen in the following figures.

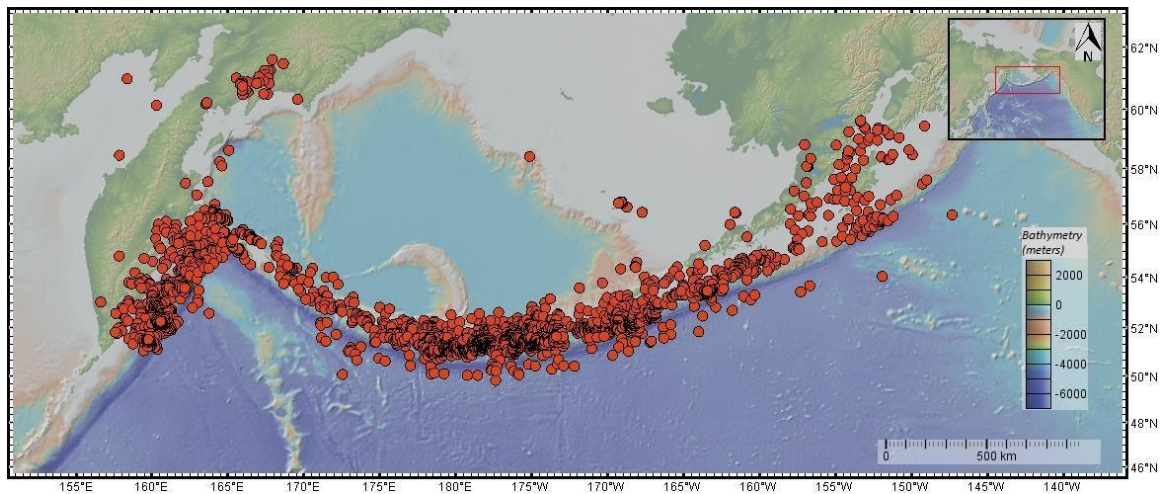


Figure 3.1. Earthquake Hypocenters on Aleutian Arc

Figure 3.1 shows all earthquake hypocenters on the Aleutian Arc. As it can be seen in the map, volcanic activity and earthquake density greatest in the center of the arc and lowest in the east.

Figure 3.2 shows the earthquake depth configuration along the arc. Most of the earthquakes are shallower than 70 km. Moreover, the west side of the Bowers Ridge has only shallow earthquakes which indicate the slab is not deep at that part of the subduction zone.

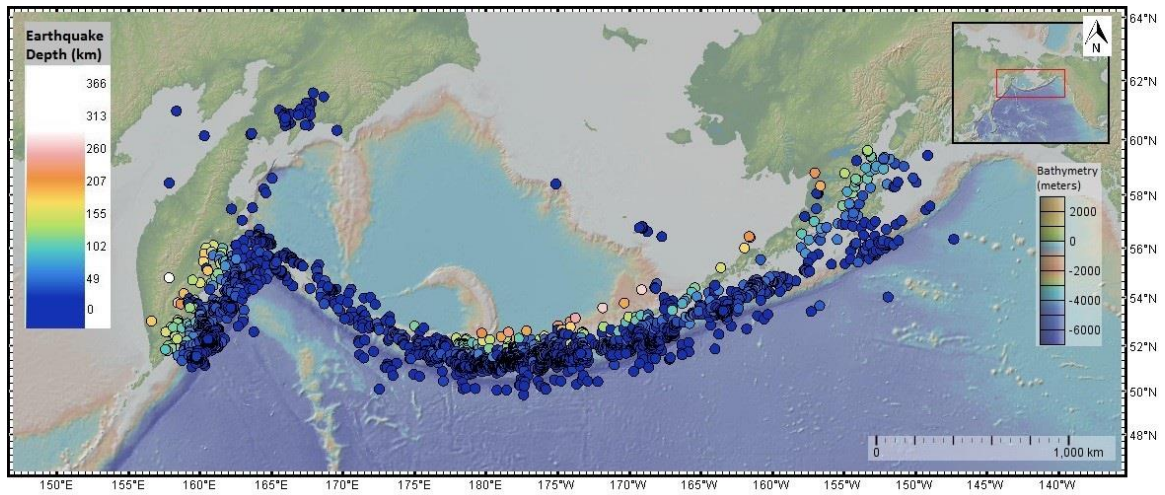


Figure 3.2. Earthquake Depths on Aleutian Arc

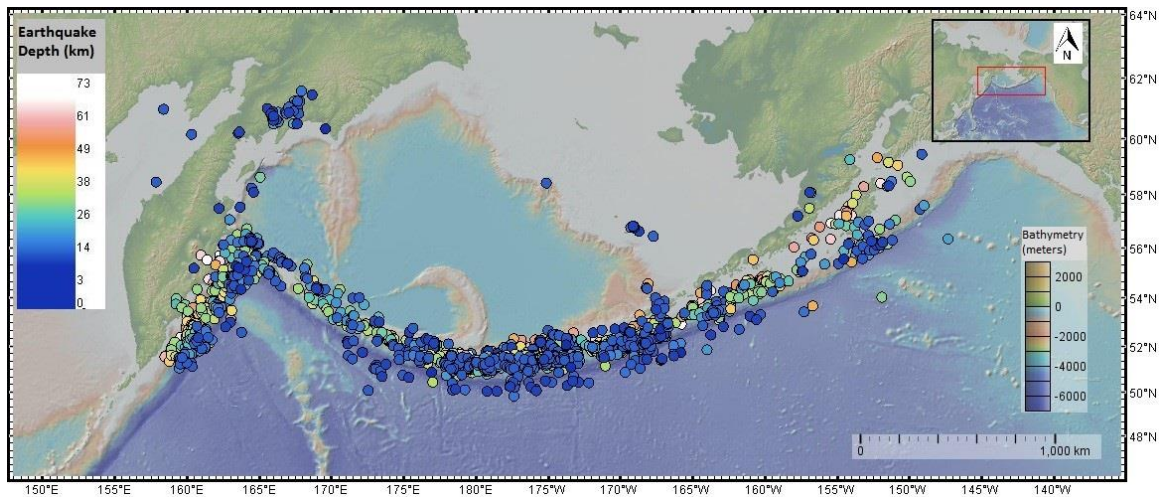


Figure 3.3. Earthquake Depth Data from Surface to 70 km

Figure 3.3 shows that all shallow earthquakes occurred from surface to 70 km depth. Shallower depth earthquakes represented by blue colors occur across the entire length of

the arc. Deeper earthquakes (represented by white and pink colors) occurred towards the center and eastern side of the arc.

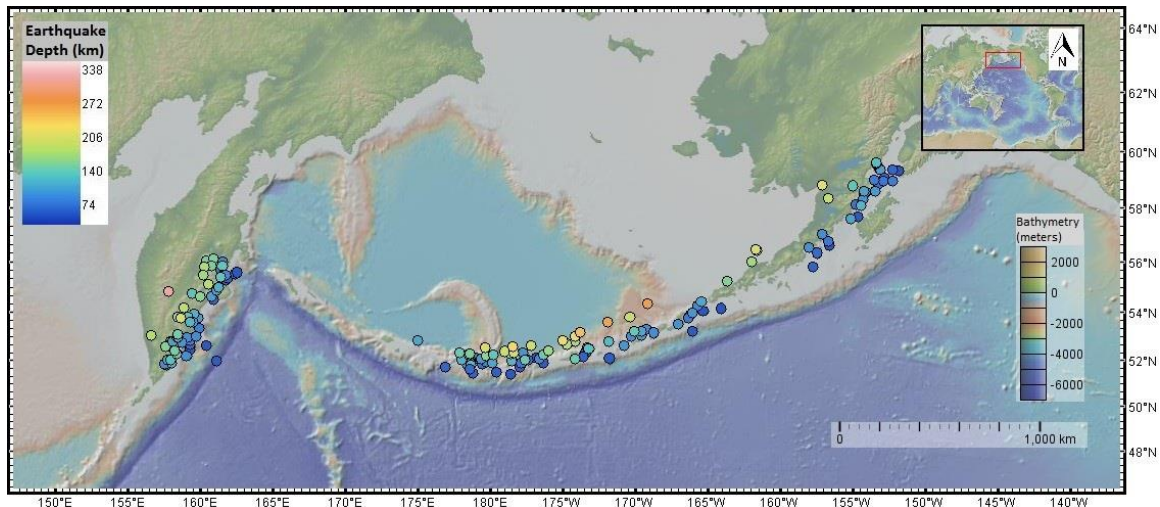


Figure 3.4. Earthquake Depth Data from 70 to 300 km

Figure 3.4 shows intermediate depth earthquakes which are between 70 and 300 km. As it can be seen from the map, there is no intermediate or deep earthquake at the western side of the Aleutian Arc. Only 167 of 1798 data are between 70 and 300 km.

Earthquakes can be described across the arc based on depth. Most parts of the arc display intermediate depth EQs. The western part of the Aleutian arcuate island arc displays shallow depth EQs and there is no moderate depth EQs at there. Shallow earthquakes occur at all part of the arc. Moreover, deep focus earthquakes are not seen at Aleutian Arc. In this class earthquakes, subduction of the slab should be very steep and this steepness of the slab depends on the convergence angle with thickness and age difference between converging plates. The convergence angle is not sufficient to produce a steeply dipping slab at the western part of the arc. The Pacific and North American plates could not reach that

convergence angle to produce steep slab and deep earthquakes. To see deep focus earthquakes, convergence angle should be perpendicular to the subduction zone. For example, convergence angle at eastern side of the arc (Alaska Peninsula) and Kamchatka Peninsula side are perpendicular to the subduction zone; therefore, there are some earthquakes occurred at 200-300 km depth range (Figure 3.4).

Figure 3.5 shows the magnitude distribution of the Aleutian Arc earthquakes. This map shows that most of the earthquakes are between 4 to 6 M_w .

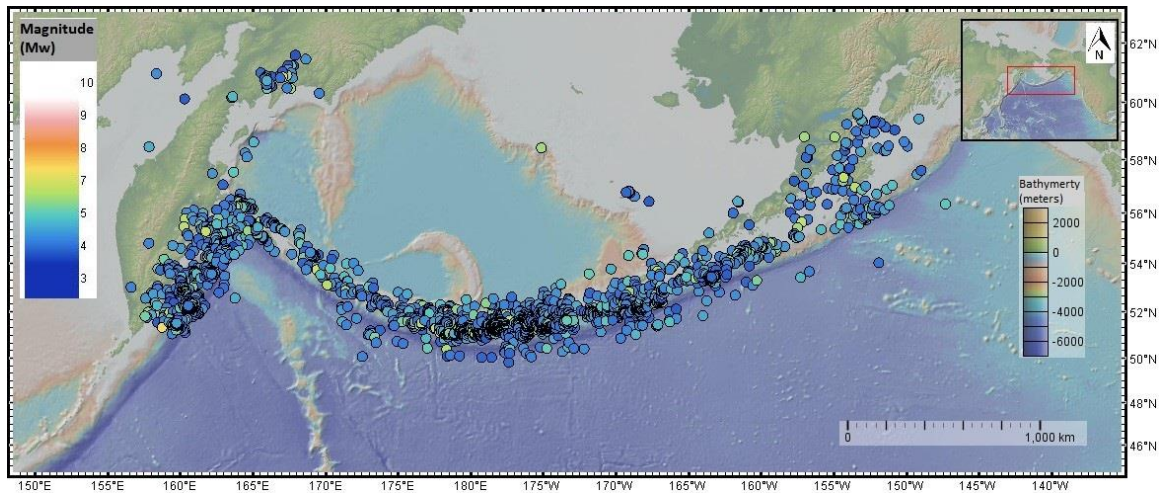


Figure 3.5. Earthquake Magnitudes on Aleutian Arc

The correlation between earthquake magnitude and depth is a simple but challenging concept. Basically, the largest magnitude earthquakes occur at shallower depths. Small magnitude earthquakes can take place at all depth in the crust.

Earthquake depths and volcanic activity are two key factor to make a prediction about the slab structure and steepness. Shallow earthquakes, between the surface to 70 km depth, are

seen all over the arc but the moderate-depth earthquakes are just seen at center and eastern side of the arc. This depth class does not provide accurate information for slab appearance.

As a result, while the convergence obliquity increases towards the west, the depth of earthquakes become shallower. At the sliver plate region where convergence is almost parallel to the trench, volcanic activity is decreasing and earthquake occurrence becomes much less.

4 DISPLACEMENT PARTITIONING

4.1 ARC-PARALLEL & ARC-NORMAL STRAINS

McCaffrey (1996) used deflection angle of earthquake slip vectors to estimate arc-parallel slip rates of forearc and to estimate arc-parallel strain rates from changes in slip rates along the strike for the world's major convergent plate margins. Depending on this study, arc-parallel slip rate calculations are made for Aleutian Arc with focal mechanism data.

The aim of this part of the study is to determine the arc-parallel and arc-normal slip rate distribution along the arc and see the relation between convergence obliquity and strain rate distribution. To do this, plate convergence rates and directions at focal mechanism locations are taken from DeMets et al. (2010) and trench normal azimuth data are taken from McCaffrey (1996).

McCaffrey (1996) used earthquake data shallower than 60 kms. I used earthquake locations from focal mechanism data which is taken from The Global CMT Project for this study. I chose the data which are shallower than 70 km. McCaffrey (1996) separated the Aleutian arc into 26 regions which are approximately 150 km apart. I took these bins and used their trench normal azimuth values for arc-parallel and arc-normal plate motion rate calculations. The direction of the motion and velocity of the subducting plate, Pacific plate, relative to the forearc is taken from DeMets et al. (2010), MORVEL.

Arc-parallel component of the plate convergence velocity is V_p is calculated as $V_p = V \sin \gamma$. V is the relative plate convergence rate and γ is the plate convergence obliquity (McCaffrey, 1996).

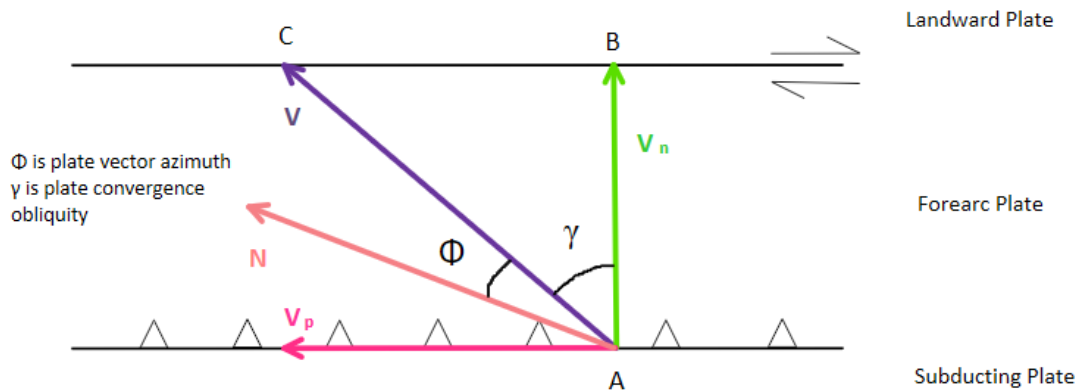


Figure 4.1.1. Displacement Partitioning Model Along Arcuate Convergent Plate Boundary

Block diagram showing the geometry of the convergence system. Convergence occurs in the direction of AC. This is the convergence direction between the subducting and overriding plate. The overriding plate covers forearc and landward plate at this figure. Convergence velocity decouples into V_n and V_p . The angle γ is the convergence obliquity angle which is between the plate convergence direction and the direction normal to the trench. Φ is the mean plate vector azimuth angle.

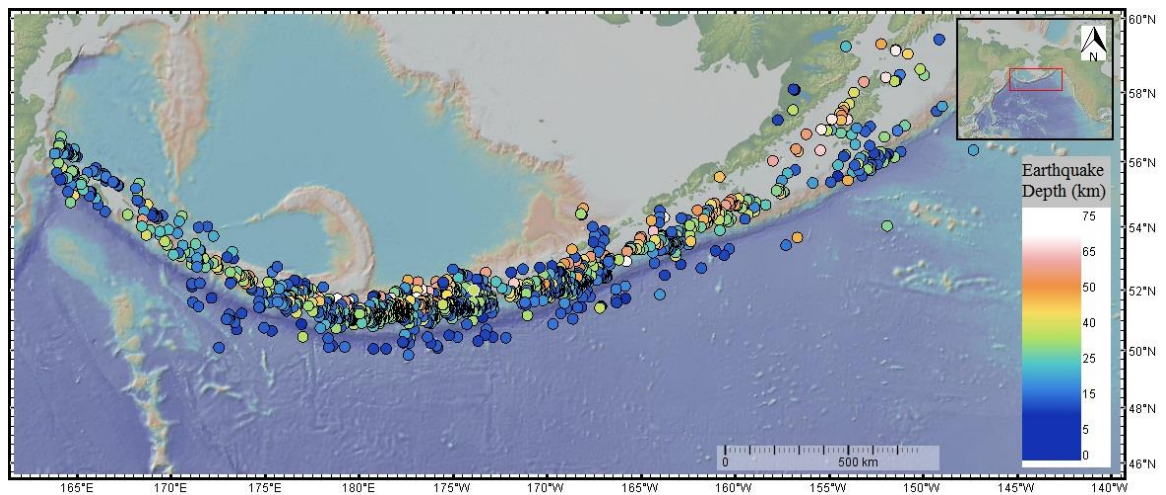


Figure 4.1.2. Earthquake Depths and Velocity Partitioning Locations

Figure 4.1.2 shows the earthquakes shallower than 70 km depth along the arc, covers from January 1976 to April 2015. These earthquake locations were used to calculate the arc-parallel and arc-normal component of the plate convergence velocities.

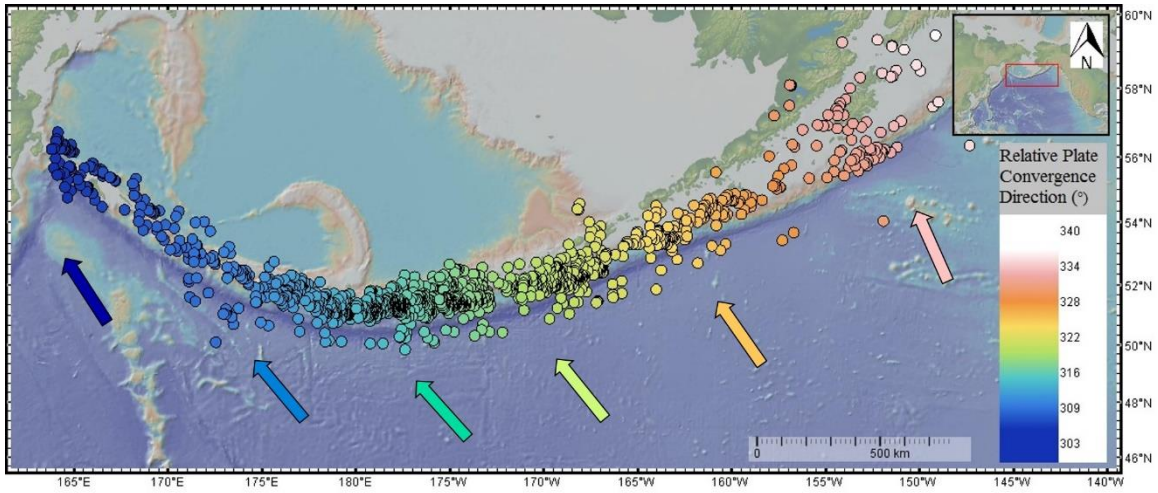


Figure 4.1.3. Relative Convergence Directions between North America and Pacific Plates

Figure 4.1.3 shows the relative convergence directions between Pacific and North American plates along the Aleutian Arc. Convergence direction becomes parallel to the arc as goes to the west direction.

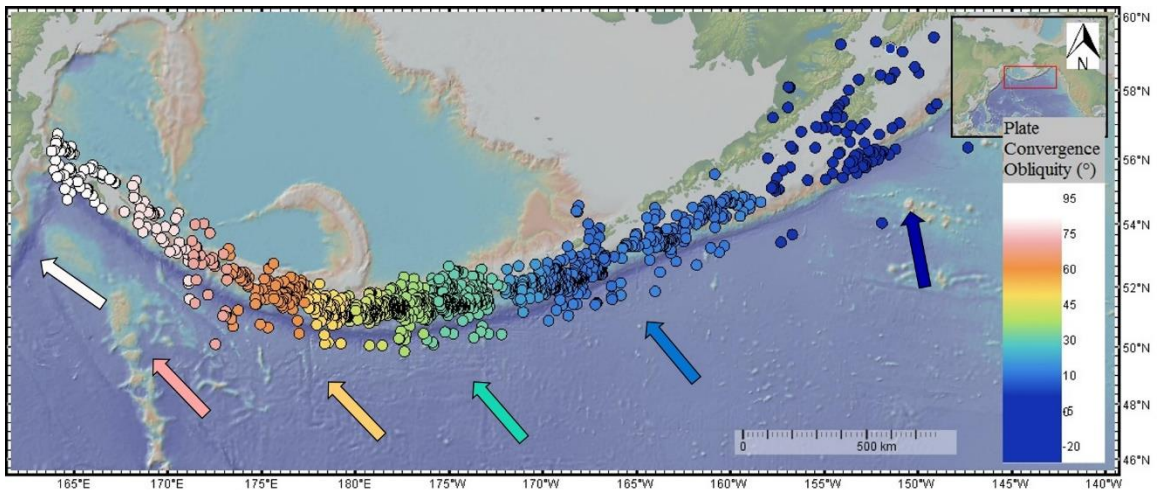


Figure 4.1.4. Relative Plate Convergence Obliquity Angles Between North America and Pacific Plates

Figure 4.1.4 shows the plate convergence obliquity variation along the Aleutian Arc. Obliquity direction at the east side of the arc is towards east. On the other hand, west of 155° W, the convergence obliquity turns toward the west direction. This is because of the arcuate shape of the arc. Moreover, convergence obliquity increase toward center and becomes parallel to the trench obliquity at the western part of the arc. These data are taken from McCaffrey (1996).

But if the arcuate shape of the arc is considered, the obliquity angles between the converging plates are more important than convergence direction. Since the obliquity and convergence angles are independent from each other; to calculate the velocity partitioning along the arc, plate convergence obliquity becomes important.

Strain partitioning structures in the Aleutian arc develop where the angle of obliquity is $\geq 20^{\circ}$ around 170° W. This area also coincides with the GPS Station AB02 which is chosen as the pivot point for the arc.

Relative plate convergence velocities are taken from DeMets et al. (2010) according to MORVEL model. Velocity values show increase toward westward of the Aleutian Arc as seen from Figure 4.1.5. They change with the same trend of convergence angles.

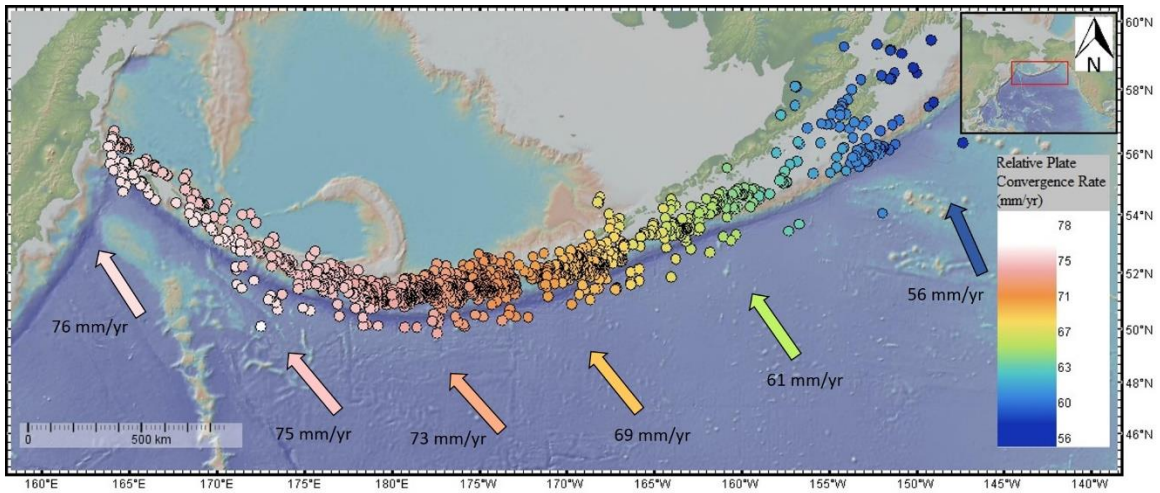


Figure 4.1.5. Relative Plate Convergence Rate Map

Arc-parallel component of the plate convergence velocity (V_p) configuration can be seen in Figure 4.1.6. V_p becomes its maximum at the western part of the arc. Since the convergence obliquity becomes parallel to the arc, this increase in the arc-parallel velocity is the expected result.

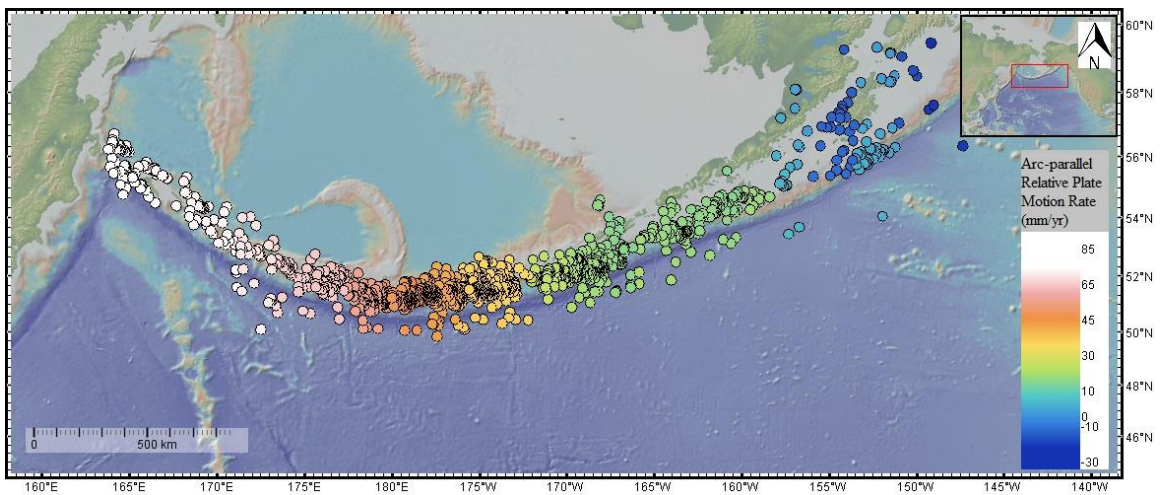


Figure 4.1.6. Arc-Parallel Relative Plate Motion Rate Map

Figure 4.1.7 shows the arc-parallel velocity change along the trench. Distance measurement starts from the east part of the arc and goes through the west direction. Distance measurement started from 145°W and finished at 164° E, approximately.

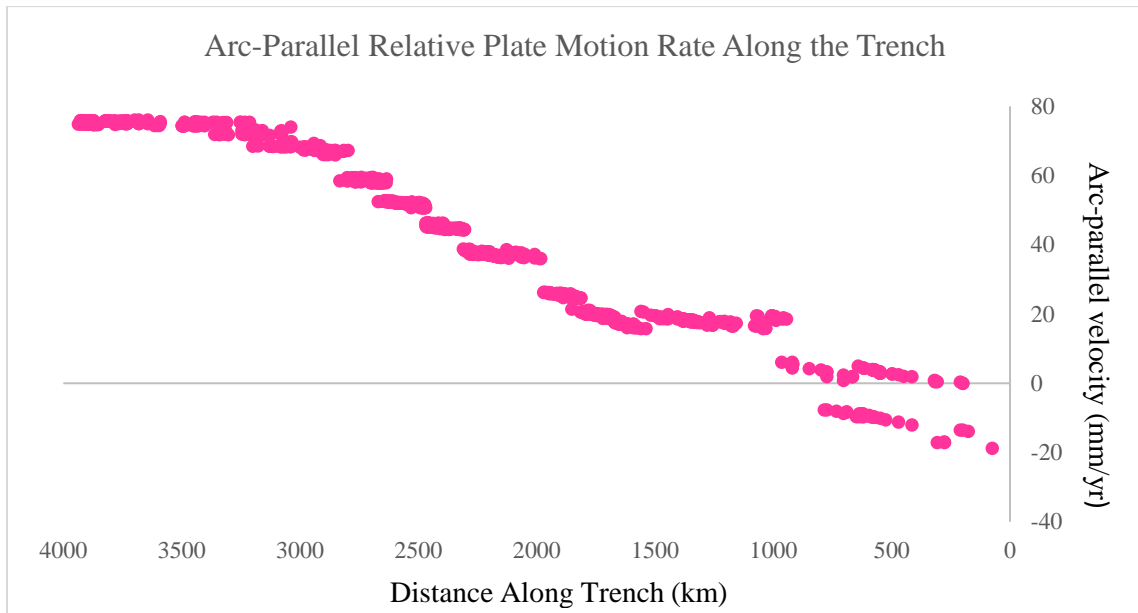


Figure 4.1.7. Arc-Parallel Relative Plate Motion Rate Along the Trench

Arc-normal convergence rate (V_n) is calculated from; $V_n = V \cos \gamma$, where V is the convergence velocity and γ is the convergence obliquity. As can be seen from Figure 4.1.8, largest values are located at east side of 170°W and gradually decreasing towards westward of the arc.

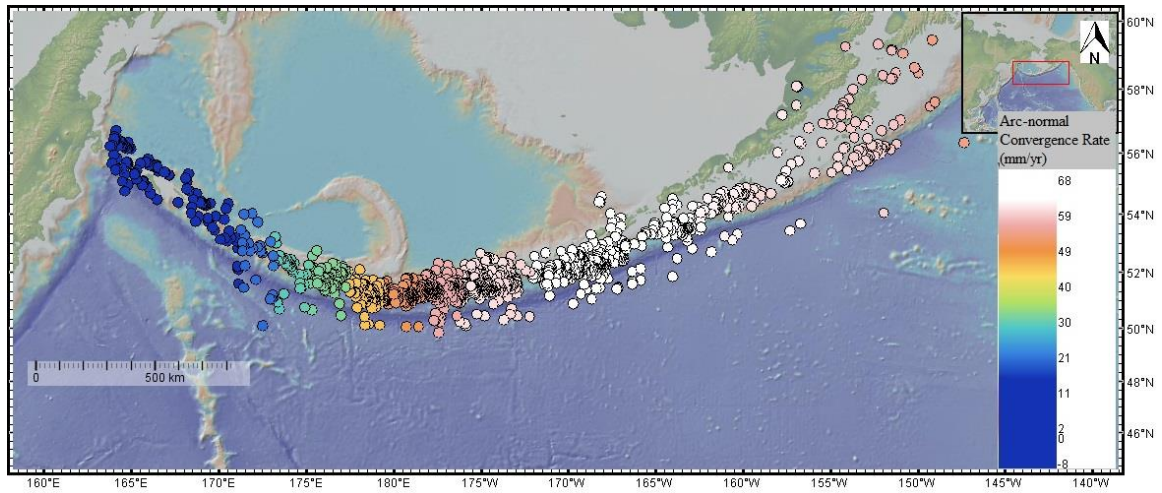


Figure 4.1.8. Arc-normal Relative Plate Motion Rate Map

Figure 4.1.9 shows arc-normal velocity along the trench which is slightly increasing westward from the Alaska Peninsula to the Aleutian Arc, however, around the center of the arc, west side of the 170°W, it decreases abruptly and becomes zero where the convergence obliquity is equal to convergence direction (around 170°E).

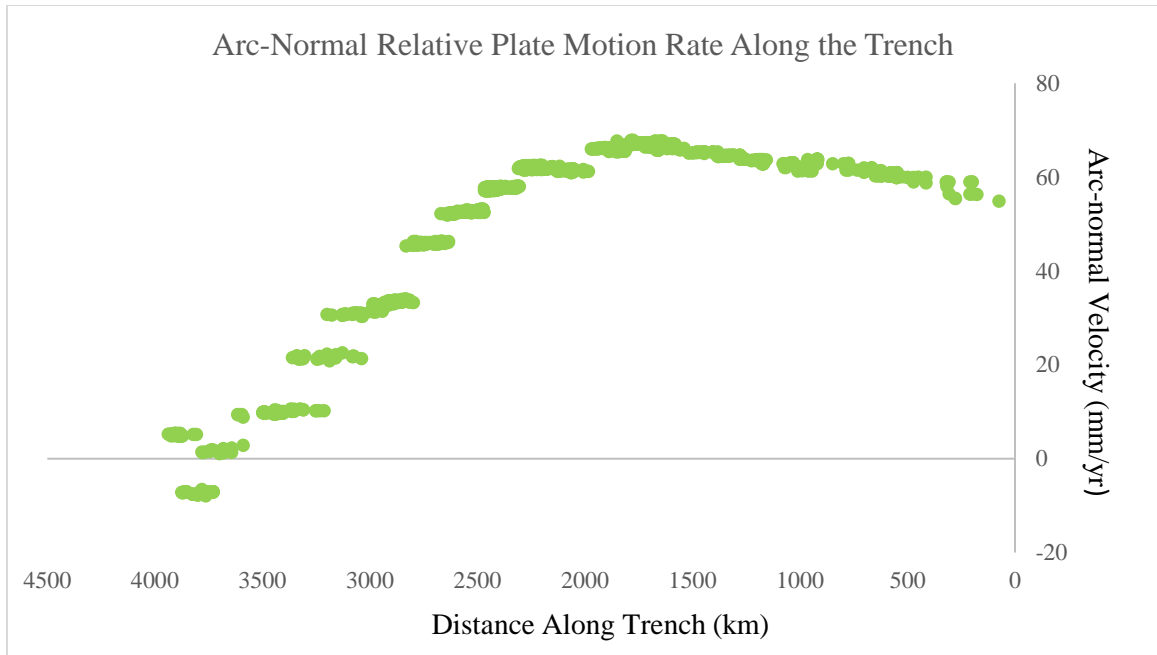


Figure 4.1.9. Arc-Normal Relative Plate Motion Rate Along the Trench

Figure 4.1.10 shows that convergence rates of plates and arc-parallel convergence rate together along the trench. At the east side of the arc, arc-parallel convergence direction is toward the east and around 15 mm/yr while the plate convergence rate is around 60 mm/yr toward the west direction. At the center of the arc, around 157°W, arc-parallel velocity changes its direction from east to west due to obliquity angle change. While going to the west side of the arc, arc-parallel velocity is gradually increasing and becomes almost equal to the convergence rate at the western side of the arc.

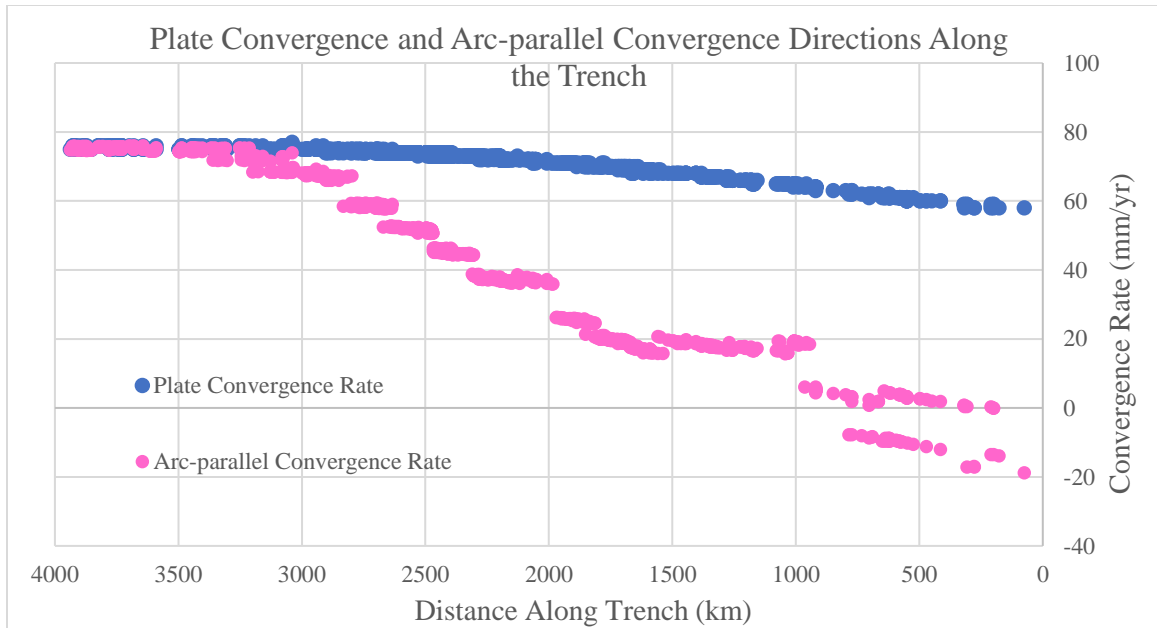


Figure 4.1.10. Plate Convergence and Arc-parallel Convergence Directions Along the Trench

Figure 4.1.11 represents the convergence rate and arc-normal component of them along the arc. East side of the trench, arc-normal convergence rates are almost equal to convergence rates as 60 mm/yr. But towards the west side of 170° W, arc-normal convergence rate starts to decrease while the convergence rate is still increasing gradually.

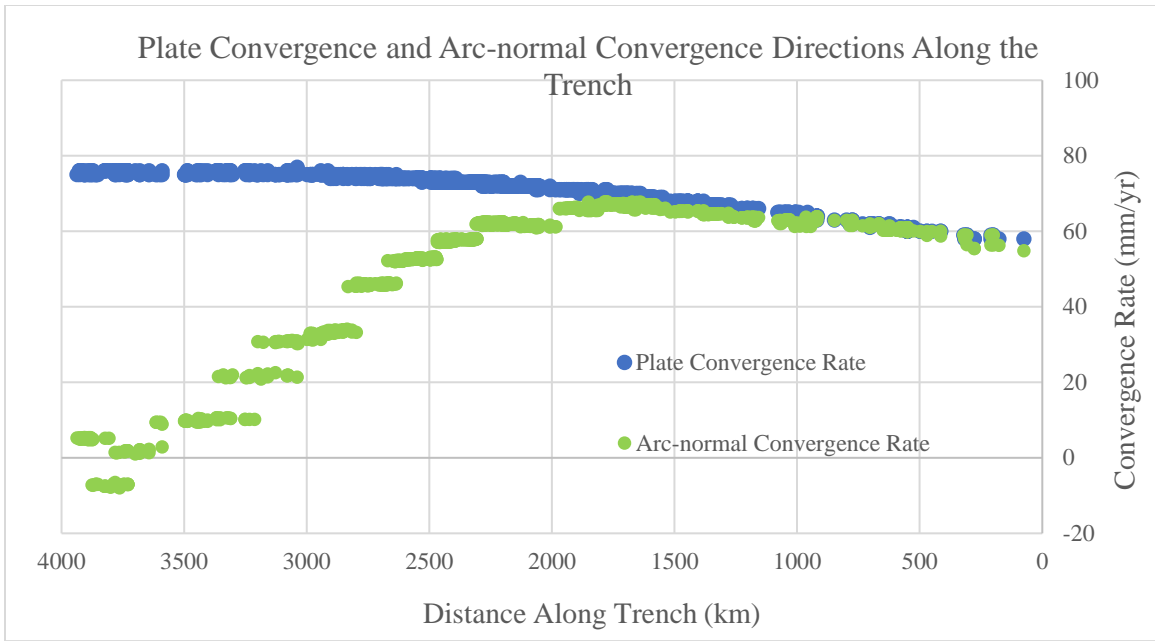


Figure 4.1.11. Plate Convergence and Arc-normal Convergence Directions Along the Trench

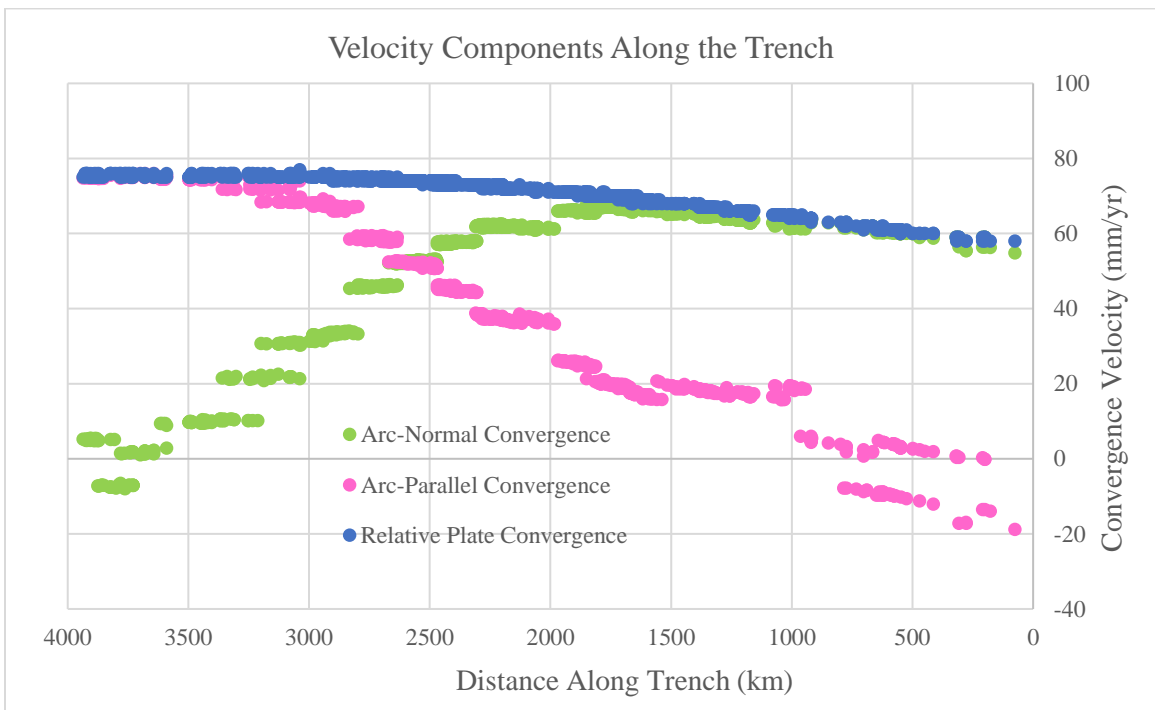


Figure 4.1.12. Velocity Components and Relative Plate Convergence Rates Along the Trench

Figure 4.1.12 shows both velocity components and relative plate convergence rates along the arc together.

4.2 VOLCANIC ACTIVITY AND MAGMA PATHWAYS

Tibaldi and Bonali (2017) studied Holocene volcano-tectonic structures to recognize the estimate magma pathways and stress distributions within the Aleutian Arc. Magma plumbing systems at volcanic arcs are complicated since magma can rise along the fractures that are associated with the regional state of stress or local state of stress. Moreover, they can rise along dykes following pre-existing structures. These magma pathway orientations can be stable or can vary because of events such as large earthquakes. In the light of this information, Tibaldi and Bonali (2017) reviewed 91 magma paths at the Aleutian Arc (Figure 4.2.1).

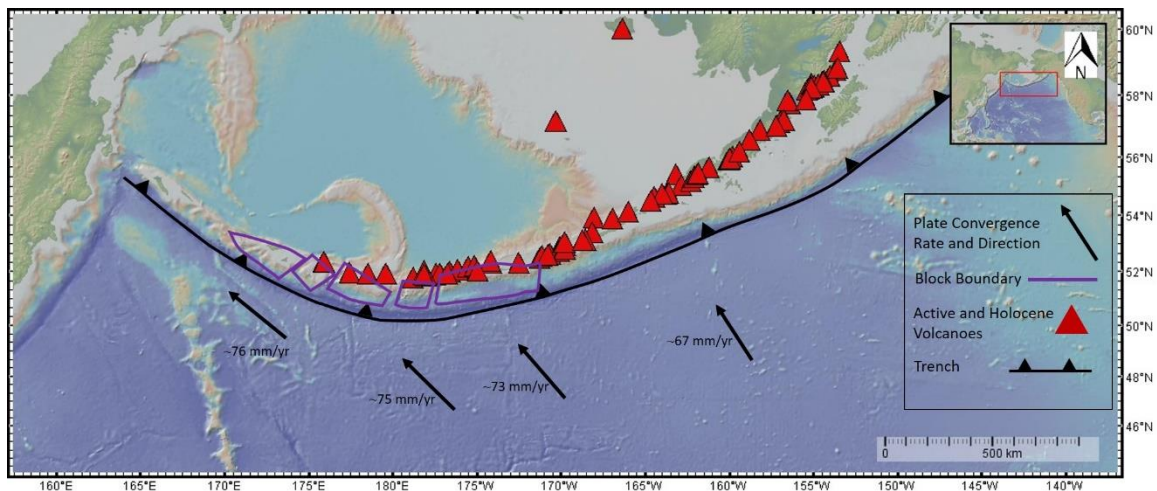


Figure 4.2.1. Active and Holocene volcanoes belonging to the Aleutian-Alaska Arc (Tibaldi and Bonali, 2017) and Rotating Blocks (Geist et. al, 1988)

Tibaldi and Bonali (2017) interpret 40 volcanoes that show shallow magma paths trending NW-SE which are perpendicular or oblique to the arc. The strikes of these volcanoes are

parallel to the regional greatest principal stress direction. Six of the volcanoes have a NE-SW trend and 3 volcanoes have a N-S trend. Also, 20 magma paths are parallel to the arc.

According to Tibaldi and Bonali (2017), the trend of the horizontal greatest principal stress along the arc is between NNW-SSE and NW-SE. Since the trend of magma pathways are parallel to the greatest principal stress direction, the relative plate convergence direction is also parallel to the greatest principal stress direction along the arc. The relative plate convergence direction between Pacific and North America plates change from 340° (NNW-SSE) at the eastern part of the arc to 303° (NW-SE) at the western part of the arc (Figure 4.2.2).

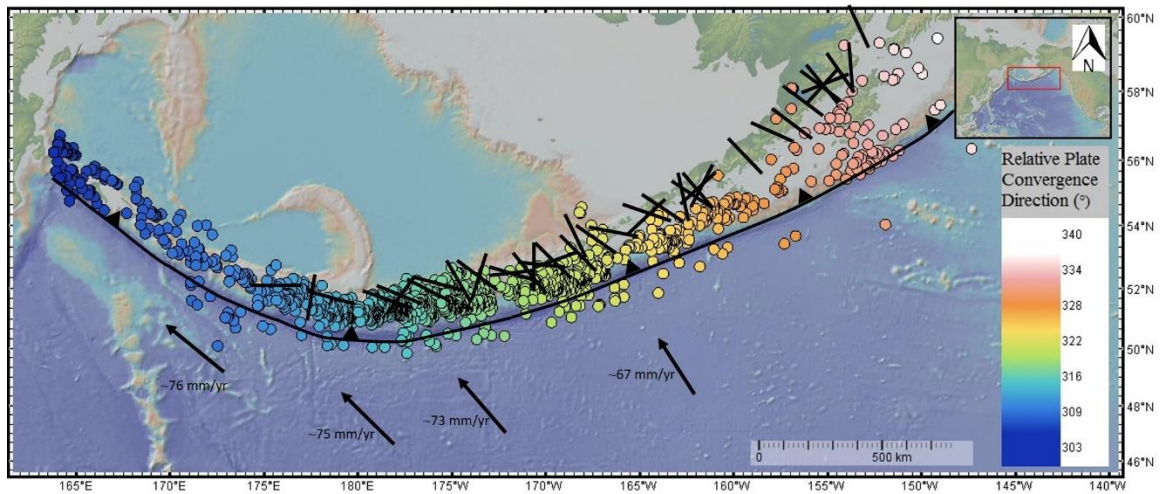


Figure 4.2.2. Relative Plate Convergence Direction and Magma Pathway Strikes

There are normal faults at the system, also. According to Tibaldi and Bonali (2017), these NNW to NW trending normal faults and dykes are coherent with the regional trend of the minimum stress direction. Since minimum stress direction at the system ranges between

NE-SW and ENE-WSW. Moreover, these arc-perpendicular normal faults and dykes are related with arc-parallel transcurrent faults which are linked to displacement partitioning along the arc (Lallemant and Oldow, 2000).

Tectonic structures along the Aleutian Arc change relatedly. Ruppert et al. (2012) show that arc-parallel strike slip faulting is dominant in the western part, arc-perpendicular strike slip faulting is dominant in the center part of the arc and normal faulting is general at the eastern part of the arc. My study also support these tectonic structures with focal mechanism data. These different dominant faulting systems at the different part of the arc are the result of the convergence angle change. Oblique subduction dominates the western part of the arc with displacement partitioning with these arc-parallel strike slip faults (McCaffrey, 1992). Arc-parallel and arc-normal convergence rate calculations also support this partitioning. From the center to the west side of the arc, there are clockwise rotating blocks defined by arc-perpendicular strike slip faults and normal faults (Geist et al. ,1988). Moreover, these rotating blocks produce triangular-shaped extensional basins in the northern limit of the sliver plate (Geist et al., 1988). This complex tectonic structure of the Aleutian Arc shows dominant magma paths at different orientations. Generally, it can be observed that the dominant magma path trends are N105° at the center part of the arc and N121° at the eastern part (Tibaldi and Bonali, 2017).

5 RESULTS AND CONCLUSIONS

The Aleutian Arc is an example of an arcuate oceanic-continental convergent margin that extends for 4000 kilometers from Gulf of Alaska to Kamchatka Peninsula. The relative convergence rate between the Pacific and North American plates is 48 mm/yr in the east and 78 mm/yr in the west of the arc (Lallemant and Oldow, 2000). Deformation along the Aleutian Arc is widely interpreted to result from oblique convergence between the relative plate motion and the strike of the margin along the arc. This obliquity results in the formation of five clockwise-rotating blocks and a forearc sliver (Ruppert et al., 2012).

The aim of this study is to better understand the geometry of these features and their potential kinematic role in accommodating oblique convergence. Forearc partitioning, rotation, and translation of the forearc sliver plate were evaluated using: 1) data from 6 GPS stations collected between 2004 and 2015, 2) 1,798 earthquake events (focal mechanisms and depth) that occurred between January 1976 to April 2015, 3) plate convergence velocities, and 4) trends of Holocene magmatic features.

There are four GPS stations located within the arc. One GPS station is not located in the block system and one station is located on the Kamchatka Peninsula. The velocities of these four GPS stations located on the blocks increase toward the west. Their velocity results are given in Table 5.1.

Table 5.1 Velocity of GPS Stations

GPS Station	Latitude	Longitude	Velocity (mm/yr)
AB01	52.210	-174.205	6.26 mm/yr - 242.97°
AB21	51.864	-176.663	15.47 mm/yr – 306.51°
AC66	51.378	179.301	23.25 mm/yr – 274.74°
AC60	52.715	174.076	32.48 mm/yr – 298.72°

Station AB01 and AB21 are located on the same block on opposite sides. Station AB01 is at the northeastern corner and Station AB21 is located at the northwestern side. From their movement direction, it can be interpreted that the northeast side of the block (Station AB01) moves towards the southwest and northwest side of the block (Station AB21) is going to the northwest. This indicates that opposite corners move in different directions. This is the evidence of block rotation.

The movement direction of Station AC66 is the combination of Station AB01 and AB21. Its movement direction deviation from major movement direction is less than the other two Stations AB01 and AB21. Station AC66 is more stable than those two stations. Moreover, Station AC60 shows a more-stable movement direction with the lowest deviation rate among the station. It is stable in its movement path.

Relative horizontal velocities of each GPS stations were calculated to understand their and blocks' motion behaviors. To calculate these relative horizontal velocities, all six stations were chosen as a fixed station and others' relative horizontal velocities were calculated according to this fixed station. Results are given in Table 5.2.

Relative horizontal velocities according to fixed reference stations show that the pivot point of the arc should be the east side of the Station AB21. Because the movement directions of the stations are towards the west direction.

Table 5.2 Relative Horizontal Velocities. Values are given in mm/yr. "E" is east direction, "W" is west direction.

	FIXED STATIONS					
	PETS	AC60	AC66	AB21	AB01	AB02
AB01	6.54 E	20.17 E	12.56 E	3.08 E		3.37 W
AB21	2.57 E	17.24 E	9.25 E		3.08 W	7.48 W
AC66	7.58 E	2.52 E		9.25 W	12.56 W	17.10 W
AC60	12.67 E		2.52 W	17.24 W	20.17 W	22.72 W

To distinguish the rotation direction and pivot point of the arc, three GPS stations (AB21, AB01 and AB02) predicted as pivot location and they are assumed as fixed stations. Figure 5.1.1 shows relative movement directions of the stations when the Station AB02 chosen as the pivot point. These movement directions are convenient with velocity directions of each station. My results show that the Aleutian Arc is undergoing clockwise rotation with respect to Station AB02 which is the pivot point of the arc. This indicates that the angle of obliquity west of 170°W is increasing.

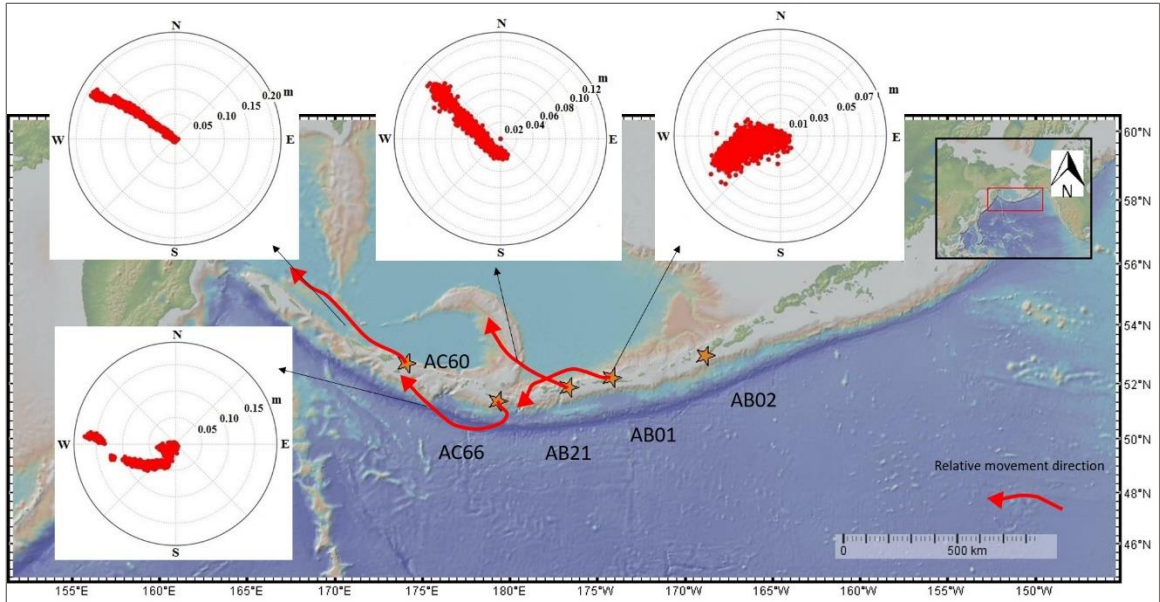


Figure 5.1.1. Comparison Map of Relative Velocity and Velocity Results of GPS Stations

Analysis of the earthquake depths show that although the convergence obliquity is increasing from east to west, depth of earthquakes become shallower. Earthquake depths are generally shallow for the Aleutian Arc.

Due to oblique convergence between the North America and Pacific plates, active strain partitioning occurs within the Aleutian Island Arc. Strain partitioning structures in the Aleutian arc develop where the angle of obliquity is $\geq 20^\circ$ around 170°W . This area also coincides with the GPS Station AB02 which is chosen as the pivot point for the arc (Figure 5.1.2).

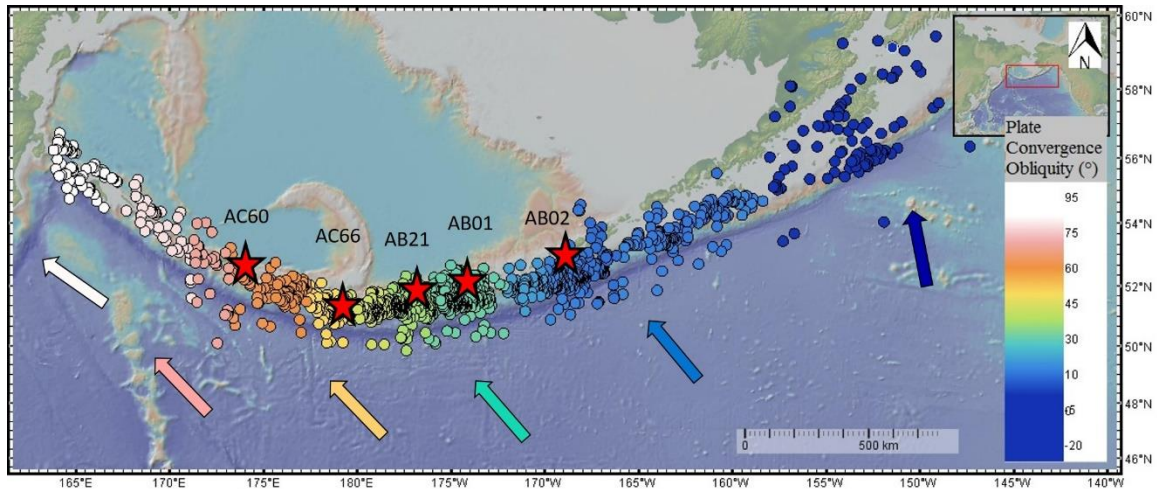


Figure 5.1.2. Plate Convergence Obliquity and GPS Stations

Arc-parallel and arc-normal convergence rates correlate with convergence obliquity along the arc. The boundary between blocks undergoing vertical axis rotation and the forearc sliver corresponds to an angle of obliquity equal to 70° (170°E) (Figure 5.1.2). Moreover, the boundary of blocks including what we interpret as a forearc sliver correlates to the angle of obliquity between the North American plate and the Pacific plate.

Holocene volcanic features also correlate with convergence directions and structural features related to the block system.

REFERENCES

- Chekhovich, V. D., O. G. Sheremet, and M. V. Kononov, 2014, Strike-slip fault system in the Earth's crust of the Bering Sea: A relic of boundary between the Eurasian and North American lithospheric plates: *Geotectonics*, v. 48, no. 4, p. 255–272, doi:10.1134/S0016852114040037.
- DeMets, C., R. G. Gordon, D. F. Argus, and S. Stein, Current plate motions, *Geophys. J. Int.*, 101, 425-478, 1990
- DeMets, C., R. G. Gordon, and D. F. Argus, Geologically current plate motions, *Geophys. J. Int.*, 181, 1-80, 2010.
- Freymueller, J.T., Woodard, H., Cohen, S.C., Cross, R., Elliott, J., Larsen, C.F., Hreinsdottir, S., Zweck, C., 2008. Active deformation processes in Alaska, based on 15 years of GPS measurements. In: Freymueller, J.T., Haeussler, P.J., Wesson, R.L., Ekstrom, G. (Eds.), *Active Tectonics and Seismic Potential of Alaska*. *Geophys. Monograph Ser.*, 179. American Geophysical Union, Washington, DC, pp. 1–42.
- Geist, E. L., J. R. Childs, and D. W. Scholl, 1987, Evolution and petroleum geology of Amlia and Amukta intra-arc summit basins, Aleutian Ridge: *Marine and Petroleum Geology*, v. 4, no. 4, p. 334–352, doi:10.1016/0264-8172(87)90011-0.
- Geist, E. L., J. R. Childs, and D. W. Scholl, 1988, The origin of summit basins of the Aleutian Ridge: Implications for block rotation of an arc massif: *Tectonics*, v. 7, no. 2, p. 327–341, doi:10.1029/TC007i002p00327.

- Krutikov, L., D. B. Stone, and P. Minyuk, 2008, New Paleomagnetic Data From the Central Aleutian Arc : Evidence and Implications for Block Rotations: Active Tectonics and Seismic Potential of Alaska Geophysical Monograph Series, v. 179, p. 135–149.
- Lallemant, H. G. A., 1996, Displacement partitioning and arc-parallel extension in the Aleutian volcanic island arc: Tectonophysics, v. 256, p. 279-293.
- Lallemant, H. G. A., and J. S. Oldow, 2000, Active displacement partitioning and arc-parallel extension of the Aleutian volcanic arc based on Global Positioning System geodesy and kinematic analysis: Geology, v. 28, p. 739–742, doi:10.1130/0091-7613(2000)28<739.
- McCaffrey, R., 1992, Oblique Pale convergence, Slip Vectors, and Forearc Deformation: Journal of Geophysical Research, v. 97, no. B6, p. 8905–8915.
- McCaffrey, R., 1996, Estimates of moderns arc-parallel strain rates in fore arcs: Geology, v. 24, no. 1, p. 27-30.
- McCaffrey, R., 2009, The Tectonic Framework of the Sumatran Subduction Zone: Annual Review of Earth and Planetary Sciences, v. 37, no. 1, p. 345–366, doi:10.1146/annurev.earth.031208.100212.
- Ruppert, N. a., N. P. Kozyreva, and R. a. Hansen, 2012, Review of crustal seismicity in the Aleutian Arc and implications for arc deformation: Tectonophysics, v. 522–523, p. 150–157, doi:10.1016/j.tecto.2011.11.024.
- Scholl, D., T. Vallier, and A. Stevenson, 1987, Geologic evolution and petroleum geology

of the Aleutian Ridge: Geology and resource potential of the western North America and adjacent ocean basins--Beaufort Sea to Baja California, v. 6, p. 123–155.

Tibaldi, A., and F.L. Bonali, 2017, Intra-arc and back-arc volcano-tectonics: Magma pathways at Holocene Alaska-Aleutian volcanoes: *Earth-Science Reviews*, v. 167, p. 1-26, doi:10.1016/0012-8252.

Wanke, M., M. Portnyagin, K. Hoernle, R. Werner, F. Hauff, P. van den Bogaard, and D. Garbe-Schon-berg, “Bowers Ridge (Bering Sea): an Oligocene–Early Miocene island arc,” *Geology* 40 (8), 687–690 (2012).

Wesson, R. L., O. S. Boyd, C. S. Mueller, and A. D. Frankel, 2008, Challenges in Making a Seismic Hazard Map for Alaska and the Aleutians: Active Tectonics and Seismic Potential of Alaska Geophysical Monograph Series, v. 179, p. 385–397, doi:10.1029/179GM22.